Experimental Characterization and Finite Element Analysis of Jute and Glass Fiber Reinforced Epoxy Composite Material for Structural Automotive Components.

A Thesis Submitted to Solid Mechanics and Design Chair in Partial Fulfillment of the Requirement for the Degree of Master of Science

In

Product Design and Development (PDD)

By:

Mr. Haftom Hailemichael

Under Supervision:

Dr. Abrha Gebregergs (*Ph.D*)

Mekelle University

Ethiopian Institute of Technology – Mekelle (EIT-M)

School of Mechanical and Industrial Engineering

Solid Mechanics and Design Chair

January - 2024

Mekelle	Tigray	Ethiopia

THESIS ACCEPTANCE APPROVAL FORM

"This is to certify that the thesis prepared by ***Mr. Haftom Hailemichael*** entitled ***"Experimental Characterization and Finite Element Analysis of Jute and Glass Fiber Reinforced Epoxy Composite Material for Structural Automotive Components."*** has been accepted for the award of the Degree of Master of Science in Mechanical Engineering (Product Design and Development), in partial fulfillment of the requirements for the Master of Science in Mechanical Engineering at Mekelle University."

Members of the Examination Board

Dr. Kalayu Mekonen		19/05/2025
External Examiner	Signature	Date
Dr Alula Gebresas		19/05/2025
Internal Examiner	Signature	Date
Dr Abrha Gebregergs		19/05/2025
Supervisor	Signature	Date
Mr Tadesse Gebray		19/05/25
Chairman	Signature	Date

Confirmation: SMD Chair

ታደሰ ገብረ ተስፋይ (MS c)
የሶሊድ መካኒክስና ዲዛይን ቼይር ሀላፊ
Tadesse Gebray Tesfay (MS.c)
Head of Solid Mechanics & Design Chair

		19/05/25
Chair Head	Signature	Date

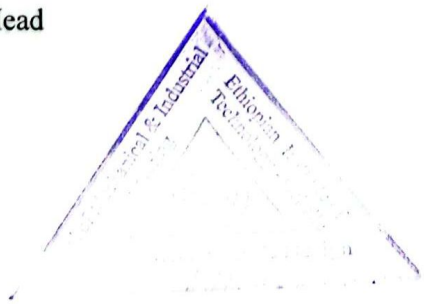

CANDIDATE'S DECLARATION

I declare that this written submission represents my ideas in my own words, but for others' idea I have used I try to sufficiently cite and put reference. I also declare that I have obeyed all principles of academic honesty and integrity and have not misrepresented (fabricated) or falsified any idea/data/fact/source in my submission. I understand that any violation of the above will cause for disciplinary action by the Institute and can also evoke penal action from the sources which have thus not been properly cited or from whom proper permission has not been taken when needed.

Name of Candidate: Mr. Haftom Hailemichael

Signature: _____

Date: _____

ADVISOR'S DECLARATION

This is to certify that the above declaration made by the candidate is correct to the best of my knowledge and the thesis is adequate for the award of the degree of Master of Science in product design and development.

Advisor: Dr. Abrha Gebregergs (Ph.D)

Signature: _____

Date: _____

Co-Advisor: Mr. ……..

Signature: _____

Date: _____

AKNOWLEDGMENT

First and foremost, I would like to thank Almighty GOD for being us here today passing all these challenges and let me complete the thesis work. Next, I would like to give special thanks to my Advisor Dr. Abrha Gebregergs (Ph.D), for his great effort in terms of supervision, support, commitment and patience from the beginning until accomplishment of my research thesis.

My infinite Gratitude goes to my parents and family members for their enduring patience, moral and financial supports. their sacrifices were truly irreplaceable by any thig the only I can say is GOD bless for your assistance at any occasions.

Many thanks are also extended to My Staff in Adigrat University and EiT-M Mechanical Engineering workshop staffs in helping and guidance for facilitating the material testing during the material properties test and Staff Friends for their Support (help) in many ways when I asked them. Finally, I would like to thanks to my family and my friends those who were supporting and motivating me for the achievement of this study.

ABSTRACT

Using of fiber-reinforced composite materials is rapidly advancing in the automotive and aerospace industries due to their superior properties, including lightweight, high strength-to-weight ratio, high impact strength, corrosion resistance, design flexibility, and dimensional stability. Traditionally, vehicle bodies have been constructed from heavy metals like steel, increasing vehicle weight and fuel consumption. This study focuses on enhancing the mechanical properties of Jute/Glass Fiber reinforced epoxy composites for automotive body applications.

The research evaluates tensile, compression, impact, and flexural strengths of unidirectional jute and glass fiber composites by varying fiber weight ratios, orientation angles, and stacking sequences. Experimentation followed ASTM standards, and the composite car bonnet was designed and analyzed using Classical Laminate Theory and optimization via Opti-Struct in Altair Hyper Mesh 2019.

Results indicated that a 50/50 weight ratio of jute to glass fibers with unidirectional orientation offered the best mechanical properties. Additionally, incorporating ±45° fiber orientations enhanced impact strength in both lateral and transverse directions. The bonnet design optimization led to a 67% weight reduction compared to conventional steel bumpers, resulting in an average fuel savings of 0.0034 L/100 km.

Thermal analysis using FEM Ansys showed that the composite bonnet had lower thermal conductivity and heat flux, with higher temperature distribution at the edges due to constraints. The thermal stress remained within safe limits, indicating no immediate failure risk.

In conclusion, the hybrid composite material with Jute/Glass fibers can effectively replace traditional steel Bonnet, offering significant weight reduction and fuel efficiency improvements without compromising safety.

Keywords: Hybrid Jute/Glass Fiber Reinforced Composite, Mechanical Property, Classical laminate Theory, Impact Strength, Altair-Hyper Work, Weight Optimization …

TABLE OF CONTENTS

LIST OF TABLES

LIST OF FIGURES

SYMBOLS

W_f	Weight of fiber
W_m	Weight of matrix
Wc	Weight of composite
W_{ff}	Weight fraction of fiber
W_{fm}	Weight fraction of matrix
V_f	Volume of fiber
V_m	Volume of matrix
Vc	Volume of Composite
V_{ff},	Volume fraction of fiber
V_{fm}	Volume fraction of matrix
ρ_c	Density of composite
E_1	Longitudinal modulus of elasticity
E_2	Transversal modulus of elasticity
E_x	In-plane longitudinal modulus
E_y	In-plane transversal modulus
G_{xy}	In-plane shear modulus
[C]	Stiffness Matrix
[Q]	Reduced stiffness Matrix
[R]	Reuter matrix
[T]	Transformation matrix
[A]	Extensional Stiffness Matrix
[B]	Coupling Stiffness Matrix
[D]	Bending Stiffness Matrix
N_x	Normal Force in x Direction
N_y	Normal Shear in y Direction
N_{xy}	Shear Force
M_x	Bending Moment in yz plane
M_y	Bending moment in xz plane
M_{xy}	Twisting moment
σ_{11L}	longitudinal tensile stress

σ_{11c}	longitudinal compression stress
σ_{22t}	Transversal Tensile Stress
σ_{22c}	Transversal Compression Stress
$V_{(X)}$	Shear Force
$M_{(X)}$	Bending Moment
δ (Δ_d)	Deflection
K	Mid-Plane Curvatures
ε	Strain
γ	Shear Strain
υ	Poisons Ratio
τ	Shear Stress
E	Impact Energy
I	Moment of Inertia
λ	Buckling

LIST OF ABBREVIATIONS AND ACRONYMS

UD	Unidirectional
FRC	Fiber Reinforced composites
PMCs	Polymer matrix composites
CMCs	Ceramic-matrix composites
MMCs	Metal-Matrix Composites
PCs	Particulate Composites
SCs	Structural Composites
HDPE	High-Density Polyethylene
MEKP	Methyl Ethyl Ketone Peroxide
ASTM	American society of testing materials
FMSS	Federal Motor Vehicle Safety Standards
CMVSS	Canadian Motor Vehicle Safety Standards
JGFREC	Jute /Glass Fiber Reinforced Epoxy Composite
CLM	Classical Laminate Method
UDL	Uniformly Distributed Load
GSE	Ground Service Equipment
UTM	Universal Testing Machine
CLT	Classical Laminate theory
FEM	Finite Element Method
CAD	Computer Aid Design
FPF	First Ply Failure load
ROM	Rule of Mixture
Mph	Miles Per Hour
SR	Strength Ratio
Eq.	Equation

CHAPTER ONE

1. INTRODUCTION

1.1. BACK GROUND

Most automotive industry uses conventional metals like steel, aluminum, magnesium and steel alloys to manufacture automobile bodies. These materials are heavy which increases weight of automobile causes for high carbon gas emission to the atmosphere. Also, the conventional materials are too costly causes economic crises. As a key technology of energy conservation and emission reduction, lightweight technology has attracted the attention of automobile enterprises and researchers. As a result, today new invention in technology material was introduced called composite provides high mechanical performance with low cost and lower weight.

Composite materials are heterogeneous solid containing at least two or more different materials with significantly different physical or chemical properties that are mechanically & metallurgical bonded together to enhance better & different mechanical, thermal or electrical properties to correct a weakness in one material by strength in the other (1). Practically, most Composite materials are composed of Two big components reinforcement and matrix. matrix surround or hold reinforcements together to create products with any shape and size. reinforcement is tougher, stronger and Stiffer than the Matrix usually can be fibrous or a particulate. These fibers can be either synthetic or Natural. A fibrous reinforcement has high strength because of high length-to-diameter (l/d) ratio is known as the aspect ratio. Continuous fibers have long aspect ratios & preferred orientation, while discontinuous fibers have short aspect ratios & random orientation. the smaller-diameter of fiber tends high-strength, greater flexibility and easy to fabrication processes.

Whereas Particulate composites have approximately equal dimensions in all directions but much weaker, less stiff and less expensive than continuous fiber composites. Particulate reinforced composites typically contain less reinforcement (40 – 50 volume percent) (1) due to processing difficulties and brittleness a Matrix phase can be polymeric, metallic or ceramic which uses load transferring to fibers, maintaining the fibers in the proper orientation and protecting them from abrasion the surface. Polymers have low strength and stiffness whereas metals have intermediate strength and stiffness but high Ductility, & ceramics have high stiffness, strength but are brittle.

Using of Natural Fiber reinforced polymer composites are being grown in almost every type of applications in our daily life because of their properties like low cost, Available, low density, biodegradable, environmentally friend (nontoxic), and nonabrasive…etc. Currently, there are variety of industrially usable natural fibers like, jute, sisal, Palm, bamboo, banana, hemp etc. available whose mechanical properties is relatively good, and may compete with glass fiber in terms of specific strength and modulus (2). Among all the natural fibers, jute is relatively cheap and commercially available in various forms. Jute fiber has many inherent advantages like luster, low extensibility, high tensile strength, moderate fire and heat resistance and long staple lengths (3) (4). Traditionally, jute is used in packaging fabrics, saking, mats, manufacturing hessian, carpet backing, bags, ropes, twines and tarpaulins. Jute fibers are also used in wide range of products like in construction for finishing, decorative fabrics, salwarkamizes, chic-saris, soft luggage, molded door panels, footwear and other innumerable useful consumer products (5). However, today major innovation comes and Jute fiber can be used as reinforcement in polymer composites in short, unidirectional or woven forms used in various applications like automotive, structures, aerospace, ship and fishing boats, sports, medical sector, packaging materials, toys and furniture's etc. The use of jute fiber is increasing hurriedly in industrial application.

1.2. APPLICATION AREA OF COMPOSITES

Since the development of synthetic resins during the 2nd half of 20th century application of composite materials comes dramatically increased especially in Aerospace industry, transport industry, structural application, Military, Automotive, Medical, Sporting goods etc. (6) (7) (8). Composites can be considered as a superior type and more unique than Conventional material which has a wide range of applications because of the following especial characteristics. The automotive industry is increasingly adopting natural fiber reinforced epoxy composites for vehicle components due to their Lightweight, High Strength-to-Weight ratio, Corrosion Resistance, Low Thermal Conductivity etc.

Drawback of composite

- √ High fabrication cost: e.g., part made of graphite/epoxy may cost 10 -15 > material costs.
- √ High moisture absorption and partially flammable.
- √ Repair of composites like crack is not a simple process compared to that for metals.

Some common applications areas of composite are

- *Aircraft***:** wings, fuselages, Jet engines, Turbine blades, Turbine shafts, Compressor blades, Airfoil surfaces, Fan blades, Flywheels, doors, Rotor shafts in helicopters etc.
- *Automobiles:* bodies like Engines, bearing materials, Piston, cylinder, connecting rod, crankshafts, roof, floor, frame, front & rare Bonnet, chair, A-pillar and B-pillar…
- *Building and construction***:** (e.g., doors, panels, frames, and bridges)
- *Chemical engineering***:** (e.g., pressure vessels, storage tanks, piping, and reactors)
- *Space craft***:** Antenna system, Solar reflectors, Satellite structures, Radar, Rocket engines

Figure 1:1 Some Application of composite

Finally, reports by Pandey et al. (9) and Bledski et al. (10) indicates the fact that a 25% reduction in the weights of vehicles can lead to a saving of 250 million barrels of fuel, which will translate into about 220 billion reductions in energy cost and a substantial reduction of the yearly CO_2 emission. weight reduction of the car body can be a solution to these problems since 57 kg weight reduction is equivalent to 0.09-0.21 km per liter fuel economy increase (11). Anthony. (12) states that Vehicle weight Savings about from 40% - 45% of total Weight for cost effectiveness if the conventional materials are replaced by fiber reinforced composite materials. Again, Helms and Lambrecht: studied about 100Kg weight reduction of trucks saves the fuel an average of 0.06 l per 100 km i.e. about $0.03l/(100km)$ on flat highway & up to $0.1l$ /100 Km in urban traffic situations.

1.3. STATEMENT OF THE PROBLEM

A lot of automobile bodies are being assembled in different large and small-scale Automotive companies in our country today. Most of these automobile bodies are made from steel and alloy steel material having high weight and imported at high cost. This higher weight causes higher fuel consumption of automobiles resulting high gas emission to the atmosphere which is currently the main concern. Natural fiber Reinforced composite having lighter weight, higher Strength, Low cost, good impact tolerance can Replace the costly and heavy Conventional material without compromising the required strength.

1.4. OBJECTIVES

1.4.1. General Objective

The general objective of this study is improving Automotive Boy using Hybrid of jute and Glass Fiber Reinforced Epoxy Composite material.

1.4.2. Specific Objective

- ✓ To characterize Mechanical Property of the Composite material experimentally based on fiber Weight Ratio, Fiber Angle of orientation and Stacking Sequence.
- ✓ To Design and analysis the Hybrid composite car body (Hood or Bonnet).
- ✓ To make Size & Stacking Sequence Optimization using Opti Struct in Altair-Hyper work.
- ✓ To make thermal analysis of the car bonnet using FEM in Ansys.

- ✓ To validate the optimized Composite Bonnet against the existing steel bonnet.

1.5. Thesis Outline

The thesis is organized in to six chapters: The first chapter gives all about the introduction of composite material, Problem statement and objectives. Chapter 2. Contains a literature review to provide a basic knowledge of the main subjects presented in this thesis. It presents the research works carried out by various investigators specifically on jute fiber reinforced polymer composites. Chapter 3. Provides information of the raw materials used, fabrication technique, Experimental Mechanical Property characterization of the composites under different variables and Software Analysis. Chapter 4. presents Design and analysis of the composite car Bonnet. Chapter 5. Presents both experimentally the physical and mechanical properties test results and Analysis result of the composites. Chapter 6. Provides conclusions drawn from the experimental and analysis study and recommendation for future research work.

1.6. SCOPE OF THE STUDY

This thesis report aims to comprehensively investigate the characterization of composites through theoretical analysis using analytical or numerical impact analysis, incorporating various fiber weight ratios and fiber angles of orientation in the composite laminate, alongside empirical experimentation involving mechanical testing such as tensile, impact, and flexural tests. Additionally, it encompasses the design and analysis of a composite car Bonnet, considering factors like material selection, geometry, and load conditions, followed by an optimization process utilizing Opti-Struct in Altair Hyper Works software to optimize weight and stacking sequence. validating the optimized composite body against the existing design, ensuring its effectiveness and potential for improvement. Overall, this thesis report provides a holistic exploration of hybrid composite materials for automotive bonnet, encompassing theoretical characterization, experimental validation, design and analysis, and optimization techniques.

1.7. SIGNIFICANCE OF THE RESEARCH

This study of Jute and glass Fiber reinforced Epoxy matrix composite material for automobile body application is expected to develop a composite material with higher strength and stiffness and lower weight. this Indirectly reduces gas (petroleum) consumption of the automobile results increase in

cost and decrease harmful gas emission to the atmosphere. So finally, if this composite material replaces the expensive and heavy metals like steels which is developed for various engineering and structural applications in Automotive industries, aerospace, chemical industry, commercial and military aircrafts industries for window and doors frames, industrial furniture, machine cover & ducts, etc.…a lot of benefit will be achieved.

- Light weight which leads to low fuel consumption
- Getting products with improved strength
- Can be as source of income (business) and Job opportunity can be created.

CHAPTER TWO

2. LITERATURE REVIEW

2.1. BASIC CONSTITUENTS OF COMPOSITE MATERIALS

Composites are a combination of at least two macroscopic components (elements) of matrix and the reinforcement working together to produce material properties that are different their own. i.e. Composite = Reinforcement + Matrix.

2.1.1. Reinforcement

Reinforcer are materials either Fibrous or Particulate whose main functions in composite are (13)

- ✓ To carry the load in a structural composite almost from 70 to 90%.
- ✓ Provides extra Mechanical properties (stiffness, strength) and thermal properties.

All of the different fibers used in composites have different properties and so affect the properties of the composite in different ways. For most of the applications, the fibers need to arrange into some form of sheet, known as a fabric, to make handling possible.

2.1.2. Matrix

The matrix are materials whose main purpose in composite are (13)

- ✓ To surround the fibers protects against Mechanical, chemical & environmental attack
- ✓ To transfers the stress (applied load) to the fibers
- ✓ Keeps the fibers in a desired position, orientation
- ✓ Offers rigidity and shape to the structure
- ✓ Provides a good surface finish quality

For the fibers to carry maximum load, the matrix must have a lower modulus and greater elongation than the reinforcement. Otherwise, the matrix would fail before the load was transferred to the fibers. The resin also reduces the propagation of cracks in the composite. This is because of greater ductility and toughness of the plastic matrix, relative to the fibers. Good bond between the fibers and the resin is required because Weak bonding causes fiber pullout and delamination of the structure.

2.2. CLASSIFICATION OF COMPOSITES

Composite materials can commonly classify based on the following two distinct levels Figure 2:1:

2.2.1. Classification based on matrix constituent : -

1) **Polymer matrix composites (PMCs)**: -are the most commonly applicable and uses a polymer-based resin as the matrix, and some fibers such as carbon, glass and aramid as reinforcement. Can be either Thermoset or Thermoplastic. Thermoset have well bonded and not reversible 3D molecular structure after curing whereas Thermoplastic have 1 or 2D molecular structure that can be reversed to regain its original property during cooling (curing).

2) Metal-matrix composites (MMCs): - typically use SiC fibers embedded in a matrix made from an alloy of aluminum and magnesium, copper, titanium, and iron are increasingly being used.

3) Ceramic-matrix composites (CMCs): - Uses ceramic as the matrix and reinforced by short fibers SiC and boron nitride which uses in lightweight structures.

2.2.2. Classification based on reinforcement

1. Particulate Composites (PCs): - are composed of particles in flakes or powder form distributed in a matrix body. Concrete, Fly Ash and wood particle boards are some examples of this category.

2. **Structural composites (SCs**): - grouped into 2: laminated and sandwiched panel composites. Laminated Composites are composed of layers of materials held together by a matrix.

3. **Fiber Reinforced composites (FRC)**: - are composed of fibers embedded in matrix can be continuous or discontinuous. discontinuous (short) fiber if its composite properties like elastic modulus vary with fiber length but if not is called continuous.

Factors for fiber selection of Fiber Reinforced Composite with a polymer matrix are

- ✓ Mechanical and physical properties.
- ✓ Elongation at failure.
- ✓ Adhesion (bond ability) and wetting for matrix.
- ✓ Availability, price and processing costs.

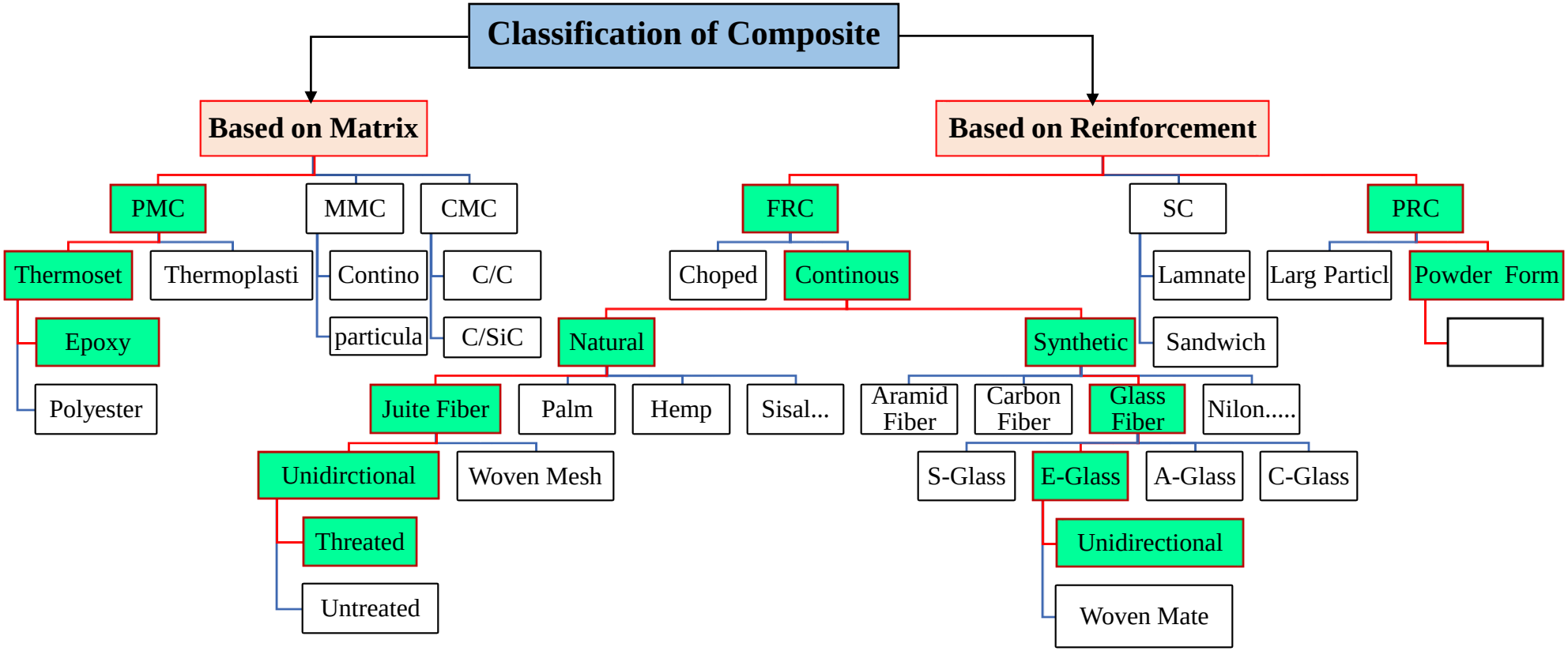

Figure 2:1 Classification of Composite Laminate Diagram (13)

2.3. LAMINATED COMPOSITE AND IT'S FAILURES

Laminates are sheet structures which are made by stacking layer by layers (plies or laminae) in a specified sequence. laminate composite can be in hybrid form made of two or more fibers lamina. The hybrid effect was investigated by Hayashi & defined as the apparent failure strain enhancement of the low elongation fiber (carbon) in a carbon/glass hybrid composite (14).

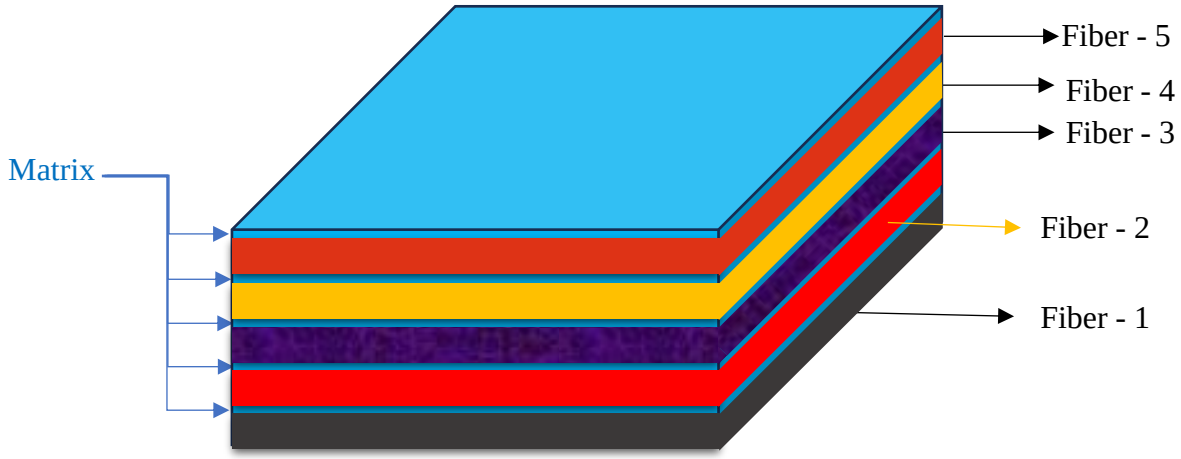

Figure 2:2 Hybrid Fiber Reinforced Laminate Composite

This study focuses on Hybrid composites fabricated from unidirectional fibers of Jute and Glass with particulate reinforcement fiber and Epoxy laminates having different six layers or plies. A laminate will fail under increasing mechanical and thermal loads in any of the six-principal plane until all plies fail. So, these failures can be either from fiber or matrix.

2.3.1. Fiber Failure modes

Fiber can fail under tensile, bending, impact and compressive loading (15). Under tensile loading a number of fiber breaks occur in the vicinity of each other leading to failure initiation. The failure mechanism and strength depend on whether the ply is unidirectional or woven fabric. A unidirectional ply loaded with tensile stress σ_t (along the fiber direction) will fail when the ultimate stress reaches the critical limit. This limit will be the tensile or compressive strength of the fibers in the respective mode of loading.

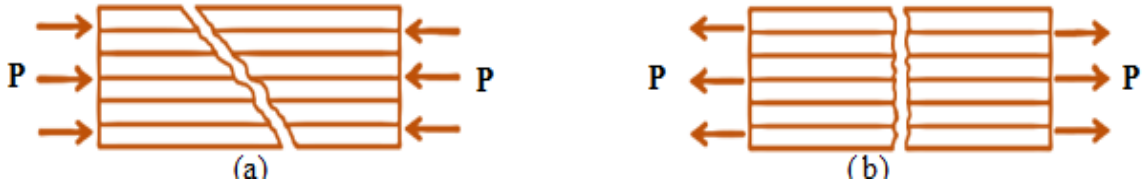

Figure 2:3 Fiber compression failure (a) and Fiber tensile failure (b)

Again, Compressive failure is associated with micro-buckling of fibers within the matrix. A compressive strength of the lamina is not only influenced by the compressive strength of the constituents but also by the elastic stiffness and shear strength of the matrix (16). also, Flexural stresses in the fiber caused due to buckling will result in bend zones that give rise to failure planes.

2.3.2. Matrix Failure Modes

The matrix material can fail in tension, flexural, impact or compression based on the nature of loading in the direction perpendicular to the fibers. For unidirectional composites, transverse tensile failure is very critical in high stress and strain concentrations (17). The fracture plane in transverse tensile loading is perpendicular to the loading direction. In transverse compression, a unidirectional composite may fail due to a crack at an angle to the loading direction (18).

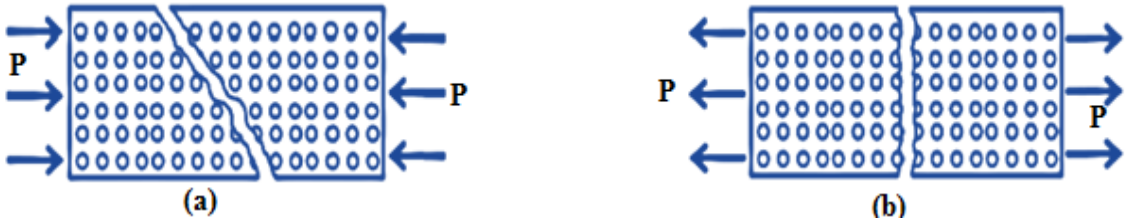

Figure 2:4 Matrix compressive failure (a) and Matrix tensile failure (b)

Matrix has the same Longitudinal and transversal Mechanical property value because of they are isotropic in all direction.

2.3.3. Delamination

Delamination is a through thickness failure form of laminate by which it occurs when fiber pullout from the surrounding matrix. Delamination usually occurs in the interface between plies of different fiber orientations. Interlaminar strength reduces when composite structures are subject to impact and thereby lead to catastrophic failure. Delamination behavior can be Mode I (tensile separation)

and Mode II (shear induced separation) or mixed Mode I/II as shown in fig bellow. Numerous experimental tests and numerical techniques are utilized to characterize and evaluate the extent of interlaminar delamination.

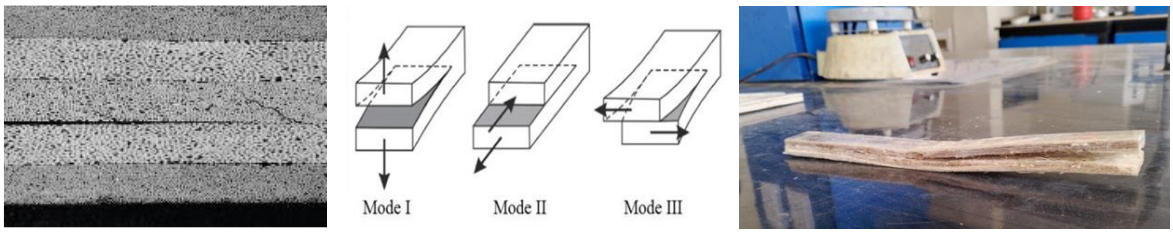

Figure 2:5 Delamination of Laminate and different modes of inter-laminar delamination

The critical energy release rate characterizes the amount of energy necessary for interlaminar fracture in a particular mode. Mode I is characterized by the standardized Double Cantilever Beam test and Mode II energy release rate is determined from the End Notch Flexure test. The energy release rate in both tests is determined from a measured applied load *P*, displacement *δ and* an initial crack length *a* as it propagates under the influence of load. Practically delamination failure is mostly mixed mode (combination) of Mode I and II.

2.4. VEHICLE WEIGHT REDUCTION

Fuel economy can be improved by reducing vehicle weight, by reducing aerodynamic drag and by increasing the thermodynamic efficiency of the engine. Some advanced materials with high specific stiffness and strength properties are adopted into the automotive applications. From the research study (19), every 10% of weight reduced from the average new car or light truck can decrease fuel consumption by 6.9%.

In past years, many technological improvements have been developed in order to increase fuel economy; they are listed in Table 2:1 shows how much potential fuel economy could be obtained.

Table 2:1 Fuel Economy Improvement Potential of Conventional Vehicle Technologies (19).

Technology	Fuel economy improvement potential
2-stroke engines	15% to 20% (compared to 4-stroke engines of similar power output)
4-stroke direct injection stratified charge engines	18% to 23%

Direct-injection diesel engines	25% to 40% (compared to similar displacement gasoline engines)
Continuously variable transmissions (CVTs)	3% to 10%
Lightweight materials: aluminum, composites,	10% to 20% (assuming weight reduction of 30% without compromising safety, comfort, or performance)
Reduced rolling resistance	5% to 8% (assuming 30% reduction in rolling resistance)

Table 2:1 is telling us that fuel economy could increase 10% to 20% if weight reduction is about 30%. weight reduction of vehicle to improve fuel economy could be achieved in three cases.

I. Redesigning the vehicle substructure:

II. Reducing vehicle size:

According to a study (19), weight savings of 9 - 12% could be achieved by changing large vehicle by mid or small size.

III. Lightweight material substitution:

Using Advanced light weight like composite with higher strength could improve fuel economy.

2.5. CAR BONNET AND ITS IMPACT ANALYSIS

Car bonnet (hood) is the hinged cover that protects the engine component of a vehicle. it is designed to provide access to the engine for maintenance while protecting it from external elements.

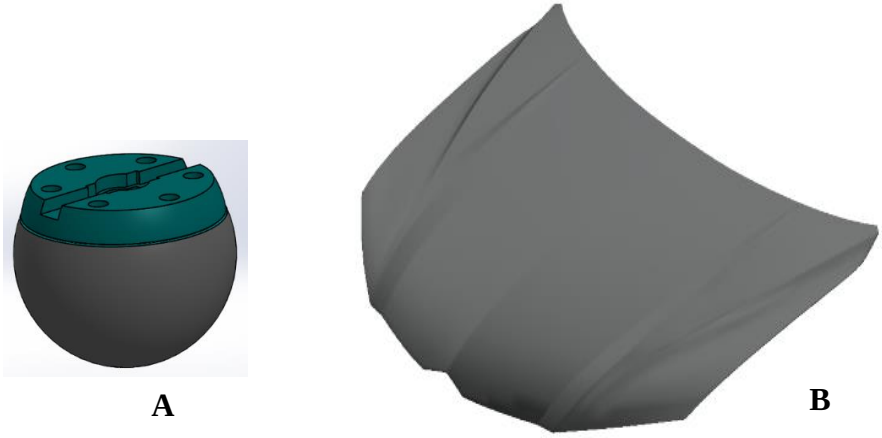

Figure 2:6 Three-Dimensional View of Head Form Impactor (A) and Car Bonnet (B)

2.5.1. Types of car bonnet systems:

Ther are different types of bonnets but among them are listed below.

1. **Conventional Hinged Bonnet:** Most vehicles have a hinged bonnet that opens towards the windshield using hinges at the front of the vehicle.
2. **One-Piece Tilt-up Bonnet**: This type of bonnet opens by tilting up from the front and provides easier access to the engine for maintenance.
3. **Solid Bonnet:** is the most common type made from a single metal (usually aluminum, steel).
4. **Composite Bonnet**: made from materials like glass fiber or carbon fiber known for being lighter. This type bonnet is being dealing with for this thesis work.

2.5.2. Components of car bonnet system:

The car bonnet system includes the bonnet itself, hinges, latches, struts, insulation, and other components that enable the bonnet to open and close smoothly and securely. It is crucial for the proper functioning and safety of a vehicle

1. **Bonnet**: The external panel that covers the engine compartment.
2. **Hinges**: Attached to the vehicle body, these allow the bonnet to pivot open and close.
3. **Struts**: Support the bonnet when it is open to provide easier access to the engine.
4. **Insulation**: Helps reduce engine noise & prevent heat transfer from the engine to the bonnet.

2.5.3. Requirements on the bonnet

The most important requirements of car bonnet are in terms of safety for pedestrians, drivers and engine protections etc. The requirement of this study is to investigate a material provides better properties such as lower weight, density, better mechanical properties to replace the existing conventional bonnet material. The largest category requirements considered are:

- ✓ Pedestrian safety (energy absorption)
- ✓ Passive safety
- ✓ Stiffness requirements

But there are still needed demands to be met fulfilled when a complete bonnet is taken in consideration, are such as:

- Hinges and Latches System Safety
- Corrosion of bonnet and front fenders

- Open/close endurance of bonnet
- Over opening strength of bonnet

I. Pedestrian Safety Test

Euro NCAP is a division working with safety aspect tests of cars in form of pedestrian protection since about 7000 pedestrians per year are killed by traffic accident in the European Union (20). About 14% of all road accidental events in Europe are with pedestrians. Most accidents occur within city areas where the speeds are moderate. In these tests, the potential risk at injuries to pedestrian head, pelvis, upper and lower leg are assessed.

To estimate the potential risk of head injury when a vehicle striking an adult or a child, a series of impact tests is carried out at 40 km/h using an appropriate head-shaped impact mass (4.8 kg). Impact test for pedestrian protection is done as illustrated in figure bellow in three cases:

- The impact of the head-shaped mass onto the vehicle bonnet

To estimate the potential risk of head injury when a vehicle striking an adult or a child, a series of impact tests is carried out at 40 km/h using an adult or child head form impact mass.

- The impact of a leg-shaped mass to the front bonnet

To estimate the potential risk of pelvis and upper leg injuries in the event of a vehicle striking an adult, a series of impact tests is carried out at 40 km/h using an adult upper leg form impact mass.

- The impact of an upper leg-shaped mass to the leading edge of the bonnet.

To estimate the potential risk of leg injuries in the event of a vehicle striking an adult, a series of impact tests is carried out at 40 km/h using an adult leg form impact mass.

Figure 2:7 Head impact (Crash) testing of Car Bonnet at 40 km/h

II. Head-shaped mass

The material which is used to perform testing is called head form. The fatal injuries with respect to pedestrians are originated by the head impact. Hence, the investigation in terms of pedestrian safety is mostly focused on bonnet impact testing. Head form consist of three main parts an outer/skin part

which is made by polyethylene/rubber, an inner (sphere) part and a covered (End Plate) part which are made of aluminum as shown in figure 4. The head form also include an accelerometer to calculate the acceleration during the impact. Parameters such as impact angle and weight of the head form differ from child to adult since this criterion depends on the length and weight of the person. The angle and weight are 65^0 and 4.8 kg respectively for adults while 50^0 and 3.5 kg for children respectively.

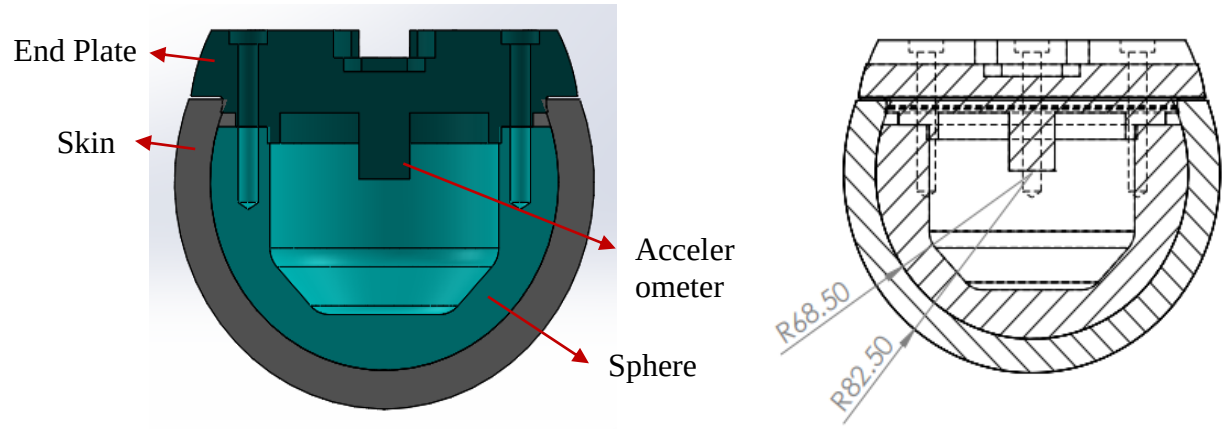

Figure 2:8 Sectional View of head form like impactor

III. Child Head Impact Test on Car Hood (Bonnet)

According to ISO 16850: 2007 and ISO 14513: 2016 A children's (adult's) head form model is used to impact a car bonnet to evaluate the performance of vehicles bonnet against pedestrian safety. car bonnet is assumed to be an Elasto-Plastic material card. the tests are required to achieve the essential improvements in the construction of vehicles, the tests are designed in such a way that they will represent the Real-world accident scenario.

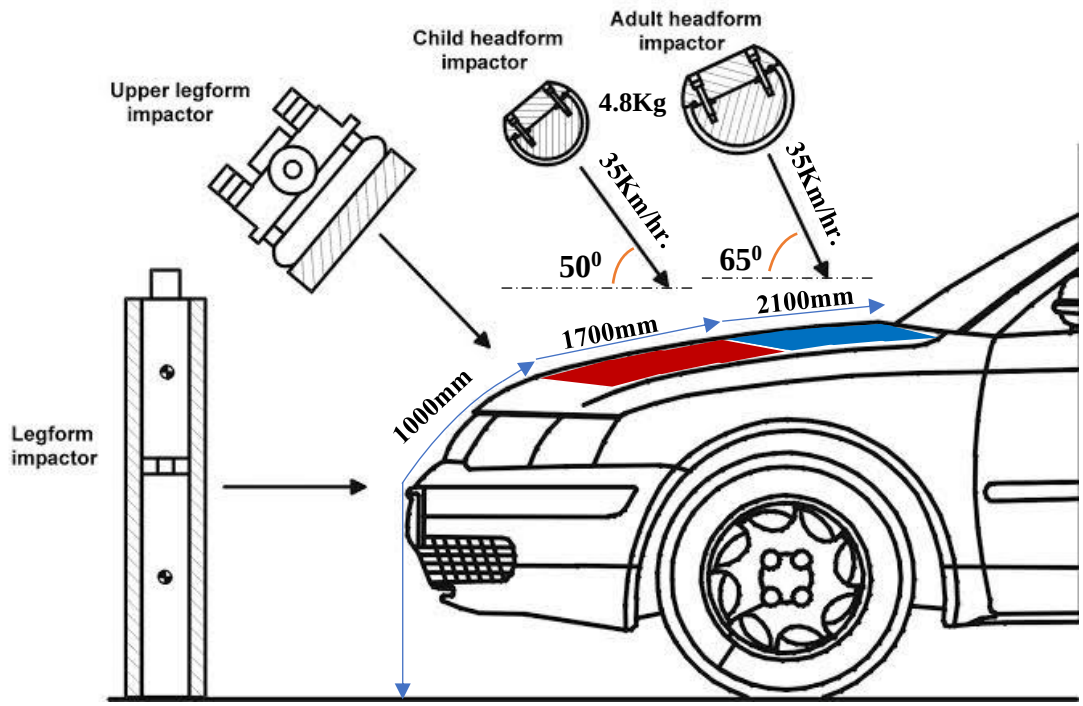

Figure 2:9 Child or Adult Head Form Impact Test of the Car Bonnet

The different impactors used in predicting the performance against pedestrian safety are the lower leg foam and upper leg foam impactors (representative of the adult leg) and the adult and child head foam impactors (representative of the adult head and child's head). Head injury is a more life-threatening and most common cause of pedestrian deaths in pedestrian vehicle collisions. It was decided to focus on these impactors and test procedures as a part of this study.

IV. Wrap Around Distance (WAD):

When a car crashes on the pedestrian, the whole human body wraps around the front shape of the car, and the head impacts on the bonnet or the windscreen. The distance at which the head impacts on the car from the ground is mentioned as Wrap Around Distance (WAD) as shown in fig above. To be specific the WAD is a measurement of the distance from the ground to the head impact zone over the outer surface of the car. during the crash analysis, based on the Wrap Around Distance (WAD), two test areas will be created namely the Child head impact zone and the adult head impact zone. The child head impact zone is between 1000 to 1700 mm WAD and the adult head impact zone ranges between 1700 to 2100 mm WAD respectively shown Figure 2:9 above.

V. Head injury criteria (HIC)

The head foam impactors are used to test the behavior on vehicle structures such as the hood. In a pedestrian-vehicle impact, the kinematics and severity of pedestrian injuries are affected by the impact locations on the vehicle and body velocities after impact. The objective of this project is to analyze the pedestrian kinematics in a Pedestrian-Car accident scenario and determine the Head Injury Criteria (HIC) from the head resultant acceleration, for head impacts on the vehicle hood.

The equation used for the measurements of the head injury of the whole model for the pedestrian head impact was Head Injury Criteria (HIC). It has been used to predict the risk of engine hood to a pedestrian during the collision.

HIC is calculated according to the below Equation

$$HIC = \max_{t_1, t_2} \left\{ \left[\frac{1}{t_2 - t_1} \int_{t_1}^{t_2} a(t)dt \right]^{2.5} (t_2 - t_1) \right\} \quad (2:1)$$

When,

a: the Resultant Acceleration (as a multiple of 10 m/s^2 or about 1 g), **t_1, t_2**: two-time instants (in seconds), which define the start and end of the recording when HIC is at maximum. Values of HIC at the time interval t_1- t_2.

2.6. JUTE FIBER COMPOSITE AND RELATED JOURNALS REVIEW

Jute is multi-celled in structure which is an annual plant that grows 2.5 - 4.5 m long and flourishes in monsoon climates (21). This plant grows and found mainly in southern part of our country. Jute is a lingo-cellulosic fiber because its major chemical constituents are lignin and cellulose. Among different natural fibers, jute fibers are easily obtainable in fiber and fabric forms with good thermal and mechanical properties (22). Many Studies have been shown on enhancing the performance of natural like jute fiber-reinforced polymeric composite materials by characterizing mechanical, physical and chemical properties based on their Fiber surface treatment, fiber Weight or volume ratio, hybridization effect, fiber Angle of orientation, stacking sequence, & filler material addition.

(23) **Ajith Gopinath et al. (2014).** Experimental Investigations on Mechanical Properties of Jute Fiber Reinforced Composites with Epoxy and Polyester Resin Matrices. It discusses impact of fiber treatment on mechanical properties, and comparison between jute-polyester and jute-epoxy composites. The result shows that jute epoxy treated at 5% NaOH gives higher tensile but lower Flexural strength and lower Impact Strength than jute polyester. Again, the study highlights the

significance of fiber-matrix adhesion, fiber dispersion, and orientation in determining the overall strength of the composites.

(24) **Torres, G.B et al. (2023).** The study investigates the incorporation of untreated and alkaline-treated jute fibers into natural rubber for counter sole shoe manufacturing. Alkali treatment improved fiber properties without compromising mechanical performance, with treated fibers showing increased tensile strength and comparable flexibility. 5% NaOH treated Jute Fiber samples exhibited 8% less hardness, 70% more tensile strength, and the same flexibility compared to their pure rubber counterparts. Scanning electron microscopy (SEM) was used to investigate the morphology of the composites in detail as analyzed using the Lorenz-Park equation and confirmed by SEM analysis.

(25) **Hua Wang et al. (2019).** This study investigates the effects of chemical treatments on jute fibers and their subsequent impact on the properties of jute fiber/epoxy composites. Analysis of mechanical properties, surface morphology, and FTIR spectra reveals improved interfacial adhesion and reduced void formation in composites with treated fibers. SEM images of fractured coupons demonstrate the enhanced performance of composites with chemically modified jute fibers, highlighting the importance of chemical treatment in optimizing the mechanical properties of jute fiber composites.

(26) **Anna Dilfi K.F et al. (2018)** The study explores the impact of surface modifications on jute fiber-reinforced epoxy composites, focusing on alkali, silane, and combined treatments. Via SEM analysis, it assesses the surface topography of treated and untreated fibers. Mechanical and thermomechanical properties of composites were compared, highlighting improved performance with combined modification due to enhanced interfacial adhesion. The chemically treated fibers showed lower water absorption rates, but exposure to moisture led to reduced properties, potentially due to fiber degradation.

(27) **S.H. Mahmud a et al. (2023).** It studies the mechanical properties (tensile, bending and impact strength), water absorption properties and ϒ-irradiation effect of jute/polyester and glass/polyester composites material. Result revealed that tensile strength, bending strength, tensile modulus, bending modulus, and impact strength increased by approximately 14, 28, 20, 21, and 13%, respectively, for the case of jute/polyester composites while glass/polyester composites demonstrated 13, 27, 15, 14, and 22% increase of the values, respectively. It concludes that hybridizing synthetic and natural fibers enhance strength and reduce costs.

(28) **Dabade et al (2013):** used polyester matrix to study the effect of fiber weight ratio and fiber length of palmyra fiber on the tensile properties. It was observed that the tensile properties of palmyra fiber showed improvement up to a fiber length of 50mm and thereafter the tensile property degraded gradually stating an optimum fiber length for maximum tensile strength. Further, the tensile properties showed improvement up to a fiber weight ratio of 55% and then decreased with further increase in the fiber weight ratio.

(29) **Amit Bindal et al. (2013).** Studies mechanical property characterization on hybrid of Jute and Glass fiber reinforced polyester composite material based on different weight ratios. Experimental results revealed that hybridization of composite with natural and synthetic fibers shows enhanced tensile strength, flexural strength, and impact strength. The content of natural reinforcement was found to be in the range of 25–33.3% for best results. The effect of treated jute on flexural properties was more than tensile properties, which was due to greater stiffness of jute fibers. Chemical treatment of jute fibers lowers the water absorption and results were comparable to glass fiber reinforced polyester composites. addition of jute also reduced the overall cost by 22.18%.

(30) **Md. Zahidul Islam et al. (2023).** Studies on mechanical property characterization of hybrid jute/hemp reinforced polyester composite material 30%, 50%, and 70% by volume and at 3% and 5% NaOH alkali treatment. From result shown the composite materials that underwent testing with a 50 vol% fiber loading and 3% NaOH exhibited the maximum tensile strength (26.6 MPa), tensile modulus (733.56 MPa), flexural strength (62.7 MPa).

(31) **M. R. Hassan et al. (2016).** The study investigates a hybrid composite material combining hessian cloth (natural fiber) and glass fiber (synthetic fiber) in a polyester matrix using a hand lay-up process. Results indicate promising tensile strength, flexural strength, and hardness in the natural-synthetic fiber hybrid composites. The composite with three layers of glass fibers and two layers of hessian cloth demonstrated the highest tensile and flexural strengths at 104.63 MPa and 134.65 MPa, respectively. Higher hessian cloth content led to increased water absorption, while higher glass fiber content resulted in greater hardness at 39.9 HV.

(32) **M. Muthuvel et al. (2013).** The study explores hybrid glass/natural fiber composites for aerospace and naval applications, focusing on mechanical properties like tensile, impact, and flexural strength. Hybrid design of woven glass and jute fiber mats led to a 20% cost reduction and

23% weight saving compared to commercial solutions. Laminates, including varying glass layers, were fabricated for testing, maintaining a total fiber weight ratio of 42% following ASTM.

(33) **M. R. Sanjay** and **B. Yogesha (2016).** Studies on the hybridization effect of jute/E-Glass fibers reinforced Epoxy composite material on mechanical properties. The result of the test shows that hybrid composite of jute/ E-glass fiber has far better tensile, flexural, impact, and inter laminar shear strength properties than that of jute fiber composite. But it is found that hybrid composite has better strength as compared to jute fiber composite fabricated separately with glass fiber.

(34) **Muhammad Usman Ghani et al. (2022).** Study the effect of stacking sequence on PBS-based Glass-Jute hybrid composites on their Mechanical properties, electron microscopic images and moisture absorption properties at ambient temperature. The TGA test was conducted to study their thermal properties. experimental results showed that the stacking sequence of the fiber layers has a significant effect on the overall performance of GJ hybrid composites. glass fiber layers on their outer surfaces showed optimum mechanical, thermal, and water resistance properties.

(35) **A Murdani, and U S Amrullah (2021)**. Studies the effect of fiber stacking sequence on flexural behavior of Jute, glass, and carbon fibers reinforcement polyester composite material. The composites were fabricated using vacuum bagging method cured at room temperature. The combinations of fiber as the reinforcement are configured by arrange two and three types of fiber. As a natural fiber, jute exists in all kind of combination. The result shows that stacking sequence of the fibers give significant different flexural behavior regardless the effect of the fiber strength.

(36) **Thaís da Costa Dias et al. (2022).** Study the effect of hybridization and stacking sequence on the mechanical and physical properties of the glass/jute fiber reinforced polyester composite laminates. The composites were characterized via C-scan analysis, density, volume fraction of constituents and optical microscopy analyses. Result shows that the longitudinal properties were higher than transverse properties for all laminates. The hybrids presented intermediate density and mechanical properties compared to pure glass and pure jute laminates. In addition, the pure glass and the hybrid laminates displayed acceptable failure morphology in the in-plane shear test, but not the pure jute laminate.

(37) **Mahammad Sharif B (2016)**. Investigates experimentally the impact of jute and carbon fiber reinforced Epoxy bio-composite material on the tensile properties of the composites at different

temperatures. Result shows that For FGE series at temperatures from 0 to 50°Cthe tensile strength is seems to be stable, which indicates the mechanical behavior of GFRP composites remains almost same this temperature range and after this range as temperature decreases tensile strength increases. Again, at high temperatures above 100°C flexural strength reduces due to the change of state in the polymer.

A lot of composite laminates due to impact were studied theoretically and experimentally. The damage modes mostly found were delamination, matrix cracking & plastic indentation. The authors showed that the damage area for low velocity impact is increased as the impact energies increase, & through the impact duration the stiffness will decrease.

(38) **Choi and Hong:** used finite element method for their analysis with modified Hertzian contact law to evaluate the impact load history, deflection, dynamic strain and compared favorably with the experimental tests. They considered higher order shear deformation & large deflection effects.

(39) **Ubels et.al:** studied the impact damage of stiffened composite plate experimentally and showed that with increasing impact load the transferred shear and delaminated sub laminates became the ultimate failure mechanism.

Again, many scholars have done a lot of research on structural optimization design. Professor Gao Yunkai uses DMTO method to optimize the thickness and layup direction of CFRP automobile bonnet simultaneously, which reduce the weight of automobile bonnet by 51.1% (40). Ahad Torkestani studies the influence of different materials (aluminum, steel, carbon fiber epoxy resin, glass fiber epoxy resin) on head injury criterion (HIC). By optimizing the composite stacking sequence, the HIC and the weight of automobile bonnet are reduced by 42.6% and 46.8% respectively (41). Chen Lina of Hunan University adopts multi-objective topological optimization design to deal with the design margin of the automobile bonnet.

The thickness of the components of the automobile bonnet is the variable, and the mass, modal and head damage are the response values. An agent model is established to obtain the optimal plate thickness combination (42). Lee et al. study the hierarchy optimization of composite materials. The hierarchy optimization of composite materials has been carried out by using different optimization techniques such as size optimization, shape optimization and topology optimization (43). Sha Yundong et al, optimizes the laying scheme of composite axial structure to improve its bearing capacity and critical buckling load (44). Ding Ling adopts step-by-step optimization method to carry out optimization of laminate design on the full composite structure of unmanned aerial vehicle wing,

so that the strength coefficient of wing composite structure increased to 0.98 from 1.45 after optimization, the maximum deformation of wing decreased to 179.918 mm from 145.894 mm after optimization, and the buckling load coefficient increased to 1.087 from 1.863 after optimization. The stress distribution of the wing is more uniform and the utilization rate of the composite is improved (45). As an important structural part of the autobody, the automobile bonnet has high requirements on stiffness, vibration and strength. Therefore, the optimization design of the automobile bonnet has always been the focus of the autobody lightweight.

2.7. The Research Gap in Earlier findings

The extensive literature survey presented above reveals the following knowledge gap in the research reported so far:

1. The jute fiber-based products has many low-end applications such as in housing, packing, furniture and transportation, but its potential use in tribological application where synthetic fibers are widely used is less.
2. Although a numerous research efforts have been devoted to the short and woven jute fiber-based polymer composites, however the study on unidirectional nonwoven jute fiber composites is less.
3. Optimization process is also limited for most studies shown on the literature above.
4. Thermal analysis of the composite car bonnet is limited.

CHAPTER THREE

3. MATERIAL AND METHODOLOGY

3.1. MATERIALS

Proper material selection is one and the most critical tasks for proper mechanical design. The material used for this thesis work with their mechanical and Physical property are listed as follow.

3.1.1. Jute Fiber

Jute is a bast fiber whose scientific name is Corchorus capsularis of Tiliaceae family. Plant of jute takes nearly 3 months to grow to a height of 12 - 15 feet (21). Jute plant is cut and kept immersed in the water for Retting process during season to get long and pure Jute Fiber. Jute fiber is lower in weight higher specific strength & stiffness, low cost, low density, nonabrasive, and biodegradable.

Figure 3:1 Jute Tree in Southern Part of Ethiopia in Sidamo

A) Physical Properties of Jute Fiber:

Density, fiber length, diameter, aspect ratio (length/diameter), cost, and availability of the natural fibers are important to determine their compatibility in natural fiber reinforced polymer composites (46). Jute fiber has lower density as compared with other natural fibers which is 1.2g/cm^3 (47). Table 3:1 below shows some Physical and Chemical Properties of Jute fiber.

Table 3:1: Physical and Mechanical property of Some Natural & Synthetic Fibers (48) (49)

Type of fiber	Density (g/cm^3)	Tensile strength (MPa)	Elongation (%)	Elastic modulus (GPa)
Kenaf	0.6–1.5	223–1191	1.6–4.3	11–60
Sisal	1.3-1.5	400-700	1.4-2.1	9-55

Flax	1.3-1.6	340-1600	1.9-12	8.5–40
Hemp	1.1-1.6	285–1735	0.8–4	14.4–70
Banana	0.5–1.5	711–789	2.4–3.5	4–32.7
Jute	**1.3–1.5**	**385-850**	**1.1–3.3**	**25-81**
Cotton	1.5–1.6	200–800	2.1–12	5.5–15.1
Bamboo	1.2–1.5	500–575	1.9–3.2	27–40
Coir	1.15–1.6	131–593	14–40	3–7
Pineapple	1.56	150–1627	2.4	11-82
E-Glass	2.5–2.55	2000–3500	0.5–3	70–73
S-Glass	2.5	4570	2.8	86
Carbon	1.4–1.78	3400–4800	1.4–1.8	230–425

Figure 3:2 Extracted Fiber and Unidirectional Mat of Jute Fiber

3.1.2. Glass Fiber

Unidirectional E- type glass fiber relatively having High strength, low density, low cost, available, Resistant to heat & Good chemical resistant (50).So for this project Unidirectional E- glass type is selected because of the above advantages.

Figure 3:3 Unidirectional E-type Glass Fiber mat

Table 3:2 Physical Properties of Unidirectional E –type glass fiber (50)

Fiber Physical Properties	Values
Density (g/cm3)	2.54
Diameter (μm)	3-20
Tensile Strength (Mpa)	3400
Young's Modulus (Gpa)	72
Elongation (%)	4.7
Relative Cost	low

3.1.3. The Matrix

A. Epoxy Resin

Epoxies are thermoset polymers known for their excellent adhesive properties, high tensile and compressive strength, chemical and thermal stability, excellent heat resistance. Epoxies are widely applicable in automotive, aerospace, and construction industry. They are widely employed as adhesives, coatings, and sealants. They are very effective at bonding unlike materials (metals, woods, stone, plastics, etc.) and acting as gap-filling agents to enable bonding between poorly conforming surfaces. Glycidyl epoxy is selected for this work because this resin is widely used in the manufacturing of coatings, composite materials and electronics and is known for its excellent mechanical properties. According to ASTM D1652, C613 & ASTM D3418 the Proportion and Properties of Epoxy resin is represented in table given below

Figure 3:4 Epoxy resin with its Hardener

Table 3:3 Physical and mechanical properties of epoxy resins (51) (52).

Properties	Value
Appearance	Color less
Flexural strength (MPa)	40–67
Density (g/m^3)	1.2–1.3
Viscosity at 25 ◦C (kg/m s)	0.25–0.75
Heat distortion temperature (◦C)	50
Modulus of elasticity (MPa)	3100 to 3800
Tensile strength (MPa)	90 to 120
Max percentage elongation (%)	4
Impact strength (kg/m2)	9

B. Hardener

The hardener is a highly viscous liquid that is mixed with resin in appropriate ratio during the composite preparation process. Amines are the most commonly used curing agents for epoxy cure. Primary and secondary amines are highly reactive with epoxy. The catalytic activity of the catalysts affects the physical properties of the final cured polymer. It aids in the solidification and hardening of the wet, smooth composite by initiating a chemical reaction without altering its own composition with the resin. The ratio of Epoxy to hardener used for this project is 2:1 according to ASTM D1652, ASTM D3418 and as recommended in various sources (51).

Table 3:4 Physical & Chemical Properties of the Hardener (52).

Parameter	Value
Melting point	40-80°C
Boiling Point	200-300°C
Density at (20ºC)	0.9-1.2 g/cm³
Viscosity at (20ºC)	20 Mpa

3.1.4. Tools, machines and other necessary stuffs

The main tools which used for the project are Oven, manual stirrer, electronic balance, Roller, cutter, wood plate, ruler, press load, cups, stirrer, Testing machine etc.

A. Electronic Balance: Uses for weighting Resin & Fibers to ensure their precise measurement.

B. Release wax: It uses in laminate to stop bonding of the molding material with the mold.

✓ ELECTRONIC BALANCE	✓ CUTTER
✓ Release wax	✓ Cleaner
✓ Hammer	✓ Brush
✓ Gloves	✓ Caliper
✓ Roller	✓ Scissor
✓ Cloth	✓ Meter etc.…

Figure 3:5 Some Tools, Machines and necessary stuffs using for composite production

3.2. METHODOLOGY

3.2.1. Materials Preparation

A) **Jute Fiber**: - Jute fiber was extracted manually and through Chemical extraction. To enhance Adhesion (bond ability) between the cellulosic Jute fiber and the polymer matrix, it was treated with a 5% NaOH solution (400 ml in water) at 50°C for one day, followed by washing with cold water and applying force to extract the fibers (53).

B) **Glass Fiber: -** The fiber glass which was bought from ANA Fiber Plc at cost of 140birr/kg was cut at proper size based on the mold dimensions (size) for sample production.

C) **Matrix: -** The Epoxy resin was bought from Addis Abeba resin supplier at a cost of 600 birr/liter, was mixed with the hardener at the proper ratio of 2:1.

3.2.2. Mold Preparation

It is a rectangular shaped frame made up of either wood, sheet metal or plastic sheet used for preparation of specimen. its approximate Size is 300x200 x4mm and consists of three parts called,

1. Rectangular side plate (frames): it is supporting part cutting up by the size and thickness of specimen uses to maintain proper sample shape and size as needed without wasting of the resin.

2. Cavity: is the central & essential part of mold working area of specimen size with its allowance.

3. Base plate: is thick plate at the bottom to withstand the pressing load & resin from wasting.

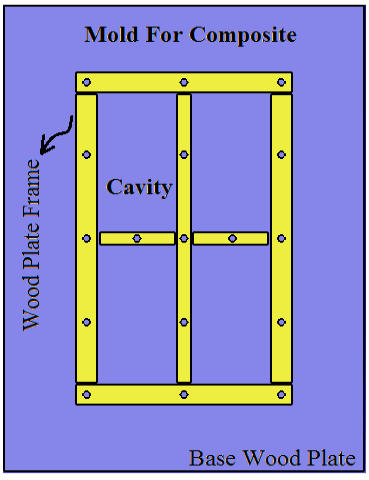

Figure 3:6 Wood Plate Composite Mold

3.2.3. Compositions of the Composite Material

In the design, manufacturing, and assessment of composite materials, it is essential to ascertain the proportions of ingredients, like ratio of fibers to matrix, present. This is used for several reasons:

- To prepare and estimate the size of the composite laminate
- To get better laminate mechanical property by varying these values.
- To minimize wastage of composite constituents

The overall Properties of composite material is computed from the property value of each constituent within the hybrid, multiplied by its corresponding weight or volume fraction in the mixture.

$$P_I = P_1V_1 + P_2V_2 \quad (3:1)$$

when, P_I = property of Composite to be investigated

P_1 & P_2 = property of first and second system respectively

V_1 & V_2 = Volume Fraction of first and second system respectively

Therefore, to go through the rule-of-mixtures here are the steps to be followed.

Step-1: Weight & Weight Fraction (Ratio) of Fiber to Matrix

Depending on the pressing load available on the laboratory it is possible to estimate the amount of fiber to resin in percent. the composite sample is assumed to contains 6 hybrid plies either Jute fiber or Glass Fiber mat with an approximate average thickness (0.4mm) and average weight of single ply measured using digital caliper and electronic balance respectively (54).

$$Wc = W_f + W_m \quad (3:2)$$

Where Wc is total weight of composite, W_F weight of fiber &W_m weight of matrix.

Again, to calculate weight fraction of fiber W_{ff} & weight fraction of matrix W_{fm}

$$W_{ff} = \frac{W_f}{W_c} = \frac{W_f}{W_f+W_m} \quad (3:3)$$

$$W_{fm} = \frac{W_m}{W_c} = \frac{W_m}{W_f+W_m} \quad (3:4)$$

But $W_{fm} + W_{ff} = 1$

Step-2: Volume & Volume fraction of Fiber and matrix (V_{Fiber}, V_{Matrix})

Even though determination of volume and Volume fraction of fiber and matrix is not such quite simple like weight ratio it can be calculated using the following formula

$$V_c = V_f + V_m = \frac{W_f}{\rho_f} + \frac{W_m}{\rho_m} \quad (3:5)$$

The total composite volume fraction (V_{cf}) must be unique i.e. $V_{cf} = V_{ff} + V_{mf} = 1$

So, the volume fraction of fiber and volume fraction of matrix can be described as

$$V_{ff} = \frac{W_f * \rho_m}{W_f * \rho_m + W_m * \rho_f} \quad (3:6)$$

$$V_{mf} = \frac{W_m * \rho_f}{W_m * \rho_f + W_f * \rho_m} \quad (3:7)$$

Where: Vc = total volume of composite, V_f , V_m = fiber & matrix volume, ρ_f, ρ_m = fiber & matrix density, V_{Ff}, V_{mf} = fiber & matrix volume fraction.

Table 3:5 Typical Fiber Volume Fraction Ranges Composite material (55)

Reinforcement	Range of Fiber Volume Fraction (%)
Unidirectional	**50-70**
Non-Crimp	45-65
Woven, braided	35-55
Random mat	10-30

Step-3: Theoretical Density of the composite

When the fibers and matrix of a composite material are synthetic, their density can be provided by the manufacturer. However, if they are natural, their density must be determined experimentally or obtained from existing literature. For instance, the density of Epoxy resin has been reported as 1.25g/cm^3 in some journal (56). With this information, the theoretical density of the composite in relation to weight fraction can be calculated using the following equations.

$$\rho_c = \frac{W_c}{V_c} = \frac{W_f + W_m + W_p}{V_c} = \frac{1}{\frac{W_{ff}}{\rho_f} + \frac{W_{fm}}{\rho_m} + \frac{W_{fp}}{\rho_p}} \quad (3:8)$$

Where ρ_c is total density of composite, $W_c = W_f + W_m, + W_p$ and $V_c = V_f + V_m + V_p$

Table 3:6 Weight and Weight Fraction of Fiber and Matrix of Hybrid Composite

Samples	**Symbol**	**Weight of Fibers (g)**	**Total Wt. of Matrix (g)**	**Epoxy Wt. (g)**	**Hardner Wt. (g)**	**Total wt. of Composite (g)**	**Jute W_f (%)**	**Glass W_f (%)**
S_1	JJJJJJ	137.2	108.32	72.21	36.11	245.52	55%	-
S_2	JGJJGJ	141.9	106.54	71.03	35.51	248.44	36.7%	18.3%

S_3	JGJGJG	145.4	104.56	69.71	34.85	249.96	27.5%	27.5%

Table 3:7 Volume and Volume Fraction of Fiber and Matrix of Hybrid Composite

Samples	**Fiber W_{FF} (%)**	**Matrix W_{FM} (%)**	**Volume of Fiber V_F**	**Volume of Matrix V_M**	**V_{FF} (%)**	**V_{FM} (%)**	**ρ_c**
S_1	55%	0.45	107.67	89.07	0.55	0.45	1.26
S_2	55%	0.45	113.46	89.07	0.56	0.44	1.32
S_3	55%	0.45	103.66	89.07	0.54	0.46	1.38

Step-4: Ply thickness:

The thickness of plies can be simply calculated from the Volume of the plies. But volume is number of grams of mass of fibers (Kg) per density (Kg/m^3) of the fibers.

Total volume (V_T) = l x b x t = $\Leftrightarrow t = \frac{V_T}{lxb}$ again $V_T = \frac{W_f}{\rho_f}$

$$t = \frac{W_f}{l*b*\rho_f}$$

In terms of mass of fraction of fibers, the thickness can be expressed as

$$t = W_f \frac{1}{l*b}\left[\frac{1}{\rho_f} + \frac{1}{\rho_m}\left(\frac{1-W_f}{W_f}\right)\right] \quad (3:9)$$

3.2.4. Sample Preparation of Composite for mechanical Testing

A) Hand Layup Method:

The hand lay-up technique is a straightforward and cost-effective method primarily used for processing thermosetting polymer-based composites. Safety precautions, such as wearing gloves and eye protection, are crucial due to the acidic and toxic nature of the chemical hardener, which includes anhydrides (acids), amines, polyamides and dicyandiamide posing potential risks to the eyes and skin. To prevent the polymer from adhering to the mold, a release gel is applied to the mold surface. Thin plastic sheets, approximately 0.1 mm thick, are placed on the top and bottom of the mold plate to ensure a smooth surface finish for the final product.

The process involves cutting unidirectional Jute and glass fibers to fit the mold size and weighing them. The liquid thermoset polymer Epoxy is gently mixed with the hardener (curing agent) in a glass mixing cup to prevent melting during the exothermic reaction. The resulting mixture is poured onto the mat already positioned in the mold and evenly spread using a roller. Subsequent layers of mat are added, and excess air and polymer are removed by applying slight pressure with a roller. This layering process is repeated until the desired laminate layers are achieved. Once the layers are stacked, a covering plastic sheet is placed, and gel is sprayed on the inner surface of the top mold plate. The mold is then closed, and a load of approximately 200N is applied and left for 24-48 hours, depending on the specific polymers and hardener ratio. After curing at room temperature or a specified temperature, the mold is opened, and the composite sample is removed and further processed or cut into the required specimen size according to ASTM standards.

The hand lay-up method requires readily available tools and involves minimal infrastructure investment compared to other methods. It is commonly used in the production of aircraft components, automotive bodies, boat hulls, dashboards, decks, kitchen and office goods, among others. It is essential to ensure the uniform distribution of the matrix throughout the fibers and a strong bond between the fibers and matrix when producing laminate samples.

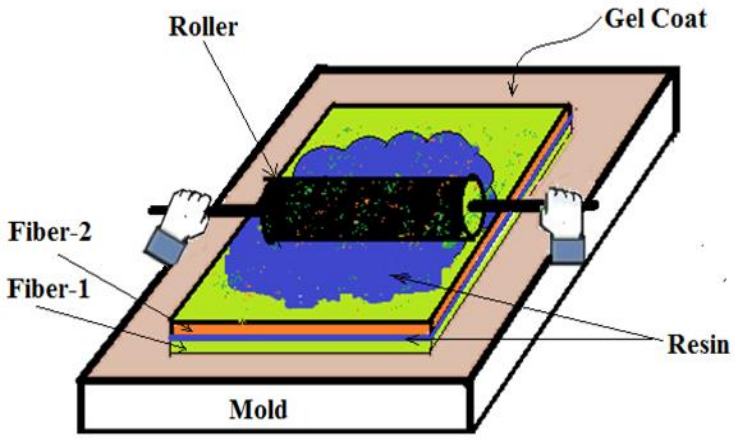

Figure 3:7 Hand layup method of Sample Preparation

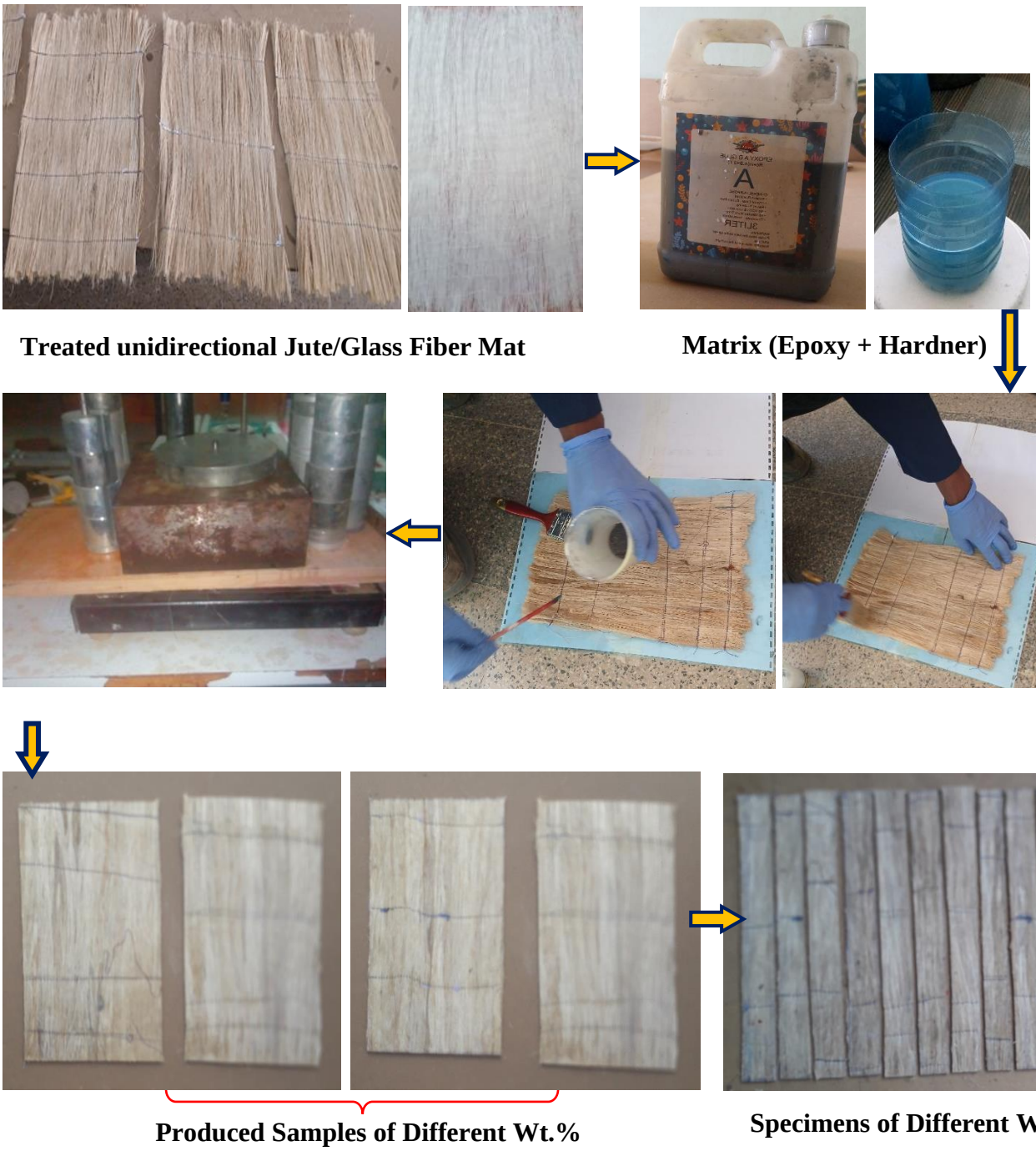

Figure 3:8 Composite Laminate Sample Preparation process

B) Specimen Preparation

Specimen is a small piece with its Appropriate dimension taken from sample produced for test to know mechanical properties like Tensile test, Compression test, Flexural test, Impact test and Water absorption test according to ASTM and taking three per each weight ratio to estimate average value.

3.3. MECHANICAL PROPERTY CHARACTERIZATION OF THE COMPOSITE

The mechanical properties of any polymer composites depend on various factors such as

- Physical & Chemical properties of fiber
- Volume (Weight) fraction of Fiber
- Inter bonding between matrix and fibers
- Orientation and geometry of fibers

Generally, the mechanical properties of Uniformly oriented long fiber reinforced polymer such as tensile, compression, Impact and flexural strength increased with increase in weight fraction of fiber.

3.3.1. Tensile Test of Specimen

Tensile testing in composite according to ASTM D3039-76 (57) is used to measure the longitudinal force required to break a polymer composite specimen and the extent to which the specimen stretches or elongates to that breaking point using Universal Testing Machine. Tensile tests produce a stress-strain diagram, which is used to determine tensile modulus.

A) Specimen size: The most common specimen size for ASTM D3039 is a constant rectangular cross section, 250 mm long 20 mm wide, and 4mm thickness.

B) Test procedure: Specimens were placed in the grips of a Universal Test Machine at a specified grip separation and pulled until failure a speed of 5mm/min according to the machine specification. finally, the results were recorded on the computer attached to the machine installed in our campus @ civil department.

Figure 3:9 Universal Testing Machine and Specimen before Test

The tensile strength, percentage elongation and tensile modulus of composite material were calculated using equations below.

$$\text{Tensile strength} = \frac{\text{load at break}}{\text{width}} \times \text{thickness}$$

$$\%\ \text{elongation} = \frac{\text{elongation at rupture}}{\text{initial gauge length}}$$

The slope of the curve defines Modulus of Elasticity. The modulus of elasticity (Young's Modulus) is the ratio of stress in Mpa to strain in millimeters per millimeter (mm./mm.)

$\text{Modulus (Mpa)} = \frac{\Delta\text{Stress(Mpa)}}{\Delta\text{Strain(mm/mm)}}$, To find the modulus by taking any two points on the modulus line, & divide the differential between their stress values in Mpa to the strain differential in mm/mm.

3.3.2. Impact Test of the Specimen using ASTM D1822:

Impact test (58) is impact resistance of material which measures the amount of force needed to break a specimen under a high-speed load introduced through a swinging pendulum.

A) Specimen Size: The Charpy impact test was carried out for the sample's specimens with dimensions of 100mm x 20mm x 4mm as shown in Figure 3:10 bellow.

B) Test Procedure After fixing of specimen pendulum is released and allowed to strike until failure occurs. The machine pendulum energy engaged for the testing was 2 Joule with a speed of 2 m/s & having 25-kg weight mounted in material testing laboratory in our campus.

Finally, the Impact energy measured in joule was recorded from the apparatus.

Figure 3:10 Impact Testing Machine and Specimen before test

3.3.3. Flexural Test of Specimen based on ASTM D7264

According to ASTM D7264 (59) Flexural test of composite measures the force required to bend

using rectangular cross section bar supported on a beam. for this test 3-point loading was applied.

A) Specimen size: Standard specimen thickness is 4 mm, width is 20 mm and length is 20% longer than the support span (rectangular cross section of (150x20x4) mm^3). If the standard specimen is not available, alternative specimen sizes may be used.

B) Test procedure: First of all, set or arrange the 2 bending beams or bar on their proper place for three-point loading system. then specimen lies on a support span and the load is applied to the center using loading nose until fail at a specified rate. data is displayed on the computer.

I. The flexural stress in a three-point bending test is found out using the following formula

$$\sigma = \frac{3PL}{2bt^2} \quad (3:10)$$

When: σ = stress

p = Applied Force

t = thickness

II. The flexural chord modulus of elasticity is the ratio (slope) of stress range and corresponding strain Range and calculated using the following formula

$$E_f = \frac{\Delta\sigma}{\Delta\varepsilon} \quad (3:11)$$

Where: E = flexural chord modulus of elasticity (MPa)

$\Delta\sigma$ =difference in flexural stress between the two selected strain points (MPa)

$\Delta\varepsilon$ = difference between the two selected strain point

III. The data documented from the 3-point bend test above can be used to determine the inter-laminar shear strength (SS) using Equation below,

$$SS = \frac{3P}{4bt} \quad (3:12)$$

Figure 3:11 Flexural Testing machine and Specimen before testing

3.3.4. Compression Teste of Composites specimen using ASTM D 3410M

According to ASTM D 3410M (60) Compression strength test experiment involved in subjecting specimen to axial compression loading using the UTM. The dimensional size of the specimen is (100x20x4) mm. The samples were then placed between the compression anvils to commence compression testing During testing, the maximum load attained was recorded by the UTM testing system after the specimen failed. Laminate Compressive Strength (σ_c) is Calculated using the following equation.

$$\sigma_c = \frac{F_c}{A} = \frac{F_c}{tw} \quad (3:13)$$

when: σ_c = Compressive Strength

F_c = Compressive Load

w = width

t = thickness

Figure 3:12 Compression testing machine and Specimen before test

3.3.5. Water Absorption Test of the specimen According to ASTM D 570

Water absorption characteristic is another important and mandatory property for natural fiber composites since they are applied in automotive, aerospace and marine applications. Moisture Absorption of Composites is a gravimetric test method that change of moisture content by measuring the total mass over time when exposed to a specified environment.

A) Specimen size: The specimen has a dimension of (60 x 30 x 4) mm^3 shown in Figure 3:13

B) Test Procedure**:** First of all, the specimens must have dried via sun for at least 2days and then allowed to cool until they reached room temperature. The dried spacemen weighed before and after immersed using balance electro mass testing machine having a precession of 0.001 (g). This procedure is repeated until there is no discernable increase in specimen weight for each sample containing different weight fractions.

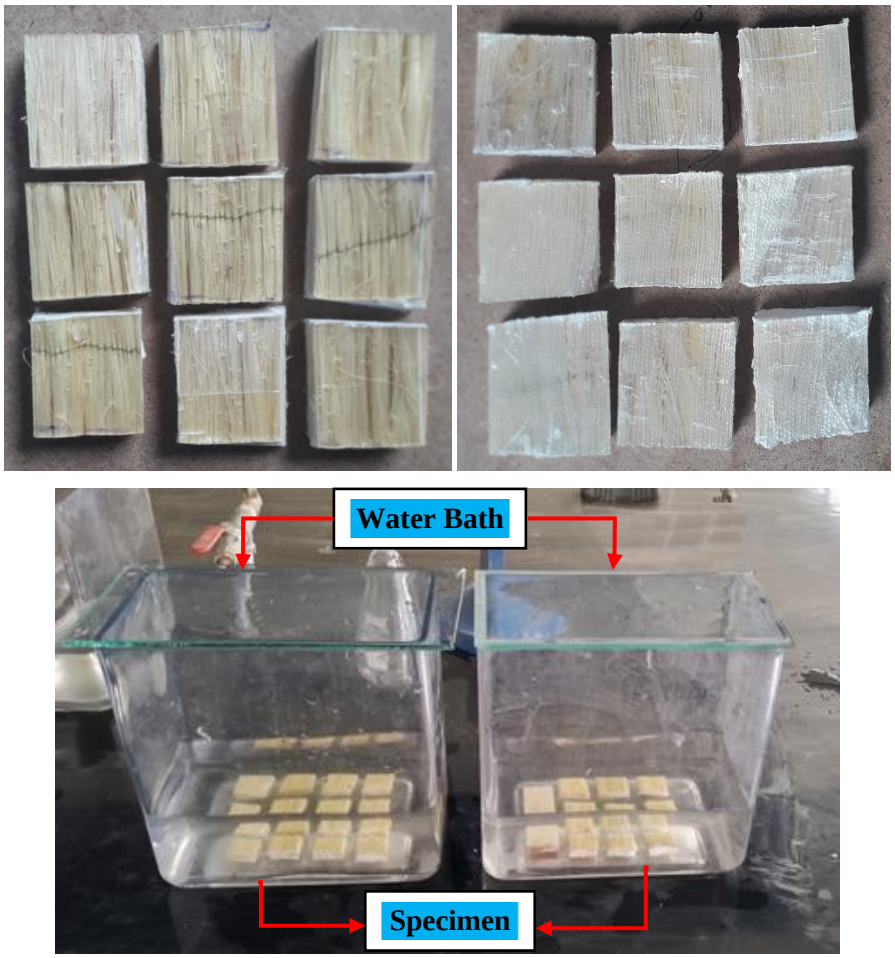

Figure 3:13 Specimen for Water Absorption Test of Different Weight Ratio

C) Immersion Time: It is a time recorded at which the composite's specimen is soaked deep in to distilled water which can be 72 hrs. The specimen removed from the water must wiped off with a dry cloth and weighed.

$$\% \text{ water absorption} = \frac{W_f - W_i}{W_i} \times 100 \qquad (3:14)$$

When W_i is initial weight and W_f is final weight of the sample after immersion.

3.3.6. Determination of density based on ASTM standards D792,

According to (61) Density of composite laminate sample can be determined experimentally using Archimedes method with distilled water whose specific mass is known (0.998 g/cm^3). dimension of the sample is 60 x 20 mm^2. the apparatus used to determine density of Laminated composite are:

A. Analytical Balance: to measure sample's weights having precision of 0.0001g.
B. Sample Holder: a wire to hold the sample when immersing into the water
C. Immersion Vessel: A beaker for holding the water and immersed specimen.
D. Thermometer: A thermometer used to measure the water temperature.

A) Test Procedure: According to Archimedes principle when an object is immersed in a liquid the apparent loss in its weight is equal to the up push and this is equal to the weight of the liquid displaced. Steps to calculate the arithmetic average of the density are.

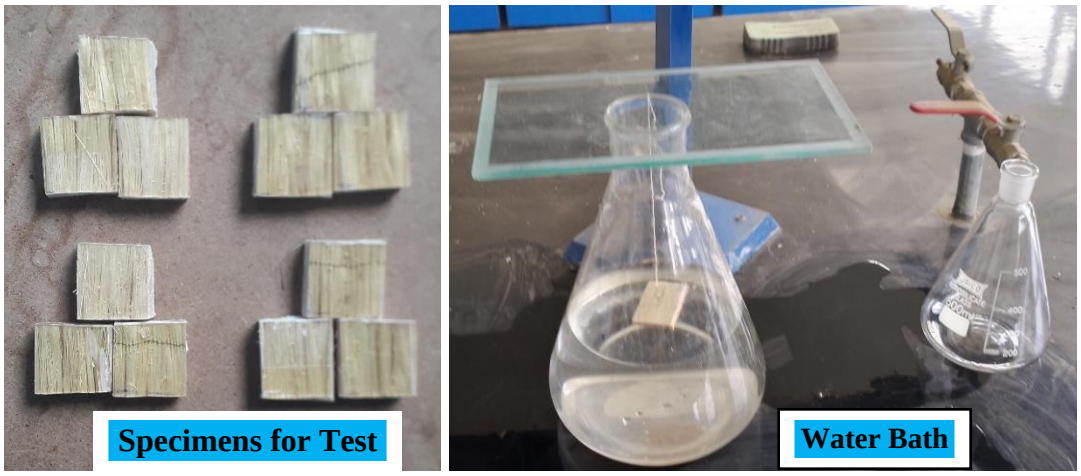

Figure 3:14 Density Determination of the composite using Archimedes method

1. First dry the specimens on oven and Measure in air to find mass in Kg.
2. Measure and record the water temperature.
3. Suspend the specimen using wire about 20-30 mm above the vessel support.
4. Determine the mass of the suspended specimen to the required precision. Record this apparent mass as of the mass of the specimen and the partially immersed wire in liquid.
5. Weigh the sample holder in water with immersion to the same depth as used in previous step.

Then the actual (measured) density of the composite is obtained using equation 3:14 bellow (62).

$$\rho_a = \frac{\rho_w W_a}{W_a - W_w - W_h} \qquad (3:15)$$

when ρ_a is the actual density of composite, ρ_w is the density of distilled water, W_a is weight of sample in air, W_w is weight of the sample in water and W_h is weight of the sample holder wire in water.

Again, the theoretical density of composite materials (ρ_t) in terms of weight fraction can easily be obtained using the following equation 3:15 bellow (63).

$$\rho_t = \frac{1}{\frac{W_G}{\rho_G} + \frac{W_J}{\rho_J} + \frac{W_m}{\rho_m}} \quad (3:16)$$

where W_J, W_E, and W_m are weight ratio and ρ_J, ρ_G, and ρ_m are densities of Jute, Glass, fiber, and Matrix respectively.

Void content of a composite may significantly affect its mechanical properties & quality of composites. i.e. higher void contents usually mean lower fatigue resistance, greater susceptibility to water penetration and weathering, and increased variation in strength properties. According to ASTM D2734 void percentage of composite is given by (64).

$$V_c = 100\left(\frac{\rho_t - \rho_a}{\rho_t}\right) \quad (3:17)$$

3.4. MACRO MECHANIC-LAMINATE DESIGN (CLT)

The classical lamination theory (CLT) is utilized to determine the stresses and strains at any position of laminates subjected to force and/or moment resultants.

Assumptions used in classical lamination theory are

- ✓ Each lamina is homogeneous & orthotropic bonded together
- ✓ Displacements < thickness(t) & (t) is much < than lengths of the plate
- ✓ Transverse and shear strains (γ_{xz} and γ_{yz}) are negligible
- ✓ The transverse normal strain (ε_z) is negligible

3.4.1. Hooke's Law for a 2D Orthotropic Unidirectional & Angle Lamina

A) For Orthotropic (Orthogonally Anisotropic)

An Orthotropic is when a material has three mutually perpendicular planes of material symmetry arranged in a rectangular array and whose stiffness matrix is given by

$\{\sigma\} = [Q]\ \{\varepsilon\}$

$$\begin{bmatrix}\sigma_{11}\\ \sigma_{22}\\ \sigma_{33}\\ \tau_{23}\\ \tau_{13}\\ \tau_{12}\end{bmatrix} = \begin{bmatrix}Q_{11} & Q_{12} & Q_{13} & 0 & 0 & 0\\ Q_{21} & Q_{22} & Q_{23} & 0 & 0 & 0\\ Q_{31} & Q_{32} & Q_{33} & 0 & 0 & 0\\ 0 & 0 & 0 & Q_{44} & 0 & 0\\ 0 & 0 & 0 & 0 & Q_{55} & 0\\ 0 & 0 & 0 & 0 & 0 & Q_{66}\end{bmatrix}\begin{bmatrix}\varepsilon_{11}\\ \varepsilon_{22}\\ \varepsilon_{33}\\ \gamma_{23}\\ \gamma_{13}\\ \gamma_{12}\end{bmatrix} \quad (3:18)$$

B) For Unidirectional along 1–2 coordinate system

A unidirectional lamina falls under the orthotropic material category. If the lamina is thin and does not carry any out-of-plane loads, one it can be assumed as plane stress conditions for the lamina.

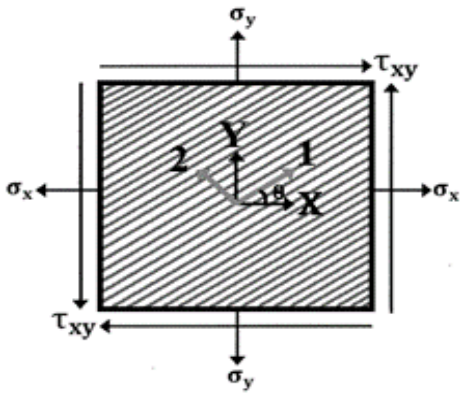

Figure 3:15 Local and global axis of an angle lamina

Therefore, taking the above Equations (3:17) and assuming, $\sigma_{33} = 0$, $\tau_{23} = 0$, $\tau_{13} = 0$ and $\gamma_{23} = \gamma_{31} = 0$ then the Hooke's law reduced to the following equation of stress–strain relationship stiffness matrix in the 1–2 coordinate system

$$\begin{bmatrix}\sigma_{11}\\ \sigma_{22}\\ \tau_{12}\end{bmatrix} = \begin{bmatrix}Q_{11} & Q_{12} & 0\\ Q_{12} & Q_{22} & 0\\ 0 & 0 & Q_{66}\end{bmatrix}\begin{bmatrix}\varepsilon_{11}\\ \varepsilon_{22}\\ \gamma_{12}\end{bmatrix} \quad (3:19)$$

Where: Q_{ij} are the reduced stiffness coefficients and whose values are given as follow

$$Q_{11} = \frac{E_{11}}{1-\nu_{21}\nu_{12}} = \frac{{E_{11}}^2}{E_{11}-E_{22}*{\nu_{12}}^2}$$

$$Q_{12} = \frac{\nu_{12}E_{22}}{1-\nu_{21}\nu_{12}} = \frac{E_{11}E_{22}\nu_{12}}{E_{11}-E_{22}*{\nu_{12}}^2} \quad (3:20)$$

$$Q_{22} = \frac{E_{22}}{1-\nu_{21}\nu_{12}} = \frac{E_{11}E_{22}}{E_{11}-E_{22}*{\nu_{12}}^2}$$

$Q_{66} = G_{12}$ when E_1, E_2 are the modulus of elasticity in the fiber (1), transverse (2) direction respectively, ν is the Poisson's ratio, τ is shear stress, G is the shear modulus, which is a function of the two elastic constants $G = \frac{E}{2(1+\nu)}$ and $\tau = \frac{G}{2\pi}$ (65). Again, the Poisson's ratio of the laminate is

the ratio of $\frac{Lateral(3\text{–}4\ \text{times}< \text{axial})}{Axial}$ (66) which is the slope obtained by plotting lateral strain against axial strain. But since the Straino meter of the universal testing machine is not working it is calculated in the fiber direction using ROM (67) ($V = V_{ff}V_f + V_{fm}V_m$).

By Inverting the above Equation (3:18) to get the compliance matrix as

$$\begin{bmatrix}\varepsilon_{11}\\ \varepsilon_{22}\\ \gamma_{12}\end{bmatrix} = \begin{bmatrix}\frac{1}{E_{11}} & -\frac{v_{12}}{E_{11}} & 0\\ -\frac{v_{12}}{E_{11}} & \frac{1}{E_{22}} & 0\\ 0 & 0 & \frac{1}{G_{12}}\end{bmatrix}\begin{bmatrix}\sigma_{11}\\ \sigma_{22}\\ \tau_{12}\end{bmatrix} \qquad (3:21)$$

C) For Angled Unidirectional along x–y coordinate system

Generally, a laminate does not consist only unidirectional laminae because of their low stiffness and strength properties in the transverse direction. Therefore, some laminae are placed at an angle. the coordinate system shown in Figure 3:15. along 1–2 is called local axis (material axis) whose direction -1 is parallel to the fibers called longitudinal direction L and direction -2 is perpendicular to the fibers called the transverse direction T. The axis in the x–y coordinate system is called the global axis or the off-axis. The angle between the two axis is denoted by an angle θ.

The global and local stresses in an angle lamina are related to each other through the angle of the lamina θ as follow.

$$\begin{bmatrix}\sigma_x\\ \sigma_y\\ \tau_{xy}\end{bmatrix} = [T]^{-1}\begin{bmatrix}\sigma_1\\ \sigma_2\\ \tau_{12}\end{bmatrix} = \begin{bmatrix}C^2 & S^2 & -2CS\\ S^2 & C^2 & 2SC\\ SC & -SC & C^2-S^2\end{bmatrix}\begin{bmatrix}Q_{11} & Q_{12} & 0\\ Q_{12} & Q_{22} & 0\\ 0 & 0 & Q_{66}\end{bmatrix}\begin{bmatrix}\varepsilon_{11}\\ \varepsilon_{22}\\ \gamma_{12}\end{bmatrix} \qquad (3:22)$$

where [T] is called transformation matrix $= \begin{bmatrix}C^2 & S^2 & 2CS\\ S^2 & C^2 & -2SC\\ -SC & SC & C^2-S^2\end{bmatrix}$, C= cos (θ) and S = sin (θ)

The global and local strains can be also related through the transformation matrix and rewritten as

$$\begin{bmatrix}\varepsilon_{11}\\ \varepsilon_{22}\\ \gamma_{12}\end{bmatrix} = [R]\,[T]\,[R]^{-1}\begin{bmatrix}\varepsilon_x\\ \varepsilon_y\\ \gamma_{xy}\end{bmatrix} \qquad (3:23)$$

where [R] is the Reuter matrix 3x3 and is defined as $[R] = \begin{bmatrix}1 & 0 & 0\\ 0 & 1 & 0\\ 0 & 0 & 2\end{bmatrix}$

Then, substituting Equation (3:24) in Equation (3:25) gives

$$\begin{bmatrix}\sigma_x\\ \sigma_y\\ \tau_{xy}\end{bmatrix} = [T]^{-1}[Q][R][T][R]^{-1}\begin{bmatrix}\varepsilon_x\\ \varepsilon_y\\ \gamma_{xy}\end{bmatrix} = \begin{bmatrix}\bar{Q}_{11} & \bar{Q}_{12} & \bar{Q}_{16}\\ \bar{Q}_{12} & \bar{Q}_{22} & \bar{Q}_{26}\\ \bar{Q}_{16} & \bar{Q}_{26} & \bar{Q}_{66}\end{bmatrix}\begin{bmatrix}\varepsilon_x\\ \varepsilon_y\\ \gamma_{xy}\end{bmatrix} \quad (3:26)$$

Where $\bar{Q}_{ij}$ are called the elements of the transformed reduced stiffness matrix and are given by

$$\bar{Q}_{11} = Q_{11}C^4 + Q_{22}S^4 + (Q_{12} + 2Q_{66})S^2C^2$$
$$\bar{Q}_{12} = (Q_{11} + Q_{22} - 4Q_{66})S^2C^2 + Q_{12}(C^4 + S^2)$$
$$\bar{Q}_{16} = (Q_{11} - Q_{12} - 2Q_{66})C^3S - 2(Q_{22} - Q_{12} - 2Q_{66})S^3C$$
$$\bar{Q}_{22} = Q_{11}S^4 + Q_{22}C^4 + 2(Q_{12} + 2Q_{66})S^2C^2$$
$$\bar{Q}_{26} = (Q_{11} - Q_{12} - 2Q_{66})CS^3 - (Q_{22} - Q_{12} - 2Q_{66})C^3S$$
$$\bar{Q}_{66} = (Q_{11} + Q_{22} - 2Q_{12} - 2Q_{66})S^2C^2 + Q_{66}(C^4 + S^2)$$

For finding the engineering Moduli of elasticity (E_x, E_y), in-plane shear modulus of elasticity (G_{xy}) and Poisson's ratio (ν_{xy}) of an Angle Lamina.

I) Modulus of elasticity in direction "X" (E_x) when $\sigma_y = \tau_{xy} = 0$ but $\sigma_x \neq 0$

$$E_x = \frac{\sigma_x}{\varepsilon_x} = \frac{1}{\bar{S}_{11}} = \frac{1}{\frac{1}{E_{11}}C^4 + \left[\frac{1}{G_{12}} - \frac{2V_{12}}{E_{11}}\right]S^2C^2 + \frac{1}{E_{22}}S^4} \quad (3:27)$$

II) Modulus of elasticity in direction "Y" (E_y) when $\sigma_x = \tau_{xy} = 0$ but $\sigma_y \neq 0$

$$E_y = \frac{\sigma_y}{\varepsilon_y} = \frac{1}{\bar{S}_{22}} = \frac{1}{\frac{1}{E_{11}}S^4 + \left[\frac{1}{G_{12}} - \frac{2V_{12}}{E_{11}}\right]S^2C^2 + \frac{1}{E_{22}}C^4} \quad (3:28)$$

III) Shear Moduli of elasticity τ_{xy} along X, Y direction when $\sigma_x = \sigma_y = 0$ & $\tau_{xy} \neq 0$

$$\tau_{xy} = \frac{1}{\bar{S}_{66}} = \frac{1}{\frac{1}{G_{12}}(C^4 + S^4) + 2\left[\frac{2}{E_{11}} + \frac{2}{E_{22}} + \frac{4V_{12}}{E_{11}}\right]S^2C^2} \quad (3:29)$$

IV) Poisons Ratio v_{xy} along X, Y direction

$$v_{xy} = E_x\frac{V_{12}}{E_{11}}(C^4 + S^4) - \left[\frac{1}{E_{11}} + \frac{1}{E_{22}} - \frac{1}{G_{12}}\right]S^2C^2 \quad (3:30)$$

3.4.2. Stress–Strain Relations of Laminate

A laminate is made of a group of single Plies bonded to each other. These relationships are developed for loads such as shear and axial forces, bending and twisting moments. coordinate system used in CLT is shown in Figure 3:16 bellow.

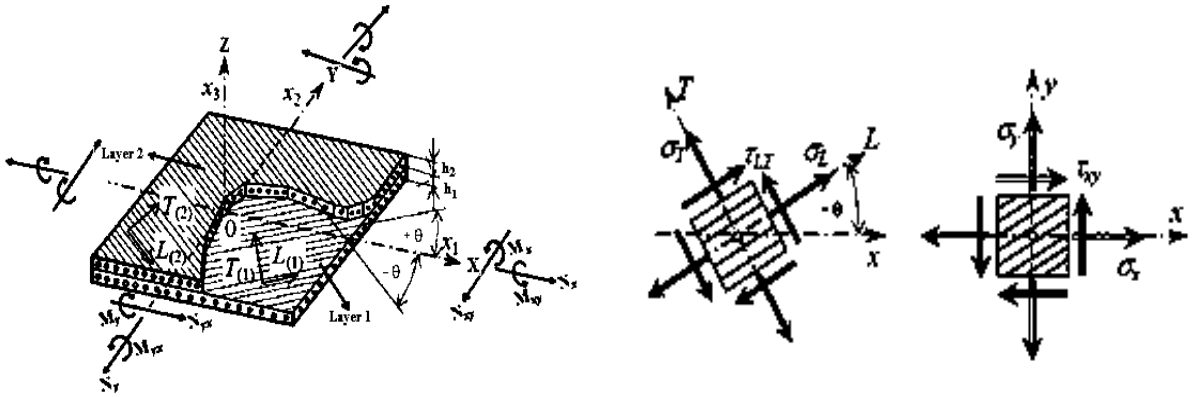

Figure 3:16 stress resultants of laminated plate along (x,y) & (L,T) Coordinate

knowing the strains at any point along the thickness of the laminate, the stress– strain equation in the global stresses in each single lamina is:

$$\begin{bmatrix}\sigma_x\\ \sigma_y\\ \tau_{xy}\end{bmatrix}=\begin{bmatrix}\bar{Q}_{11} & \bar{Q}_{12} & \bar{Q}_{16}\\ \bar{Q}_{12} & \bar{Q}_{22} & \bar{Q}_{26}\\ \bar{Q}_{16} & \bar{Q}_{26} & \bar{Q}_{66}\end{bmatrix}\left[\begin{bmatrix}\varepsilon_x^0\\ \varepsilon_y^0\\ \gamma_{xy}^0\end{bmatrix}+Z\begin{bmatrix}k_x\\ k_y\\ k_{xy}\end{bmatrix}\right] \qquad (3:31)$$

When $\begin{bmatrix}\varepsilon_x\\ \varepsilon_y\\ \gamma_{xy}\end{bmatrix}=\begin{bmatrix}\varepsilon_x^0\\ \varepsilon_y^0\\ \gamma_{xy}^0\end{bmatrix}+Z\begin{bmatrix}k_x\\ k_y\\ k_{xy}\end{bmatrix}$ is laminate strains, "Z" is distance from centroidal line and, K_x, K_y and K_{xy} are mid-plane curvatures.

3.4.3. Force and Moment Resultants Related to Midplane Strains and Curvatures

The mid-plane strains and plate curvatures are the unknowns for finding the lamina strains and stresses. The stresses in each lamina can be combined through the laminate thickness to give resultant forces and moments. The forces and moments applied to a laminate will be known, so the mid-plane strains and plate curvatures can then be found. This relationship between the applied loads and the mid-plane strains and curvatures is developed.

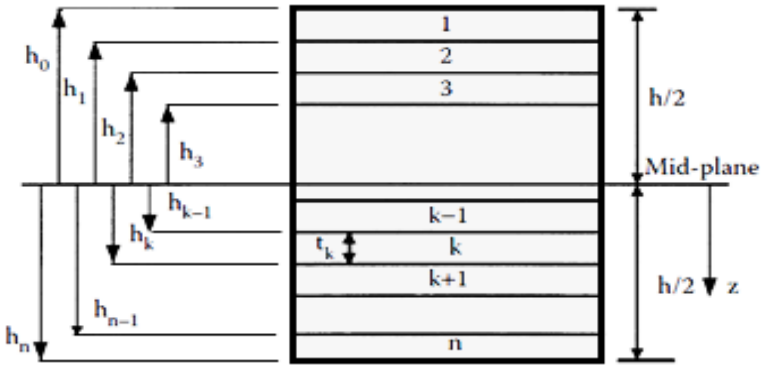

Figure 3:17 Coordinate locations of n plies in a laminate.

Consider a laminate made of n plies shown in Figure 3:17 above. Each ply has a thickness of t_k. Then the thickness of the laminate h is: $h = \sum_{k=1}^{n}(t_k)$

The resultant forces and moments can be written in terms of the mid-plane strains and curvatures:

$$\begin{bmatrix} N_x \\ N_y \\ N_{xy} \\ M_x \\ M_y \\ M_{xy} \end{bmatrix} = \begin{bmatrix} A_{11} & A_{12} & A_{16} & B_{11} & B_{12} & B_{16} \\ A_{12} & A_{22} & A_{26} & B_{12} & B_{22} & B_{26} \\ A_{16} & A_{26} & A_{66} & B_{16} & B_{26} & B_{66} \\ B_{11} & B_{12} & B_{16} & D_{11} & D_{12} & D_{16} \\ B_{12} & B_{22} & B_{26} & D_{12} & D_{22} & D_{26} \\ B_{16} & B_{26} & B_{26} & D_{16} & D_{26} & D_{66} \end{bmatrix} \begin{bmatrix} \varepsilon_x^0 \\ \varepsilon_y^0 \\ \gamma_{xy}^0 \\ k_x \\ k_y \\ k_{xy} \end{bmatrix} \quad (3:32)$$

Whenever N_x, & N_y, N_{xy}, M_x & M_y, M_{xy} are (normal force, shear force, bending moments & twisting moments) per unit length respectively. in short form it can be written

$\begin{bmatrix} N \\ M \end{bmatrix} = \begin{bmatrix} A & B \\ B & D \end{bmatrix} \begin{bmatrix} \varepsilon^0 \\ k \end{bmatrix}$ but if inverted, $\begin{bmatrix} \varepsilon^0 \\ k \end{bmatrix} = \begin{bmatrix} A^* & B^* \\ B^* & D^* \end{bmatrix} \begin{bmatrix} N \\ M \end{bmatrix}$ when $\begin{bmatrix} A^* & B^* \\ B^* & D^* \end{bmatrix} = \begin{bmatrix} A & B \\ B & D \end{bmatrix}^{-1}$ and $[C^*] = [B^*]^T$.

The Extensional Stiffness (A_{ij}), Coupling Stiffness (B_{ij}) and Bending Stiffness (D_{ij}) are given by

$$A_{ij} = \sum_{k=1}^{n} \left[\bar{Q}_{ij}\right]_k (h_k - h_{k-1}) \quad i = 1,2,6 \ldots and\ j = 1,2,6 \quad (3:33)$$

$$B_{ij} = \frac{1}{2} \sum_{k=1}^{n} \left[\bar{Q}_{ij}\right]_k (h_k^2 - h_{k-1}^2), i = 1,2,6 \ldots and\ j = 1,2,6 \quad (3:34)$$

$$D_{ij} = \sum_{k=1}^{n} \left[\bar{Q}_{ij}\right]_k (h_k^3 - h_{k-1}^3), i = 1,2,6 \ldots and\ j = 1,2,6 \quad (3:35)$$

The extensional stiffness matrix [A] relates resultant in-plane forces to in-plane strains, the coupling stiffness matrix [B] couples the force & moment terms to midplane strains & midplane curvatures, the bending stiffness matrix [D] relates the resultant bending moments to the plate curvatures.

Generally, the stress-strain relationship for K^{th} layer laminate composite along (x, y) and along the transformed Longitudinal and Transversal (L, T) axis shown from fig. 3:14 above is given by:

$$\begin{bmatrix} \sigma_x \\ \sigma_y \\ \tau_{xy} \end{bmatrix}^k = \begin{bmatrix} \bar{Q}_{11} & \bar{Q}_{12} & \bar{Q}_{16} \\ \bar{Q}_{12} & \bar{Q}_{22} & \bar{Q}_{26} \\ \bar{Q}_{16} & \bar{Q}_{26} & \bar{Q}_{66} \end{bmatrix}_k \begin{bmatrix} \varepsilon_x \\ \varepsilon_y \\ \gamma_{xy} \end{bmatrix}^k when \begin{bmatrix} \varepsilon_x \\ \varepsilon_y \\ \gamma_{xy} \end{bmatrix}^k = \begin{bmatrix} \varepsilon_x^0 \\ \varepsilon_y^0 \\ \gamma_{xy}^0 \end{bmatrix} + Z \begin{bmatrix} k_x \\ k_y \\ k_{xy} \end{bmatrix} is\ strain \quad (3:36)$$

$$\begin{bmatrix} \sigma_x \\ \sigma_y \\ \tau_{xy} \end{bmatrix}_{(LT)}^k = [T]_k \begin{bmatrix} \bar{Q}_{11} & \bar{Q}_{12} & \bar{Q}_{16} \\ \bar{Q}_{12} & \bar{Q}_{22} & \bar{Q}_{26} \\ \bar{Q}_{16} & \bar{Q}_{26} & \bar{Q}_{66} \end{bmatrix}_k \begin{bmatrix} \varepsilon_x \\ \varepsilon_y \\ \gamma_{xy} \end{bmatrix}^k \ \&\ [\varepsilon]_{(LT)}^k = [T]_k [\varepsilon]_{(xy)}^k \text{ is Strain} \quad (3:37)$$

3.4.4. In-Plane & Flexural Modulus of Symmetric Laminate

A laminate is called symmetric if the material, angle, and thickness of plies are the same above and below the midplane (Z=0). For a symmetric laminate, [B] = 0, A_{16} =A_{26} = 0 and it can be shown that [A*] = $[A]^{-1}$ and [D*] = $[D]^{-1}$. Then, Equation 3:33 can be decoupled to give

$$\begin{bmatrix} N_x \\ N_y \\ N_{xy} \end{bmatrix} = \begin{bmatrix} A_{11} & A_{12} & A_{16} \\ A_{12} & A_{22} & A_{26} \\ A_{16} & A_{26} & A_{66} \end{bmatrix} \begin{bmatrix} \varepsilon_x^0 \\ \varepsilon_y^0 \\ \gamma_{xy}^0 \end{bmatrix} \text{ or } \begin{bmatrix} \varepsilon_x^0 \\ \varepsilon_y^0 \\ \gamma_{xy}^0 \end{bmatrix} = \begin{bmatrix} A_{11}^* & A_{12}^* & A_{16}^* \\ A_{12}^* & A_{22}^* & A_{26}^* \\ A_{16}^* & A_{26}^* & A_{66}^* \end{bmatrix} \begin{bmatrix} N_x \\ N_y \\ N_{xy} \end{bmatrix} \quad (3:38)$$

$$\begin{bmatrix} M_x \\ M_y \\ M_{xy} \end{bmatrix} = \begin{bmatrix} D_{11} & D_{12} & D_{16} \\ D_{12} & D_{22} & D_{26} \\ D_{16} & D_{26} & D_{66} \end{bmatrix} \begin{bmatrix} k_x \\ k_y \\ k_{xy} \end{bmatrix} \text{ or } \begin{bmatrix} k_x \\ k_y \\ k_{xy} \end{bmatrix} = \begin{bmatrix} D_{11}^* & D_{12}^* & D_{16}^* \\ D_{12}^* & D_{22}^* & D_{26}^* \\ D_{16}^* & D_{26}^* & D_{66}^* \end{bmatrix} \begin{bmatrix} M_x \\ M_y \\ M_{xy} \end{bmatrix}$$

This shows that the force and moment terms are uncoupled. Thus, if a laminate is subjected only to forces, it will have zero midplane curvatures. Similarly, if it is subjected only to moments, it will have zero midplane strains. the uncoupling between extension and bending in symmetric laminates makes analyzing such laminates simpler.

A) in-plane longitudinal modulus E_x for Appling load $N_x \neq 0$, $N_y = 0$, $N_{xy} = 0$ is $E_x = \frac{1}{hA_{11}^*}$

B) in-plane transverse modulus, E_y for Appling load $N_x = 0$, $N_y \neq 0$, $N_{xy} = 0$ is $E_y = \frac{1}{hA_{22}^*}$

C) in-plane shear modulus G_{xy} for Appling load $N_x = 0$, $N_y = 0$, $N_{xy} \neq 0$ is $G_{xy} = \frac{1}{hA_{66}^*}$

D) The effective Poisson's ratio, vxy, is then defined as: $v_{xy} = -\frac{A_{12}^*}{A_{11}^*}$

Also, for a symmetric laminate, the coupling matrix [B] = 0; then, from Equation (3.39),

$$\begin{bmatrix} k_x \\ k_y \\ k_{xy} \end{bmatrix} = \begin{bmatrix} D_{11}^* & D_{12}^* & D_{16}^* \\ D_{12}^* & D_{22}^* & D_{26}^* \\ D_{16}^* & D_{26}^* & D_{66}^* \end{bmatrix} \begin{bmatrix} M_x \\ M_y \\ M_{xy} \end{bmatrix} \quad (3:39)$$

Using bending compliance matrix [D*] to define effective flexural moduli first Apply $M_x \neq 0$, M_y = 0, M_{xy} = 0 and then substitute in Equation (3:40) the effective flexural longitudinal modulus, flexural transversal elastic moduli, shear moduli and poisons ratio will be:

Ex, = $\frac{12}{h^3 D_{11}^*}$, E_y, = $\frac{12}{h^3 D_{22}^*}$, Gxy = $\frac{12}{h^3 D_{66}^*}$ and $v_{xy} = -\frac{D_{12}^*}{D_{11}^*}$ respectively.

- Assume the laminate bonnet plate have 6plies having symmetrical and unidirectional orientation. The plate is subjected to impact load.

Figure 3:18: Laminate of the composite Plate plies via mid plane

3.4.5. Failure Analysis of Laminate

Material failures occur when component is subjected to higher stresses & strain values beyond, they can handle. It includes fracture (breakage into several parts), buckling, and matrix cracking.

So, a laminate will fail under increasing mechanical and thermal loads until all the plies fail. Laminate failure is not catastrophic. If one ply fails the other ply in the laminate is still capable of taking more loads until all the plies fail.

A) Tsai-WU Failure Theory

Tsai-Wu result is more accurate and agree with the experimental values, because it does distinguish between the tensile and compressive strengths and shows as if it exists a failure surface in the stress-space (68). again, Tsai–Wu failure criterion used to predict the first-ply failure load.

For orthotropic lamina in a general state of plane stress for Tsai-Wu failure theory is given by

$$F_1\sigma_1 + F_2\sigma_2 + F_{11}\sigma_1^2 + F_{12}\sigma_1\sigma_2^2 + F_{22}\sigma_2^2 + F_{66}\tau_6^2 \geq 1 \qquad (3:40)$$

where $F_1 = \frac{1}{X_t} - \frac{1}{X_c}$ & $F_2 = \frac{1}{Y_t} - \frac{1}{Y_c}$ are coefficient for longitudinal strength $F_{11} = \frac{1}{X_c X_t}$ & $F_{22} = \frac{1}{Y_c Y_t}$ are coefficient for transversal strength, $F_{66} = \frac{1}{\tau^2}$ coefficient for shear & F_{12} is determined experimentally. But if no experimental value, Tsai-Wu recommends using: $F_{12} = -\frac{1}{2}\sqrt{F_{11}F_{22}}$

Magnitude of F_{12} is constrained by inequality called the stability criterion i. e. $F_{11}F_{22} - F_{12}^2 > 0$.

When

X_t = Allowable tensile stress or strain in longitudinal direction.

X_c = Allowable compression stress or strain in longitudinal direction.

Y_t = Allowable tensile stress or strain in transverse direction.

Y_c = Allowable compression stress or strain in transverse direction.

τ = Allowable stress in shear (+ve or -ve shear has the same allowable).

B) Steps for laminate Failures

The procedure followed in this paper for finding the first ply and last ply failure load following the fully ply discounted method is.

1. Enter the basic lamina properties E_1, E_2, G_{12} and V_{12}.
2. Compute the reduced ply stiffness [Q] referred to their local axis (principal material axis)
3. Enter the orientation Θ_k, number of layers n, through the thickness coordinate z.
4. Find reduced transformed stiffness matrix $[\bar{Q}]_{xy}$ for each ply of coordinate (x, y) using [Q].
5. Knowing thickness, t_k of each ply, find the coordinate of top & bottom surface h_i when i = l… n.
6. Calculate the laminate stiffness matrices [A], [B], [D] and their compliance matrices.
7. Enter the mechanical loading, $[N]_{xy}$, $[M]_{xy}$.
8. Calculate the mid plane strain $\varepsilon^0{}_{xy}$ and curvature $[k]_{xy}$ using laminate analysis above.
9. Calculate the layer strain $[\varepsilon]_{12}^{k}$ and stress $[\sigma]_{12}^{k}$ with reference to the local axis (1, 2) (Longitudinal and Transversal) axis in each layer under the given load.
10. Enter the five-lamina strength & using a appropriate failure theory to find out the strength ratio (safety factor) of each of the lamina. Then the minimum SR is the desired one of the laminates.
11. Multiply the minimum strength ratio to the applied load to get the load level of the failure of the first ply. This load is called the First Ply Failure load (FPF).
12. Calculate the laminate strength by applying unit stress in the respective direction.
13. Degrade fully the stiffness of damaged plies. Apply the actual load level of previous failure.
14. Go to step 10 to find the strength ratio (SR) in the undamaged plies. If the SR>1, multiply the SR to the applied load to get the load level of the next ply failure and go to next step
15. If SR< 1, Stiffness & Strength properties of all damaged plies reduce & go back to step 13.
16. Repeat the preceding steps until all plies in the laminate have failed. The load at which all the plies in the laminate have failed is called the last ply failure.

3.4.6. Plate Bending

Palte is a flat structure mostly subjected to in-plane loading, transverse loads (loads normal to its mid-surface). transverse loads supported by combined bending and shear action.

The bonnet of the car is assumed as plate subjected to concentrated load. Due to this load plate design was considering the maximum deflection occurred in the plate surface. This maximum

deflection can be determine using analytical modeling and finite element method software package (Altair Hyper work/opt 2019). For this study the bonnet plate boundary condition was constrained along the edges of the bonnet and subjected to concentrated load *q (x, y)* see Figure 3:19.

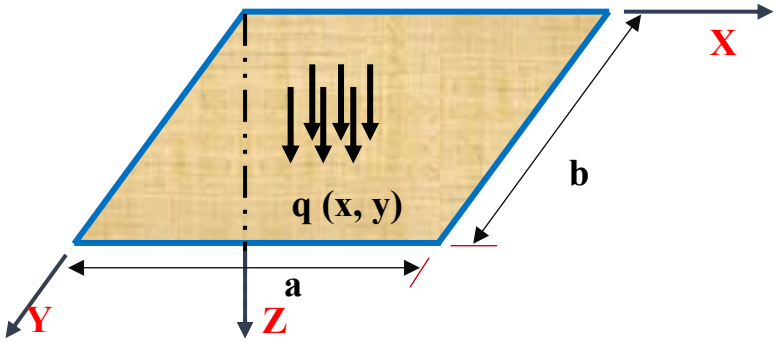

Figure 3:19 Completely clamped rectangular plate subjected to a distributed load

Bending of completely constrained plates as shown in Figure 8.12 is traditionally addressed by using the Ritz method, which is an approximate method known to yield acceptable results (69)

The Ritz method is based on the minimization of potential energy, and is the simplest method for solving plate and shell deflections using hand calculations.

Therefore, the deflection is given as:

$$W_o(x,y) = \frac{16q_o a^4}{\pi^6}\sum_{m=1}^{\infty}\sum_{n=1}^{\infty}\left[\frac{sin(2m-1)\frac{\pi x}{a}\,sin(2n-1)\frac{\pi y}{b}}{(2m-1)(2n-1)D_{2m-1,2n-1}}\right] \quad (3:41)$$

When:

$$D_{2m-1,2n-1} = D_{11}(2m-1)^4 + 2(D_{12}+2D_{66})\big((2m-1)(2n-1)R\big)^2 + D_{22}\big((2n-1)R\big)^4 \quad (3:42)$$

where R = a/b

The maximum deflection occurs at the center of the orthotropic plates (x = a/2, y = b/2) and is

$$W_o(x,y) = \frac{16q_o a^4}{\pi^6}\alpha \quad (3:43)$$

Where:

$$\alpha = \sum_{m=1}^{\infty}\sum_{n=1}^{\infty}\left[\frac{(-1)^{m+n-2}}{(2m-1)(2n-1)D_{2m-1,2n-1}}\right] \quad (3:44)$$

The maximum deflection occurs at the center of the isotropic rectangular plates (x = a/2, y = b/2) and is:

$$Wo(a/2,b/2)\,\frac{0.00342q_o a^4}{D(1+0.571R^2+R^4)_{max}} \quad (3:45)$$

CHAPTER FOUR

4. DESIGN AND ANALYSIS OF THE BONNET

4.1. DESIGN OF THE CAR BONNET

Designing a jute and glass fiber-reinforced Epoxy Composite bonnet (hood) involves considering several key parameters, specifications, and design considerations to ensure optimal performance, durability, and safety. Here's a detailed breakdown:

4.1.1. Design Parameters:

1. ***Material Selection:***
   - ✓ Unidirectional Jute and Glass Fibers Reinforced Epoxy Composite laminate.
2. ***Composite Layup:***
   - ✓ Different stacking sequence and orientation of jute and glass fibers is applied to optimize strength, stiffness, and weight of the car bonnet.
   - ✓ Consider hybrid layup designs to leverage the strengths of both fibers (e.g., using jute for impact absorption and glass for structural integrity).
3. ***Shape and Geometry:***
   - ✓ The Shape of the bonnet is ***Double Curvature Profile***, *i.e.* it is curved both horizontally and vertically in the front which enhances aerodynamics efficiency, structural rigidity and gives aesthetics.

Standard dimensions for the bonnet (hood) of a Lamborghini can vary slightly depending on the model and design specifications. But for this work Lamborghini Urus 2019 car model is selected because it is known for its low-slung and preferences styling, which influences the dimensions of the bonnet. So, the geometrical dimensions of typical Lamborghini models bonnet are (70):

1. **Length (Front to Rear):** Around 1.8 to 2.0 meters (198 cm).
2. **Width (Side to Side):** Typically, between 1.2 to 1.5 meters (145 cm).
3. **Height (Top to Bottom):** Usually around 0.5 to 0.7 meters (55 cm).
4. **Weight**: Carbon Fiber Bonnet (7-10 Kg), Steel Bonnet (15-30Kg) but for urus the steel bonnet is 18Kg.
5. **Thickness:** Carbon Fiber Bonnets (2 - 4 mm), Steel Bonnet **(**0.6 – 1.2 mm).
4. ***Load Conditions:***
   - ✓ The Load to the bonnet is Impact Load or aerodynamic forces.

4.1.2. Design Specifications:

1. ***Mechanical Properties:***
   - **Strength:** The material has good mechanical properties. Glass fibers provide high tensile strength, while jute fibers can enhance impact resistance.
   - **Stiffness:** It is stiff having higher Modulus of Elasticity (Young's modulus).
   - **Weight:** Compared to conventional metal (Al, steel) bonnets, composites can significantly reduce weight, improving vehicle performance and fuel efficiency.
2. ***Dimensional Accuracy:***
   - The Dimension of the bonnet is accurate that ensures precision and fitment to maintain structural integrity and aesthetic alignment with the vehicle.
3. ***Surface Finish:***
   - It has good surface finish to meet aesthetic standards and minimize post-processing.
4. ***Environmental Considerations:***
   - The composite bonnet is expected to resist environmental factors such as UV exposure, moisture absorption, and temperature variations.

4.1.3. Design Considerations:

1. ***Safety Standards:***
   - According Automotive safety regulations and standards the bonnet ensures the main body like engine parts against crashworthiness and fire resistance.
2. ***Manufacturability:***
   - Consider ease of fabrication, assembly, and integration into the Lamborghini manufacturing process.
3. ***Aesthetic Integration:***
   - Ensure the bonnet design aligns with Lamborghini's brand identity and enhances the vehicle's overall visual appeal.

Addressing all these design parameters, specifications, and considerations, it is possible to develop a jute and glass fiber-reinforced epoxy composite car bonnet that not only meets performance requirements but also aligns with aesthetic, cost, and environmental goals. This holistic approach ensures a balanced design that enhances both form and function in automotive engineering.

4.1.4. Design Calculation:

I: *Calculate the loads like Impact and Moment*

Having Child head form mass of impactor m_{im}, initial Speed u_{im}, time of collision 't' etc. then

Impact Load (strength), $I = \frac{E}{AK}$, K is aspect ratio = 0.5 for Glass & most natural fibers

Impact (KE) Energy, $E = \frac{1}{2} m_{im} u_{im}^2$

The bending moment of a plate subjected to a concentrated load 'P' at a distance 'd' can be calculated using the equation for bending moment:

$$M = P \times d = \frac{\sigma_s (I)}{Y}$$

II: *Select Double-Curved shape and calculate Thickness of the Composite Plate*

The Cross Section for bonnet plate is almost flat with moment of inertia $I = bt^3/12$ and $Y = t/2$. Since the composite is wanted to replace the strength of conventional materials (steel) then the momentum for steel and composite bonnet is assumed to be same.

The bending moment equation of Steel bonnet plate is $M = \frac{\sigma_s (I)}{Y}$

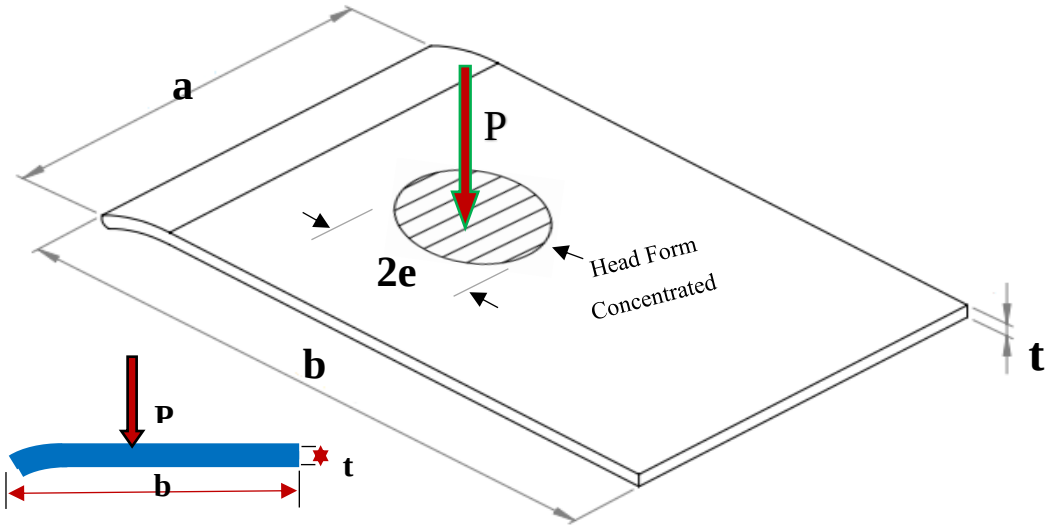

Figure 4:1 2D and 3D Cross Sections of car Bonnet Plate

$$M = \frac{\sigma_{steel} (I)}{Y} = \frac{460Mpa\ (2.08x\ 10^{-8} m^4)}{.012m/2} = 160.08Nm$$

Thickness of the composite bonnet can be determined from bending moment of steel equation.

$$\frac{M}{I} = \frac{\sigma_{comp}}{Y} \quad \text{when } I = \frac{b * t^3}{12} \text{ and } Y = \frac{t}{2}$$

$$t = \sqrt{\left[\frac{6M}{b*\sigma_{comp}}\right]} = \quad (4:1)$$

$= \sqrt{\left[\frac{6*160.08\text{Nm}}{1.45*209Mpa}\right]}$ = 3.97 = 4 mm is the total thickness of Composite laminate.

Therefore, since the average thickness single ply of jute & E-glass is 0.4mm, then around 10 layers (***JGJGJGJGJG***) are required for fabricating composite bonnet plate.

III: *Check Stress and deflection at a given load*

Assume Simply Clamped Rectangular Plate Subjected to Concentrated Load **'P'** at Center over a small area of radius **'e'**. then the stress and deflection at the concentrated point is given by.

1. Stress equation at the concentrated area

$$\sigma_m = \frac{1.5P}{\pi t^2}\left[(1+v)ln\frac{2b}{\pi e} + 1 - K_2\right] \quad (4:2)$$

2. Deflection due to 'P' at the concentrated area:

Maximum deflection of the designed pate is checked at the given concentrated loads & must be less than the Maximum allowable deflection.

$$\Delta_m = K_1 \frac{P*a^2}{E*t^3} \quad (4:3)$$

Maximum allowable total deflections due to different construction are.

Type	Plastered floor construction	Un plastered floor construction	`Un plastered roof construction
Δ_{max}	L/360	L/240	L/180

Assuming plastered floor construction, Δ_{max} = L/360.

Therefore, $\Delta_m <$ Δ_{max} - **OK!**

Table 4:1 Major Length to Minor Length ratio of the car bonnet plate

b/a									
	1	1.1	1.2	1.4	1.6	1.8	2	3	∞
K_1	0.127	0.138	0.148	0.162	0.171	0.177	0.180	0.185	0.185
K_2	0.564	0.445	0.349	0.211	0.124	0.072	0.041	0.003	0.000

when:

a, b = minor (width) & Major length of rectangular plate, (m)

P = Concentrated load, (N)

v = Poisson's ratio

E = Young's modulus, (N/m²)

t = plate thickness, (m)

e = Radius of area with force applied

σ_m = maximum stress, (N/m²)

Δ_m = maximum deflection, (m)

4.2. Finite Element Analysis of the Car Bonnet

4.2.1. Impact Analysis of the Composite bonnet Using Altair-Hyper Mesh

Altair Hyper Mesh is a high-performance finite element pre-processor software used for meshing and pre-processing of complex models in industries like automotive, aerospace, and marine engineering. It allows engineers or analysts to create finite element models for structural, thermal, and fluid analysis. Hyper Mesh is known for its powerful meshing capabilities, geometry editing tools, and solver interfaces that help streamline the simulation process.

A) CAD Model of the Bonnet with the Head form Impactor:

Three-Dimensional Modeling is a geometrical representation of the real object having full information of its volume, density, mass and inertia. the 3D modelling of the Bonnet was done using Solid work 2023 modeling software by taking the actual data from a selected type of vehicle. the file was saved in IGES form to import into Altair Hyper Work for further analysis purpose

Figure 4:23D view of Car bonnet (A) and Head like Impactor (B)

B) Steps for Impact Analysis of the Car Bonnet

1. Import geometry
2. Mesh the geometry:
3. Creating Material:
4. Creating Ply:
5. Laminate generation:
6. Defining Property:
7. Apply Loads and BC's *(Constraints*): 4.8 kg impactor @ low speed of 35Km/h
8. Create Set for each Component, Rbody and Load collector.
9. Create Group or Connect Load Collector with Set
10. Create Engine File Assistant
11. Analysis (Run) and record the *Output file*

4.2.2. Design optimization of the Composite bonnet laminate structure

Optimization process is a process of achieving maximized objective at a given variables under a constrained parameter. Opti Struct software has a comprehensive optimization technology of size, shape and Shuffle optimization. it is possible to automatically generate the appropriate laminate shape and initial thickness distribution of the fiber reinforcement according to the structure and force of the component. Steps for Design optimization process is listed below:

1. ***Analysis Type:*** Static, Dynamic,
2. ***Optimization Type*:** Sizing, Shape, Stacking Sequence.
3. ***Design Variables***: No of plies and Ply orientation are variables.
4. ***Design Constraints***: Strength ratio is the limits on the Design response.
5. ***Design Objective*:** Minimize weight, thickness and Strength.

The main objective of this analysis is to minimize the weight of the bonnet undergo minimizes cost at its maximum impact performances and stiffness. The weight of the bonnet depends on its thickness. according to the structural performance requirements, the ply angle of orientation and play thickness are optimized to obtain a final structural optimization design.

A. Size Optimization

Optimization used to get the best thickness for each ply-bundle considering manufacturing constraints.

Objective Function: Is as a function needed to be optimized by minimizing or maximizing the design variables. main goal of this study is to optimize (minimize) weight under the constraint of Tsai-Wu failure criteria and variable of ply thickness. mathematically expressed in equation (4:4);

$$f(\mathrm{u}) = \sum_{\mathrm{i}=1}^{\mathrm{n}} (\rho_{\mathrm{i}} A_{\mathrm{i}} t_{\mathrm{i}}) \qquad (4:4)$$

Where; f(u) is minimizing weight and u is design variable of Jute and glass fiber thickness.

First import model solver Deck in new Hyper mesh session created from free sized model (model name optimization sizing.3.fem). for each ply there is a size design variable created in the design variable section. rename the 'DesBoard' to 'DesSize'. specify a manufacturing thickness value (TMANUF). TMANUF defines the thickness of one manufacturable ply. This parameter is used during sizing optimization to automatically create discrete design variables such that the thickness of the ply bundle is equal to a multiple of TMANUF. Finally run and see the result.

B. Stacking Sequence Optimization

In this phase, an optimal shuffling sequence is generated for the loads and BCs applied, that is which ply should go where in the laminate. Import the model name_size_shuffling.fem file in a new Hyper Mesh session. In the laminate it may found couple of plies missing this is because of their contribution for the laminate is not required.

4.2.3. Thermal analysis of the Composite Car bonnet

Thermal analysis of a car bonnet plate is essential for ensuring the overall performance, reliability, safety, and regulatory compliance of the vehicle. It allows engineers to optimize design choices, select appropriate materials, and prevent potential thermal-related failures during both normal operation and extreme conditions. So, the thermal analysis design calculation of a car bonnet plate is crucial for several reasons:

1. **Material Selection and Optimization:** Thermal analysis helps in selecting the most suitable material that can withstand the expected thermal loads without deforming, melting, or undergoing other undesirable changes.
2. **Performance and Reliability:** The bonnet plate is exposed to various thermal loads during vehicle operation, including solar radiation, engine heat, and ambient temperature fluctuations. Analyzing these thermal loads ensures that the bonnet plate can maintain its structural integrity and functional performance over its lifespan.

3. **Preventing Thermal Stress and Failure:** Excessive heat can cause thermal stress in materials, leading to fatigue, cracking, or even catastrophic failure over time. Thermal analysis helps in identifying potential of a material to thermal stress.

I. Input Parameter for the bonnet:

- ***Material Properties*:** material of the car bonnet plate is Jute/glass fiber reinforced epoxy composites with its Thermal Conductivity (k), Specific Heat Capacity (c) and Density (ρ).
- ***Engine Heat*:** Consider the heat radiated from the Diesel engine, typically produce more heat than gasoline engines due to their higher thermal efficiency. Typically, during normal operating conditions, the temperature rise on the bonnet due to engine can range from approximately 50°C to 150°C above ambient temperature (71).

4.2.3.1. Mathematical model of heat transfer for the bonnet

Conductive Heat Transfer: Use Fourier's law of heat conduction to calculate the steady-state temperature distribution across the bonnet plate:

$\frac{d}{dx}\left(k\frac{dT}{dx}\right) = \rho c\frac{dT}{dt}$ integrating both sides it gives a heat flux Q,

$$Q = k\frac{dT}{dx} \quad (4:5)$$

Where: T is temperature, t is time, k is thermal conductivity, ρ is density & c is specific heat capacity.

4.2.3.2. Radiative Heat Transfer:

Calculate the radiative heat transfer using the Stefan-Boltzmann law:

$$Q = \sigma\epsilon A(T^4 - T_{ambient}^4) \quad (4:6)$$

Where:

- Q is the radiative heat transfer rate
- ϵ is the emissivity of the bonnet plate surface
- σ is the Stefan-Boltzmann constant
- A is the surface area of the bonnet plate exposed to radiation
- T is the temperature of the bonnet plate
- $T_{ambient}$ is the ambient temperature

4.2.3.3. Transient Thermal Analysis

Consider transient effects if the temperature changes rapidly due to sudden environmental changes or engine operations. Use the heat diffusion equation:

$$\rho c \frac{\partial T}{\partial t} = \nabla * (k \nabla T) + Q \qquad (4:7)$$

4.2.3.4. Simulation Analysis

Finite Element Analysis (FEA) in ANSYS is used to see the temperature distribution analysis on the car bonnet based on the actual vehicle structure and size, the model of the vehicle hood location designed and drawn is shown in figure below. The main Input Parameters (structural or material) parameters and specification of the model are as follow.

A) Material: the material is Jute/Glass Fiber Reinforced Epoxy with its structural parameters of the bonnet are Length = 180(cm) and width = 120(cm) from the existing bonnet whereas the material parameters of the bonnet are density = 1500 kg/cm^3, heat conductivity ($\lambda/(w.m^{-1}k^{-1})$), Specific heat capacity ($c/ (J.kg^{-1}k^{-1})$).

B) Load Conditions: Internal heat load applied as a temperature from engine ranges from 110°C to ambient temperature (22^0c).

C) Boundary Conditions: Fixed constraints along the edges of the bonnet to simulate attachment to the vehicle frame.

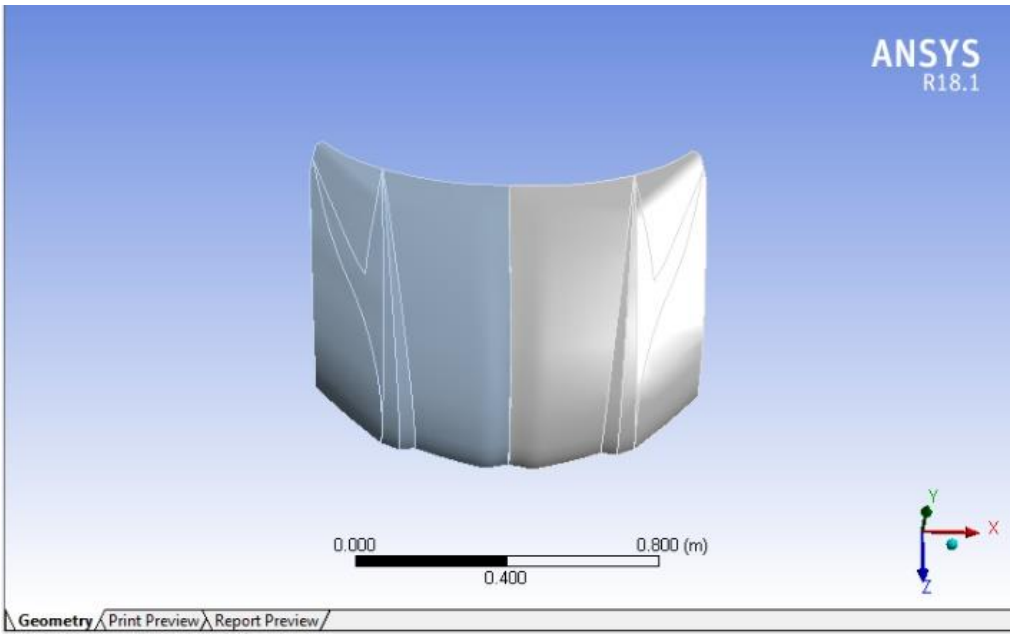

Figure 4:3Three-Dimensional model of the car bonnet

The output results In ANSYS Workbench, conducting thermal analysis of a car bonnet involves solving for the temperature distribution across the bonnet plate under steady thermal conditions. The result typically includes:

1. **Temperature Distribution:** ANSYS provides a contour plot or color map showing the minimum and maximum temperature distribution across the bonnet plate surface.
2. **Heat Fluxes:** The software calculates & displays heat fluxes across the bonnet plate surface.

Overall, the steady-state thermal analysis results from ANSYS Workbench provide comprehensive insights into the thermal behavior of the car bonnet plate. These insights are essential for optimizing the bonnet plate design, selecting appropriate materials, and ensuring reliable performance under varying thermal conditions encountered during vehicle operation.

CHAPTER FIVE

5. RESULT AND DISCUSSION

5.1. EXPERIMENTAL CHARACTERIZATION RESULT OF THE COMPOSITE

In this chapter Experimentally Physical and Mechanical properties, and Software Analysis result are presented. Experimental tests were conducted on laminate composites made of jute and glass fiber reinforced epoxy. These tests analyzed how different weight ratios and orientations of fibers affect the mechanical properties (such as tensile strength, impact resistance, flexural strength, compression strength, and water absorption) as well as the density of the composites. The goal was to identify which laminate configurations exhibit optimal properties for various applications.

5.1.1. Tensile Strength Result

The Tensile strengths test of treated unidirectional hybrid fiber of jute and Glass reinforced Laminated composite specimens was made as per the ASTM standard. the average result of stress–strain curves for jute and Glass fiber reinforced Epoxy under tensile loading was presented in Figure 5:1 below. as observed from the figure, tensile stress increased linearly with increase in strain until point of ultimate load under tensile loading.

Also, from this strength result graph relatively steep part of the curve represents elastic behavior and the slope of the curve (change Stress to Strain ratio) defines the elastic modulus. the result is calibrated result because the machine has an error and found by subtracting the error.

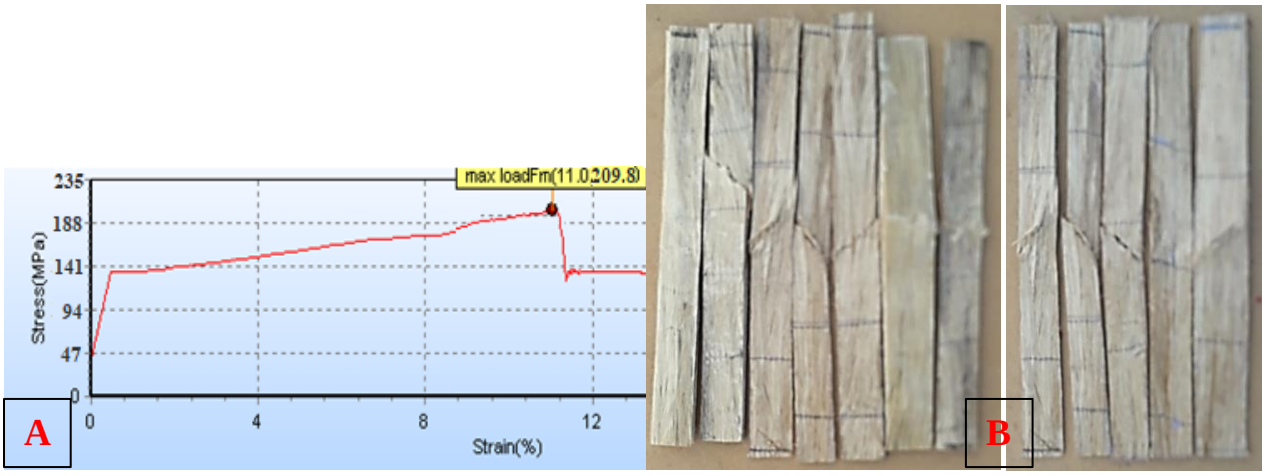

Figure 5:1 a) Stress Strain Curve b) specimen after teste

Table 5-1 Calibrated Tensile Test Result of different Samples

Calibrated Tensile Test Result				
Specimen	Ultimate tensile strength (Mpa)	Tensile strength (MPa)	Modulus of Elasticity (Gpa)	Elongation at break (%)
JJJJJJ (100,0) %	305.98	202.12	46.84	3.65
JGJJGJ (75,25) %	309.16	205.55	48.78	3.61
JGJGJG (50,50) %	313.78	209.83	49.96	3.54

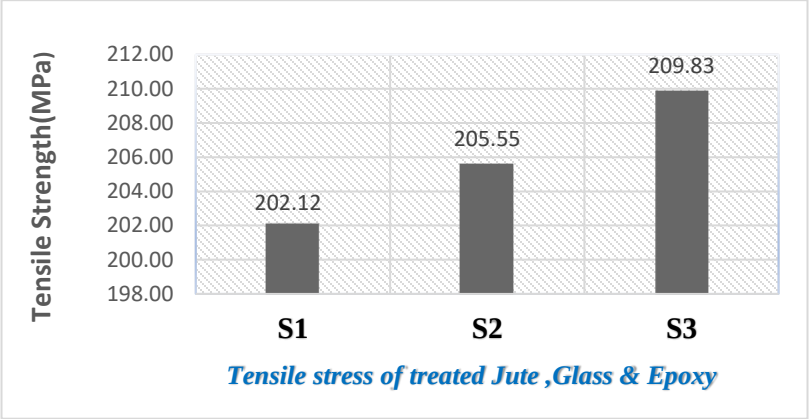

Figure 5:2 Graphical Representation of Stress Strain Curve test result

From the hybrid composite test result it is observed that the tensile strength of the samples increases with increase the weight ratio of Glass fiber to get maximum at 209.83 MPa.

Different failure modes of the samples have been observed as per the ASTM D3039 Standards when testing the specimen. The most common failures occurred are fiber pull out, fiber and/or matrix fracture, Delamination, failure at the grasp (hold) and fiber/matrix debonding. Fiber pulls out and delamination are due to weak bond (poor lamination) but the others are because of stress concentration or due to high clamping force on the composite sample.

5.1.2. Compressive Strength Result

Compressive strength of composite specimen is the opposite of Tensile strength and is evaluated by conducting uniaxial compression tests. The compressive strength value increases with increase Glass fiber mass. JGJJGJ has higher compressive strength (31.34Mpa) than the other preceding samples.

Figure 5:3 Specimen of Different Weight Ratio After Compressive Test

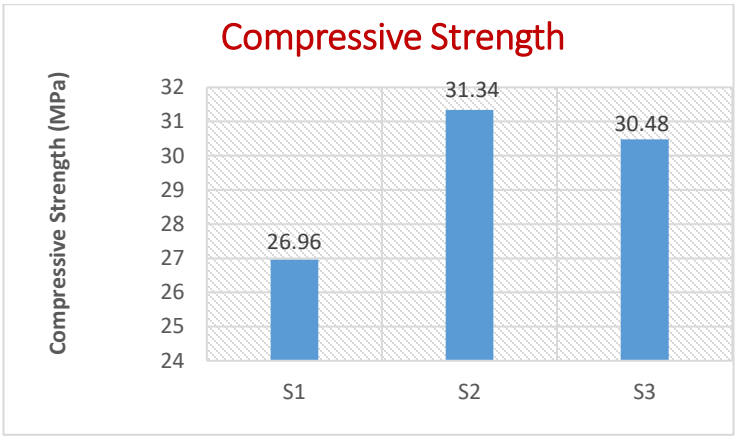

Figure 5:4 Graphical representation of compressive Strength test result

The compressive strength values of the composites range in between $[J]_5$ of 26.96Mpa & [JGJJGJ] of 31.43 MPa. Samples during compressive strength test also poses different types of failure mode. But the most common one is delamination due to lack of proper boding between fiber and matrix.

5.1.3. Flexural Strength Result

Most of the time structural body experience failure due to impacts and bending loads. To prevent such failures, composites with high resistance to both impact and bending loads are essential. Based on experimental results of flexural strength, it is evident that the data shows fluctuations, indicating a non-linear relationship. However, overall, there is a consistent trend: as the weight ratio of glass fiber increases, the flexural strength also increases.

Figure 5:5 Specimen After Flexural test

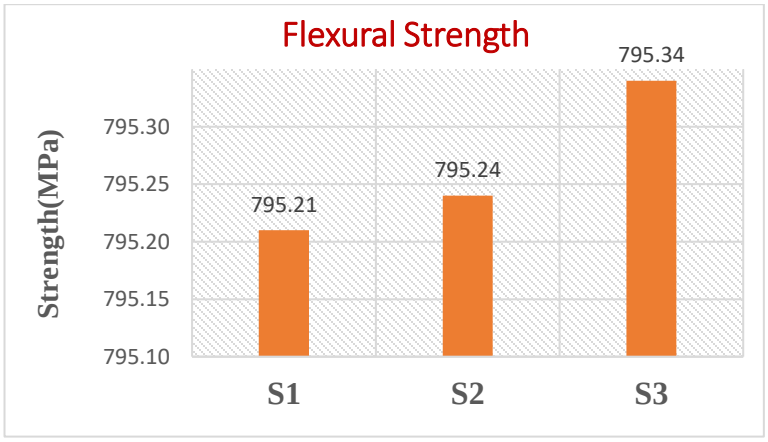

Figure 5:6 Graphical representation of flexural strength

Flexural strengths of the composite specimen are assessed by conducting three-point bend test in accordance with ASTM Standard and the average test results have its failure mode but mostly common is delamination.

5.1.4. Impact Strength Result

Impact resistance refers to the capability of composite structural materials to absorb and dissipate energy during impact or shock loading. A pendulum impact test machine was used to assess this ability. According to the experimental results, specimens with a higher weight ratio of glass fiber demonstrate greater impact strength. For instance, among the given samples, JGJGJG exhibited the highest impact strength of 348.39 J/m².

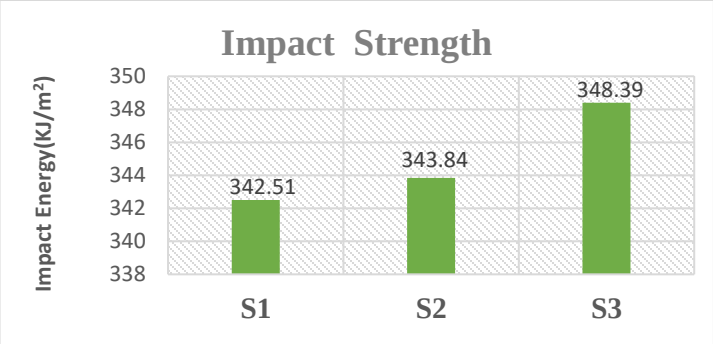

Figure 5:7 Graphical representation of impact strength

Similarly, with the other above mechanical property its common failure mode is delamination.

Figure 5:8 Specimen after Impact Test and Delamination failure

5.1.5. Water Absorption Test Result

The water absorption test result of the different weight ratio samples is listed below. From the result it is observed that it increases when the weight percent of jute fiber increases.

Table 5-2 Water Absorption Test Result of Composite Samples

	After 24 hrs.			After 48hrs.		
Samples	**Original mass (g)**	**Final mass (g)**	**Absorbed Water %**	**Original mass (g)**	**Final mass (g)**	**Water Absorbed %**
JJJJJJ	14.62	15.98	8.51	15.45	15.53	0.52
JGJJGJ	14.48	15.79	8.30	15.79	15.87	0.50
JGJGJG	14.55	15.53	6.31	14.87	14.91	0.27

As observed from the result with increasing weight percent of glass fiber decreases water absorption. Finally, from the above samples of weight ratio it should be selected with good mechanical property. since the aim of this characterization is for proper material selection with high mechanical property especially impact strength. From the above results JGJGJG has better mechanical property than the other Samples. This is further characterized based on fiber angle of orientation to Provides relatively good mechanical properties like strength and stiffness in multiple directions (Lateral and Transversal) or (both in the warp and weft directions of the fiber mat) so that it resists an impact load even when a laminate is subjected to concentrated load.

5.1.6. Characterization of composite based on the Fiber Angle of Orientation

When considering the effect of fiber angle of orientation on the strength of a composite material made up of unidirectional fiber embedded in a matrix, it is to over come

A. Composite failure occurs parallel to fibers because of if stress concentration is applied.
B. Shear failure of the matrix as a result of a large shear stress acting parallel to the fibers,
C. Tensile failure of the matrix (fiber/matrix) interface when stressed perpendicular to fibers.
D. To overcome failure during transversal impact

Further characterization is made on the composite sample having better mechanical property (sample of weight ratio of 50% jute fiber to 50% Glass fiber). characterization based on fiber angle of offers better impact resistance and damage tolerance due to the interlocking nature of the weave.

A. Effect of fiber orientation on Young's modulus of composites

The Young's modulus of a unidirectional composite is much higher when loaded in the longitudinal (0°) direction than in the transverse (90°) direction. The Young's modulus decreases with increasing fiber angle, particularly from 0° to 45° when the stiffness falls sharply by nearly 70%. The high sensitivity of the Young's modulus to fiber angle occurs for any type of unidirectional composite material, and their fibers must be closely aligned to the load direction to achieve high stiffness.

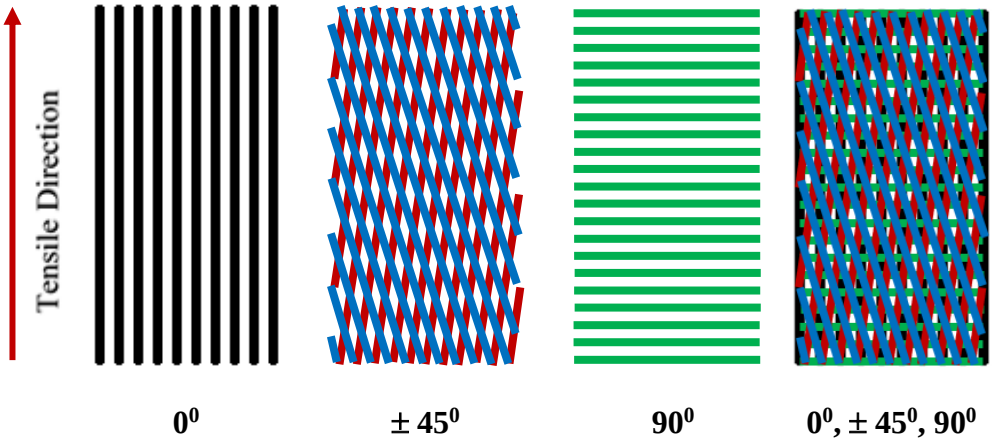

Figure 5:9 Schematic illustration of the composites with different fiber orientation

The Young's modulus of a unidirectional composite loaded at any fiber angle (Θ) between 0° and 90° can be calculated using:

$$E(\Theta) = \frac{1}{\frac{Cos^4(\Theta)}{E_1} + \frac{Sin^4(\Theta)}{E_2} + \left(\frac{1}{G_{12}} - \frac{2\nu_{12}}{E_1}\right) Sin^2(\Theta)Cos^2(\Theta)} \quad (5:1)$$

The other elastic properties of unidirectional composites are also dependent on the fiber angle. The equation bellow shows the variation in the shear modulus of Composite with fiber angle, and this property is highest at 45° and lowest when the load is applied in the fiber (0°) and anti-fiber directions (90°). The change in the shear modulus with fiber angle can be determined using:

$$G(\Theta) = 2\left(\frac{2}{E_1} + \frac{2}{E_2} + \frac{4\nu_{12}}{E_1} Sin^2(\Theta)Cos^2(\Theta)\right) + \frac{1}{G_{12}} Sin^4(\Theta)Cos^4(\Theta) \quad (5:2)$$

This composite is needed to have both Elastic Modulus and Shear Strength maximum value.

Generally, the overall mechanical Properties of the Angled fiber composite result is shown below.

Table 5-3 Longitudinal Mechanical Property result of Angled JGJGJG Samples

Angle of orientation	Tensile Strength (Mpa)	Impact Energy in (J)	Impact Strength in (KJ/m2)	Flexural Strength (Mpa)	Compression Strength In (Mpa)	Water Absorption Rate %
$[0^0 0^0]_{3s}$	209.83	30.18	348.39	795.34	30.58	8.51
$[0^0 / \pm 45^0]_s$	188.46	28.35	332.21	780.82	28.4	7.82
$[0^0 / 90^0]_{3s}$	165.74	27.9	319.79	770.23	26.7	6.70

Table 5-4 Transversal Mechanical Property result of Angled JGJGJG Samples

Angle of orientation	Tensile Strength (Mpa)	Impact Energy in (J)	Impact Strength in (KJ/m^2)	Flexural Strength (Mpa)	Compression Strength In (Mpa)	Water Absorption
$[0^0 0^0]_{3s}$	26.53	9.25	91.54	105.28	5.64	8.58
$[0^0 / \pm 45^0]s$	120.69	22.32	152.62	571.41	20.56	7.42
$[0^0 / 90^0]3s$	110.74	19.68	147.9	570.25	19.67	6.74

Generally, Properties like tensile, Flexural and compressive properties of composites decrease with the increase fiber angle of orientation from 0^0 to 90^0.in the lateral direction. But impact property increases with the increase fiber angle of orientation in the transverse (cross) direction.

5.2. IMPACT ANALYSIS RESULT OF THE BONNET USING ALTAIR-HYPER MESH

5.2.1. Stress Distribution Result of The Bonnet Plate

The stress distribution result of the Jute/Glass reinforced Epoxy laminate composite bonnet structure as shown in the fig below has maximum von mises stress of 53.78 N/mm^2 at the area of collision which is below the yield strength of the material implies there will not be an immediate failure or it is safe.

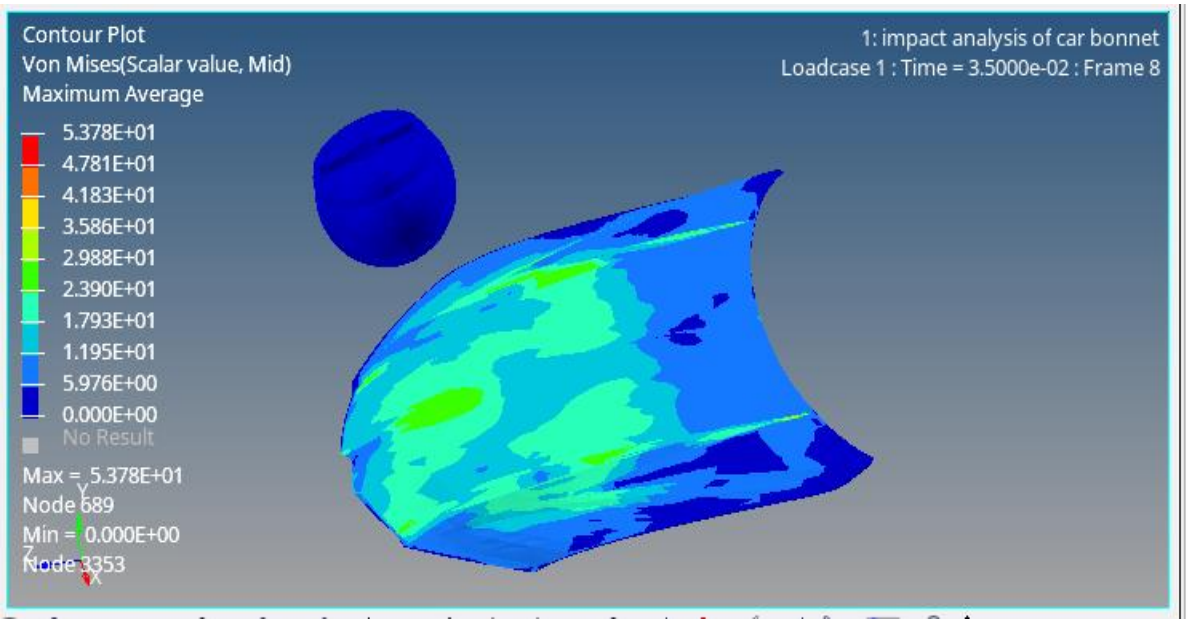

Figure 5:10 FEA Stress Distribution Analysis of the Composite Bonnet

5.2.2. Deformations Occurred in Composite Material of Bonnet Plate

The deformations occurred in the vehicle front Bonnet Plate is expected to be small or minimum as much as possible in order to minimize the damage of the vehicle's front body and the passengers. Then the Deflection for Jute/Glass reinforced Epoxy Laminate Composite Material can be observed as shown in the Figure 5:11 below and the maximum deflection obtained is 2.8 mm.

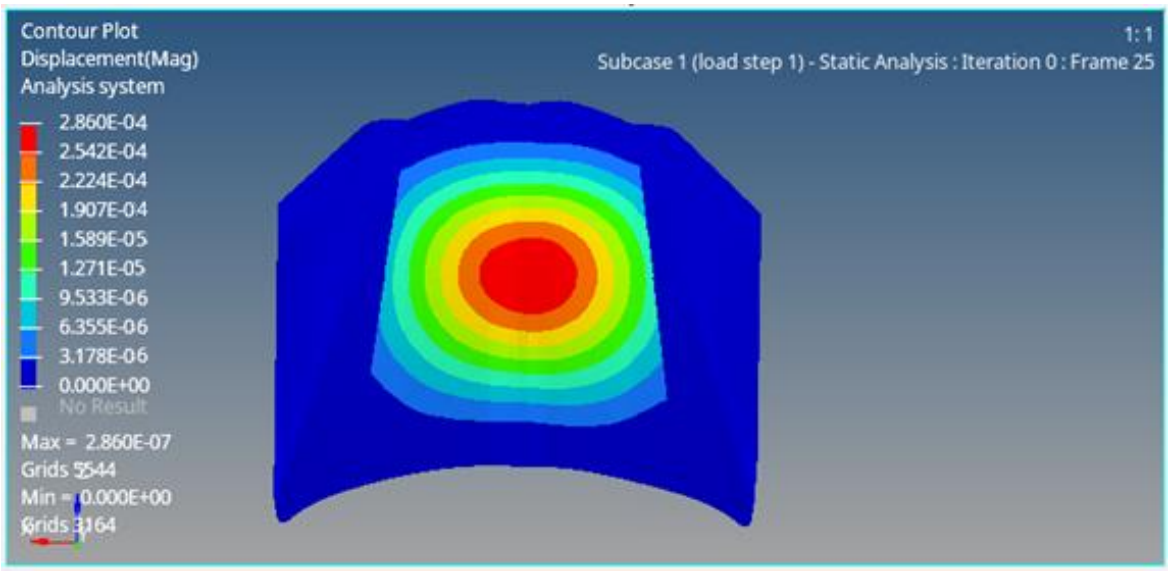

Figure 5:11 Total Deformation of Composite Bonnet and Steel Bonnet

5.3. Optimization Result of The Composite Bonnet Plate

5.3.1. Free Size Optimization Result

The 'output file (results) of the analysis for different Iterations are shown bellow

1. **Element Thickness, Orientation Thickness and Ply Thickness Results**

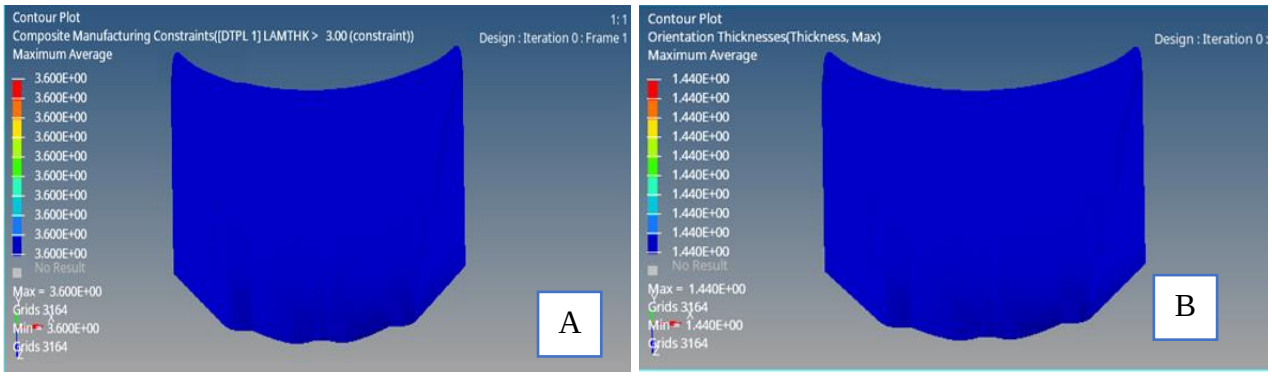

Figure 5:12 Manufacturing Thickness (A), Orientation Thickness(B) result of the Bonnet Plate

All plies have equal ply thickness of 3.6mm after optimized.

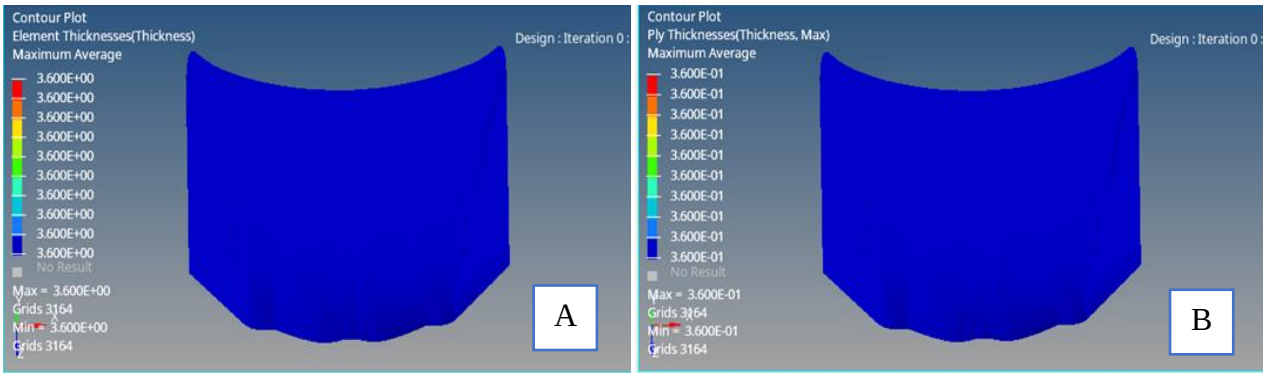

Figure 5:13 Element thickness and Ply Thickness Result of the Composite Bonnet Plate

5.3.2. Sizing Optimization Result

Open animation results in HyperView and check the thickness contours.

Run Summry:

OPTIMIZATION HAS CONVERGED

Feasible Design (All Constraints Satisfied)

==== End Of Solver Screen output ====

ITERATION 1
Soft convergence criterion satisfied;
the design did not change during the last iteration

Objective Function (Minimize Mass) = 9.25380E-03 % change = 0.00
Maximum Constraint Vaiolation % = 0.00000E+00
Volume = 7.83411E+06 Mass = 9.25380E-03

Subcase	Compliance	Epsilon
1.	3.2964421E+05	2.152508E-07

Figure 5:14 Sizing Optimization Result of the Bonnet Plate

1. **Element Thickness and Orientation Thickness Results**

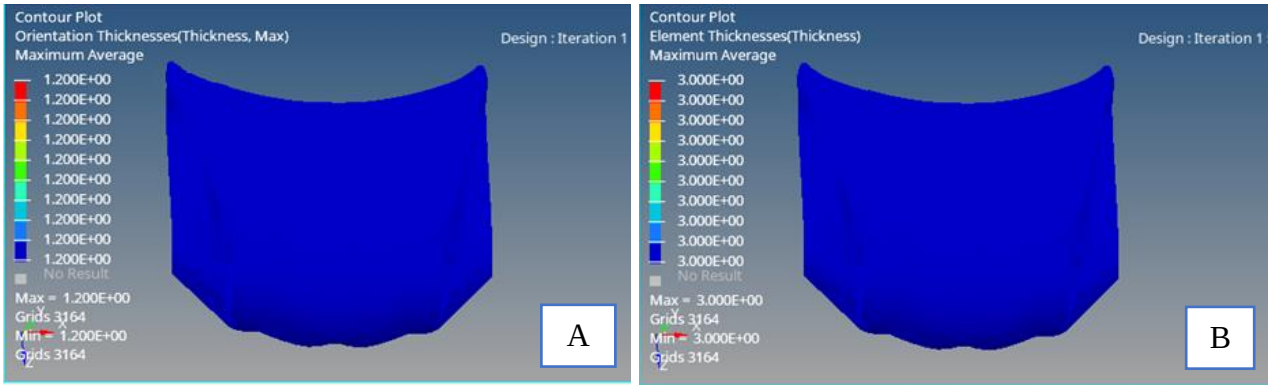

Figure 5:15 Element Thickness(A) and Orientation Thickness (B) results

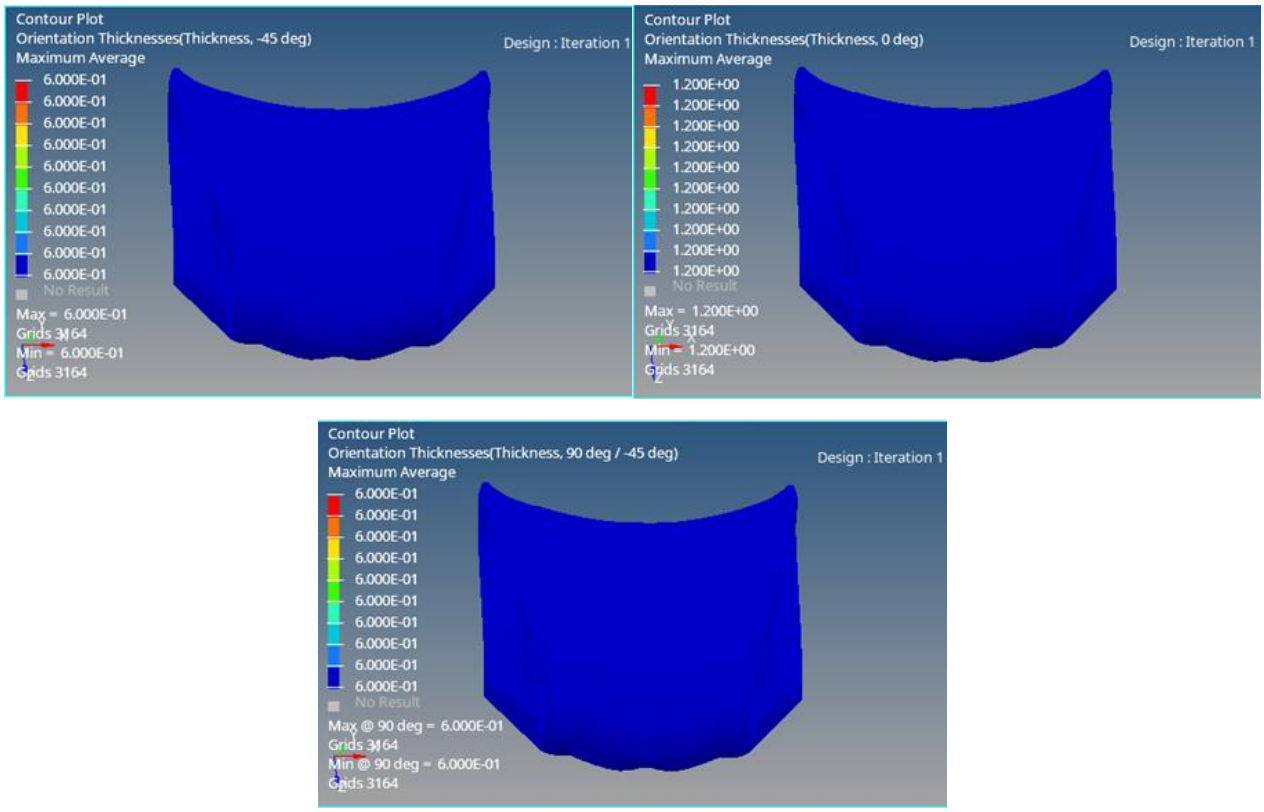

Figure 5:16 Orientation Thickness Result of each ply

The orientation thickness for 45^0, -45^0 and 90^0 is equal which is 0.6 mm

NB: Here in this analysis several Plies are either deleted or increased dueto their need.

5.3.3. Ply Stacking (Orientation) Sequence Optimization Result

Stacking sequence for STACK 1

Iteration 0	Iteration 1	Iteration 2
1101	1101	1101
2101	2101	2101
3101	3101	3101
5101	5101	5101
6101	6101	6101
7101	9101	9101
8101	8101	8101
9101	7101	7101

Legend
90.0 degrees
45.0 degrees
0.0 degrees
-45.0 degrees

Figure 5:17 Stacking Sequence of different Angled Plies Laminate

Iteration 1 or Iteration 2 are the optimized stacking sequence for the laminate stacks.

1. **Composite Stress Results: -** Under this different analysis like Shear Max., Vonmises, stress results of the laminate and for each Ply are shown.

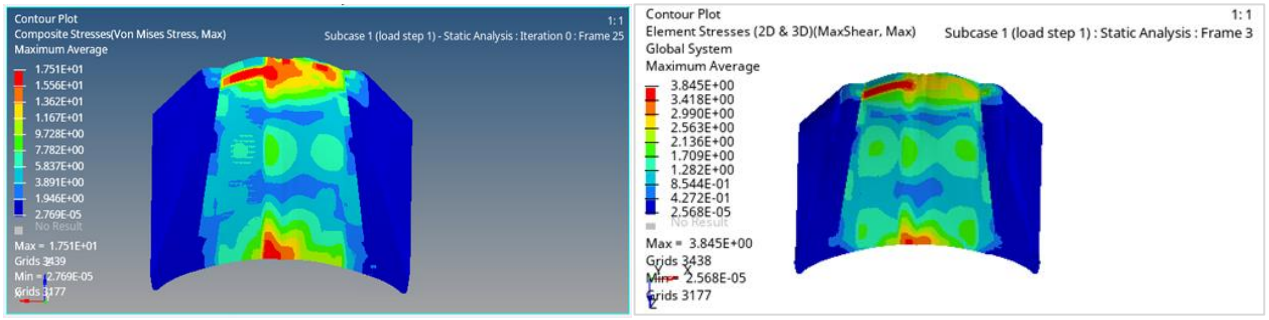

Figure 5:18 Optimized Composite Stress (von mises, Max Shear Stress) of different Angled Plies

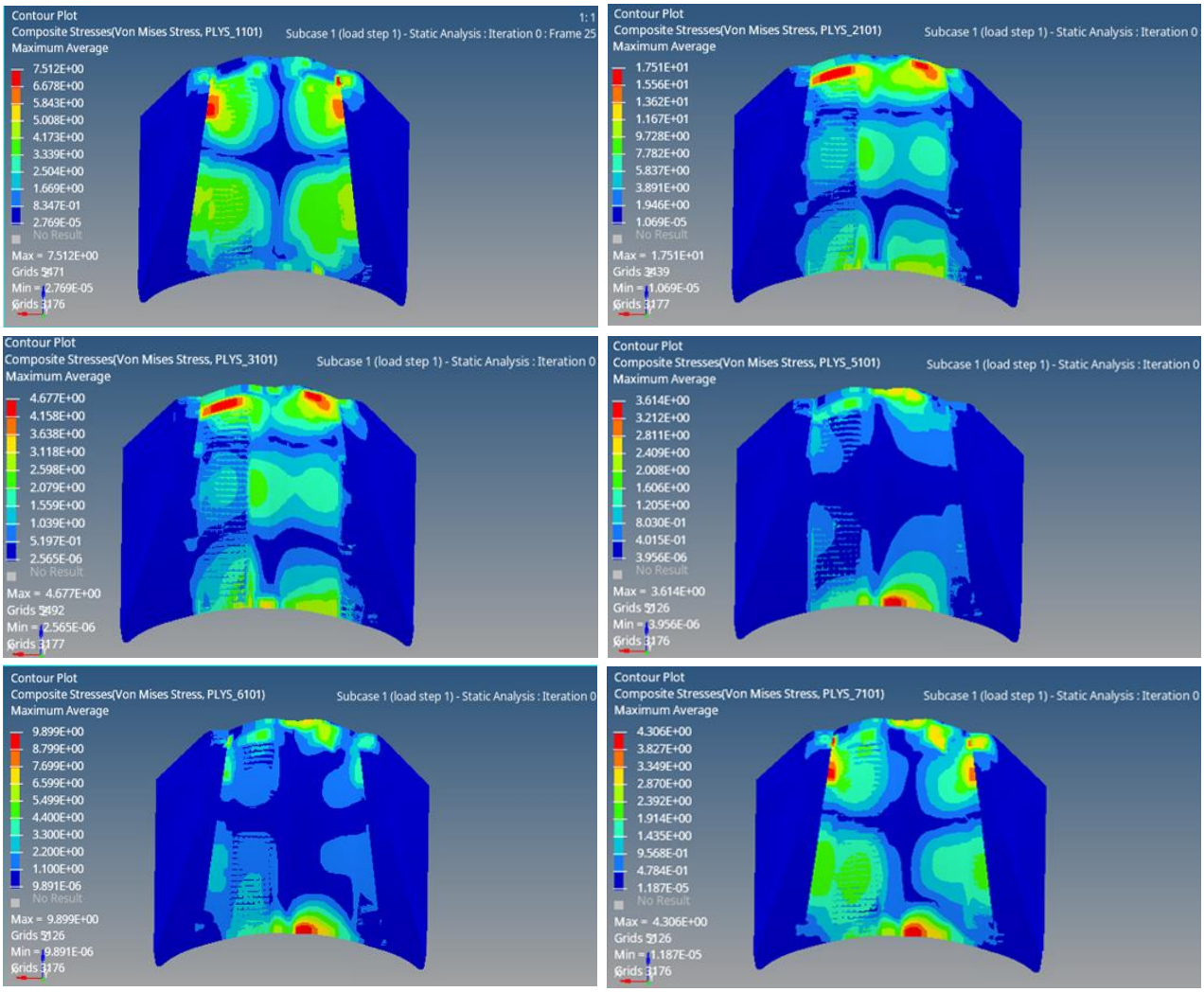

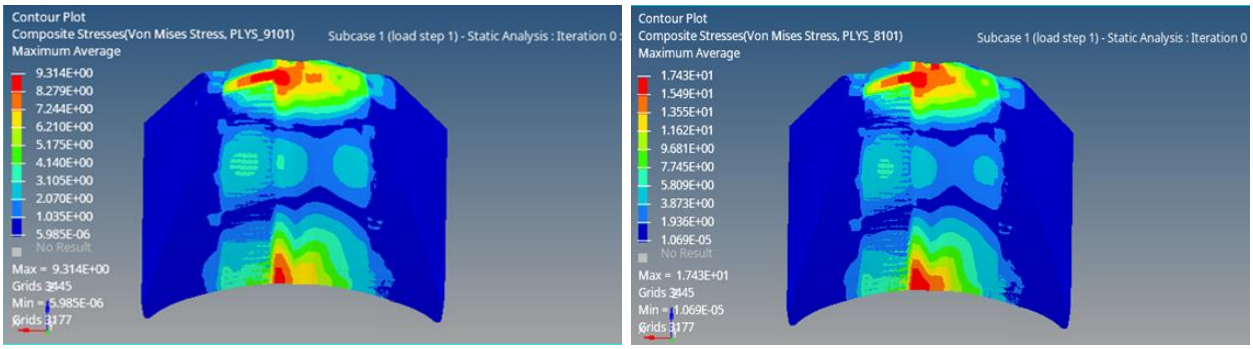

Figure 5:19 Optimized Composite Stress (Von Mises Stress) of different Angled Plies

2. **Element Stress Results:** - Again under this different analysis like Shear Max. ,Vonmises, Plain stress and Presssure results of the laminate and each Ply are shown.

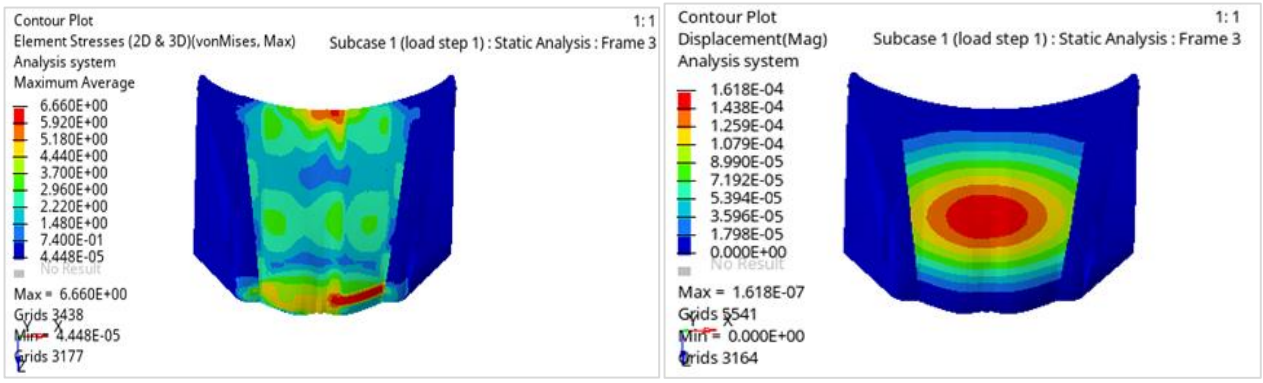

Figure 5:20 Optimized Stress & Displacement Result of the Composite Bonnet

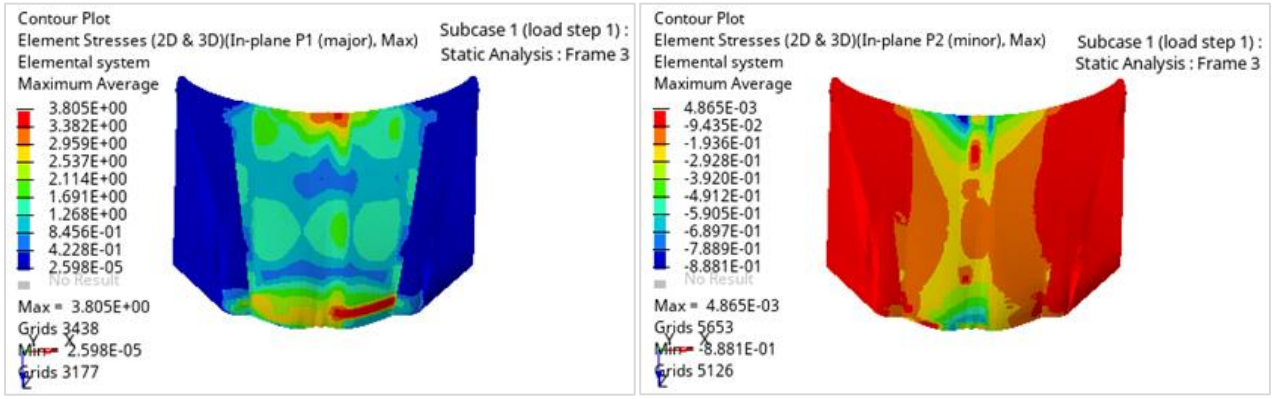

Figure 5:21 Element Stress (2D & 3D) result along Plane 1and 2 of the Composite Bonnet

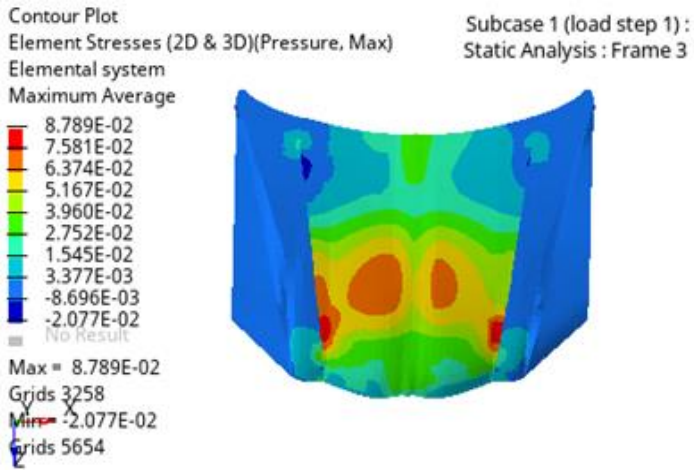

Figure 5:22 Element Stress (2D & 3D) Pressure of then composite bonnet

5.4. Thermal Analysis Result of the composite car bonnet using FEM

Finite Element Method (FEM) analysis is a powerful tool for evaluating the thermal performance of composite materials, like jute and glass fiber reinforced epoxy composites used in automotive bonnets. This analysis provides understandings into temperature distributions, thermal stresses, and deformation characteristics at a given thermal load. This document presents the FEM analysis results and discusses the implications for the design and performance of composite bonnets.

I. Temperature Distribution:

As shown in the figure below the temperature distribution across the bonnet was analyzed to understand how heat propagates through the composite material surface to give a result.

- Center of Bonnet: 67.5°C
- Edges of Bonnet: ~100.54°C

The temperature increases more significantly at the edges compared to the center this because of heat dissipation through the fixed constraints and also decrease from inner to outer surface.

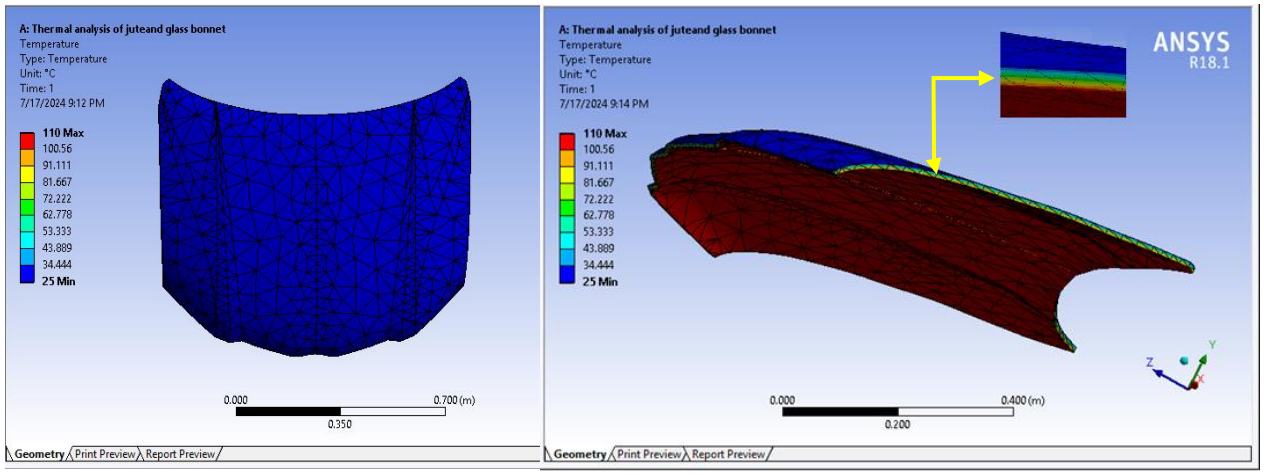

Figure 5:23 Temperature distribution of along the Composite surface of the bonnet

Generally, the temperature distribution analysis of the jute and Glass fiber reinforced epoxy composite bonnet indicates that the temperature gradient suggests that the bonnet maintains relatively even thermal conditions in the central areas but might face challenges in managing thermal loads at the edges. For improved thermal management, enhancing the heat dissipation mechanisms at the edges could be considered.

II. Heat Flux:

The heat flux for the composite bonnet is shown below. From the result it is observed that heat flux higher at the edge than at the center this is because of the constraint.

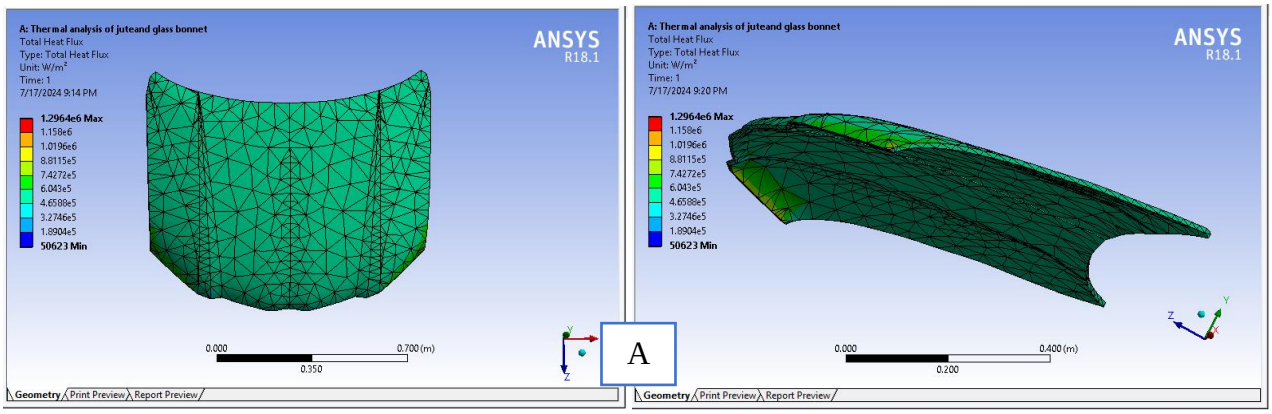

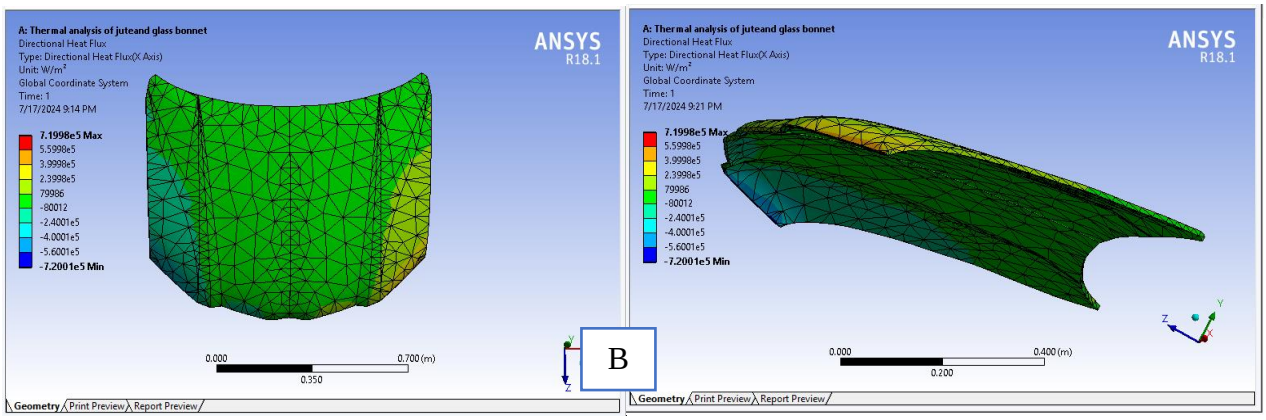

Figure 5:24 Heat Flux (A) and Heat Flux direction (B of the car bonnet

III. Thermal Stresses

Thermal stress is the stress produced due to any variation in temperature of the material. Mathematically it can be expressed as follow.

$\delta_T = \alpha L \Delta T$, when δ_T = thermal stress, α = coefficient of thermal expansion, L = length, ΔT = temperature change. The analysis of thermal stresses for Jute and Glass Fiber Reinforced Epoxy bonnet was conducted to understand the stress distribution resulting from temperature changes.

- Maximum Thermal Stress: 4.5 MPa
- Stress Distribution: Higher stresses observed near the edges due to thermal expansion and boundary constraints which causing higher stress concentrations.

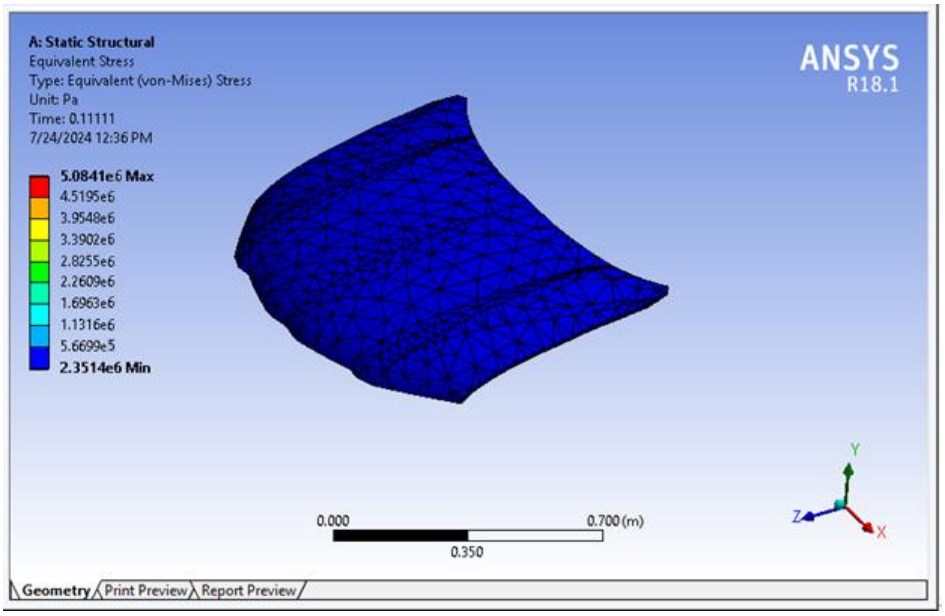

Figure 5:25 Thermal stress (von mises stress) of the composite bonnet

Finally, these thermal stresses should be considered in the design phase to avoid potential material failure. A possible design improvement could be incorporating flexible edge reinforcements to better accommodate thermal expansion and reduce stress concentrations.

IV. Thermal Deformation

The deformation due to temperature changes was analyzed to understand how the bonnet shape changes under thermal load.

- Maximum Deformation: 0.35 mm
- Deformation Distribution: Uniform deformation across the bonnet with slightly higher deformation at the center due to thermal expansion but lower at the edge because of the constraint.

The analysis reveals that the deformation due to thermal load is minimal, with the maximum deformation of 0.204 mm observed. This indicates that the composite maintains its structural integrity under the given thermal conditions. again, this low deformation value is favorable for maintaining the bonnet's shape and functionality.

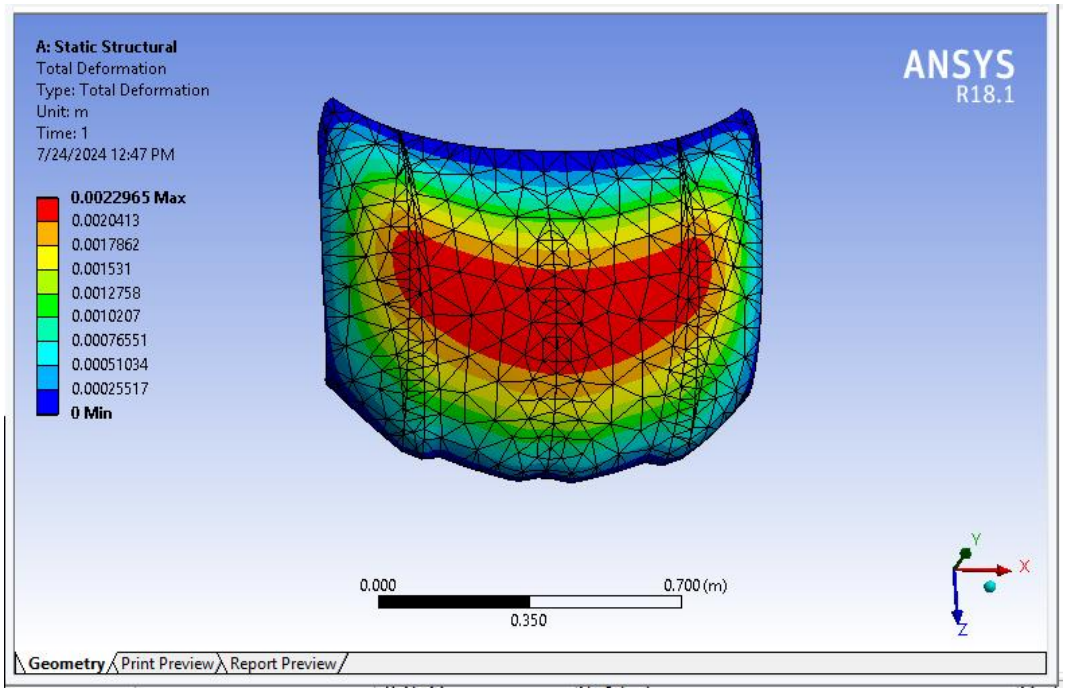

Figure 5:26 Thermal deformation of the composite bonnet

CHAPTER SIX

6. CONCLUSION AND RECOMMENDATION

6.1. CONCLUSION

The following conclusions were drawn for Jute/Glass fiber reinforced Epoxy composite based on the Experimental and Simulation results using Software (Ansys and Altair Hyper mesh).

A) ***Experimentally*****: -** Starting from Activities of fiber extraction method to fabrication process using hand layup method is made and mechanical characterization process was briefly discussed and presented under the variation of Fiber weight (volume) ratio and Fiber Angle of orientation.

- Optimum strength of different mechanical properties is obtained from Jute to E-glass fiber weight ratio at 50:50.
- From the mechanical characterization results, it observed that the Jute/Glass fiber reinforced epoxy composite material has a good mechanical property in the longitudinal direction but lower in transverse direction.
- Mechanical properties of the composite material increase with increasing E-glass fiber content.
- 0^0 unidirectional laminates have higher mechanical properties.
- Adding fiber angle of orientation improves Impact strength in both longitudinal and transversal direction when subjected to impact load. i.e. [0^0, $\pm45^0$] have better impact strength.

B) ***Simulation result***: - Impact analysis was done for Jute/Glass fiber reinforced Epoxy composite material for automotive Bonnet using Altaire Hyper mesh software & Ansys.

- The composite bonnet Plate has a lower deformation of 2.8 mm which is insignificant.
- The internal energy absorbed due to impact load is 1570J which has better energy absorption.
- The maximum equivalent Von-Mises stress exerted in the composite bonnet is 53.78 Mpa which is very much lower than the Materia strength implies have a capability of to withstand at the collision load.
- Comparing the laminates composites JGJGJG] bonnet with structural steel bonnet has better in strength and about 67% weight reduction which leads better performance of vehicle.
- Also, in the cost perspective composite bonnet is 78.5% less than steel bonnet.

Finally, it can be concluded that Jute/E-glass fiber reinforced epoxy composite meets most of the requirements like high strength to weight ratio, higher crashworthiness, high stiffness to weight ratio, less deformation and high von mises stress so that it can replace the existing steel bonnet.

6.2. RECOMMENDATION FOR FUTURE WORK

Since there is no complete solution to engineering problem adding the next further studies is good.

- Using poor fabrication process of hand-lay-up technique affects mechanical property result of Composite material so using other advanced manufacturing process technique is good.
- Economic Analysis & Structural analysis (aerodynamic analysis) of the Composite Bonnet.
- Deep thermal analysis Study of the composite bonnet is mandatory.
- Water absorption ability is the main drawback of composite material for automobile application which is seriously recommended for further study.
- Shear Testing Machine is limit throughout the country universities it is good if accessible.
- Finally, Federal Government or Automotive Private Company owner should take an Initiatives & give place for Natural Fiber Reinforced Composite in Engineering Structural application & do more on it.

References

1. *Campbell, F.C. 2010 : Structural Composite Materials ASM International® Materials Park, OH 44073-0002.*

2. N. Chand, M. Fahim, Tribology of Natural Fiber Polymer Composites, CRC Press, Florida (2008).

3. M. S. Islam, S. K. Ahmed, The Impacts of Jute on Environment: An Analytical Review of Bangladesh, Journal of Environment and Earth Science, 2 (2012), pp. 24-31.

4. B. K. Ghosh, A. Jethi, Growth and Instability in World Jute Production: A Disaggregated Analysis, International Journal of Electronics and Communication Technology, 4 (2013), pp. 191-195.

5. B. K. Ghosh, A. Jethi, Growth and Instability in World Jute Production: A Disaggregated Analysis, International Journal of Electronics and Communication Technology, 4 (2013), pp. 191-195.

6. Fardin Khan et al., Advances of composite materials in automobile applications – A review, Journal of Engineering Research 2023, https://doi.org/10.1016/j.jer.2024.02.017.

7. Venkatesh Naik et al. A Review on Natural Fiber Composite Materials in Automotive Applications, Engineering Science, 2022, 18, 1–10.

8. Rozaini Othman Et L., Application Of Carbon Fiber Reinforced Plastics In Automotive Industry: A Review, Research Get 2019 https://www.researchgate.net/publication/33791740).

9. Pandey JK, Ahn SH, Lee CS (2010) Recent advances in the composite Materials application.

10. Bledzki AK, Franciszczak P, Osman Z (2015) Elbadawi M (2015).

11. X. Cui, H. Zhang, S. Wang, L. Zhang, and J. Ko, "Design of lightweight multi-material automotive bodies using new material performance indices of thin-walled beams for the material selection with crashworthiness consideration," Mater. Des., vol. 32, no. 2.

12. Anthony Mascarin, IBIS Associates, Inc. Ted Hannibal, IBIS Associates,.

13. M. Sanjay, Composites Manufacturing: Materials, Product, and Process Engineering, florida: CRC Press, 2002.

14. Hayashi.T, "On the Improvement of Mechanical Properties of Composites by Hybrid Composition," in Proc. 8th International Reinforced Plastics Conference.

15. M. Andersoon and P. Liedberg, "Crash behavior of composite structures: A CAE benchmarking study," 2014.

16. A. Matzenmiller, J. Lubliner, and R. L. Taylor, "A constitutive model for anisotropic damage in fiber-composites," Mechanics of Materials, vol. 20, no. 2, p. 125–152, 1995.

17. I. M. Daniel and O. Ishai, Engineering Mechanics of Composite Materials,2nd Edition, 2013.

18. M. Andersoon and P. Liedberg, "Crash behavior of composite structures: A CAE benchmarking study," 2014.

19. Anup Bandivadekar, Kristian Bodek, Lynette Cheah,Christopher Evans, Tiffany Groode, John Heywood,Emmanuel Kasseris, Matthew Kromer, Malcolm Weiss, "Reducing Transportation's Petroleum Consumption and GHG Emissions," LFEE 2008-05 RP, Massachusetts Institut.

20. Masoumi, Mohammad Hassan Shojaeefard, Amir Najibi, Comparison of steel, aluminium and composite bonnet in term of pedestrian head impact, Safety Science. 1371(2011) 1371-1380.

21. J. Summerscales, N. P. J. Dissanayake, A. S. Virk, W. Hall, A Review of Bast Fibres and their Composites. Part 1 – Fibres as Reinforcements, Composites: Part A, 41 (2010), pp. 1329–1335.

22. S. Dalbehera, S. K. Acharya, Study on Mechanical Properties of Natural Fiber Reinforced Woven Jute-Glass Hybrid Epoxy Composites, Advances in Polymer Science and Technology: An International Journal, 4 (2014), pp. 1-6.

23. Ajith Gopinath, Senthil Kumar.M, Elayaperumal A, Experimental Investigations on Mechanical Properties of Jute Fiber Reinforced Composites with Polyester and Epoxy Resin Matrices, Procedia Engineering 97 (2014) 2052 – 2063.

24. Torres, G.B. et al. Eco-Friendly Natural Rubber–Jute Composites for the Footwear Industry. Polymers 2023, 15, 4183. https://doi.org/10.3390/ polym15204183.

25. Hua Wang, Hafeezullah Memon, Elwathig A. M. Hassan et al. Effect of Jute Fiber Modification on Mechanical Properties of Jute Fiber Composite, Materials 2019, 12, 1226 and doi:10.3390/ma12081226.

26. Anna Dilfi K.F., Aiswarya Balan, Hong Bin, Guijun Xian, Sabu Thomas, Effect of surface modification of jute fiber on the mechanical properties and durability of jute fiber-reinforced epoxy composites, Society of Plastics Engineers in POLYM. COMPOS, 2018.

27. S.H. Mahmud, S.C. Das, M.Z.I. Mollah,d, M.M. Ul-Hoque a, et al. Thermoset-polymer matrix composite materials of jute and glass fiber reinforcements: Radiation effects determination, journal of materials research and technology 2023 and 6635, 26:6623 -.

28. Padhi P K and Satapathy A 2013 Tribology Transactions 56, 789-796.,.

29. Amit Bindal, Satnam Singh, N. K. Batra, and Rajesh Khanna, et al. Development of Glass/Jute Fibers Reinforced Polyester Composite, Indian Journal of Materials Science Volume 2013, Article ID 675264, 6 pages http://dx.doi.org/10.1155/2013/675264.

30. Md. Zahidul Islam, Emel Ceyhun Sabir et al., Experimental investigation of mechanical properties of jute/hemp fibers reinforced hybrid polyester composites, SPE Polymer DOI: 10.1002/pls2.10119.

31. M. R. Hassan, M. A. Gafur, A. A. Rana, M. R. Qadir, et al. Characterization of jute and glass fiber reinforced polyester based hybrid composite, Bangladesh J. Sci. Ind. Res. 51(2), 81-88, 2016.

32. M. Muthuvel, G. Ranganath, K. JanarthananK. Srinivasan, et al. Characterization Study of Jute and Glass Fiber Reinforced Hybrid Composite Material, International Journal of Engineering Research & Technology (IJERT) Vol. 2 Issue 4, April - 2013 ISSN: 2278-.

33. M. R. Sanjay, B. Yogesha, Studies on Mechanical Properties of Jute/E-Glass Fiber Reinforced Epoxy Hybrid Composites, Journal of Minerals and Materials Characterization and Engineering, 2016, 4, 15-25 http://dx.doi.org/10.4236/jmmce.2016.41002.

34. Ghani, M.U., Siddique, A. and Abraha, K.G et al. Performance Evaluation of Jute/Glass-Fiber Reinforced Polybutylene Succinate (PBS) Hybrid Composites with Different Layering Configurations. Materials 2022, 15, 1055. doi.org.

35. A Murdani, and U S Amrullah, Flexural behavior of jute, glass, and Carbon fiber reinforced Polyester hybrid composites, Materials Science and Engineering 1173 (2021) 012067 doi:10.1088/1757-899X/1173/1/012067.

36. Dias, T.d.C. etal. Experimental Investigation on the Mechanical and Physical Properties of Glass/Jute Hybrid Laminates. Polymers 2022, 14, 4742. https:// doi.org/10.3390/polym14214742.

37. Mahammad Sharif Budihal, Preparation And Tensile Characterization Of Jute Based Bio Composites, International Journal of Research in Engineering and Technology eISSN: 2319-1163 | pISSN: 2321-7308.

38. Jonsan A. Zakus, T. Nicholas, H. F. Swift, L. B. Greszczuk, Curran D.R.," Impact Dynamics", John Wiley and Sons, Inc. (1982).

39. Kiesling et.al [Kiesling T.C., Chaudhry Z., Paine J.S.N., and Roger C.A., "Impact Failure Modes of Thin Graphite Epoxy Composites Embedded with Super Elastic Nitnol" the AIAA/ASME/AHS/ASC 37th SDM Conference, Satlake City, UT, April 15-17,(1996).

40. Gao Y, Gao Y, Qian R, Xu Y et al (2018) Concurrent optimization of ply orientation and thickness for carbon fiber reinforced plastic (CFRP) laminated engine hood. SAE Technical Paper 2018-01-1121. https://doi.org/10.4271/2018-01-1121.

41. Torkestani A, Sadighi M, Hedayati R (2015) Effect of material type, stacking sequence and impact location on the pedestrian head injury in collisions. Thin-Walled Struct :130–139.

42. University, Chen L (2013) Research on Lightweight Design Method of Engine Hood Based on Pedestrian Protection. Hunan.

43. Lee SL, Lee DC, Lee JI et al (2007) Integrated process for structural-topological configuration design of weight-reduced vehicle components. Finite Elem Anal Des 43(8):620–629.

44. 12(12):2933–2940, Yundong S et al (2016) Optimization design for laminate scheme of fiber reinforced composite shaft. J Aerospace Power.

45. Ding L (2014) Structure Optimal Design for All Composite Wings of an Unmanned Aerial Vehicle. Changchun Institute of Optics, Fine Mechanics and Physics, Chinese Academy of Sciences.

46. Mohamed.H, Gheitha, Mohamed. A, Wahe.G, Naheed.S, Mohammad.A, Mohmad J,c,∗, Othman Y. Alothmanc :- studies the Flexural, thermal and dynamic mechanical properties of Palm fibers reinforced epoxy composites, international journal University Putra Malaysi.

47. Mohamed.H, Gheitha, Mohamed. A, Wahe.G, Naheed.S, Mohammad.A, Mohmad J,c,∗, Othman Y. Alothmanc :- studies the Flexural, thermal and dynamic mechanical properties of Palm fibers reinforced epoxy composites, international journal University Putra Malaysi.

48. AL-Oqla F M, Alothman O Y, Jawaid M, Sapuan S M, and Es-Saheb M H 2014 Processing and properties of date palm fibers and its composites Biomass bioenergy 1-25.

49. R. Kumar, M. I. Ul Haq, A. Raina and A. Anand, Int. J. Sustain. Eng., 2009, 12, 212-220, Doi: 10.1080/19397038.2018.1538267.

50. International Journal of Advance Engineering and Research Development (IJAERD)International Conference of Trends in Information, Management, Engineering and Sciences (ICTIMES)Volume 5, Special Issue 02, Feb.-2018.

51. Mittal, V., Saini, R. and Sinha, S. Natural fiber-mediated epoxy composites—A review. Compos. Part B Eng. 2016, 99, 425–435.

52. Patel, R.V., Yadav, A. and Winczek, J. Physical, Mechanical, and Thermal Properties of Natural Fiber-Reinforced Epoxy Composites for Construction and Automotive Applications. Appl. Sci. 2023, 13, 5126. https://doi.org/10.3390/app13085126.

53. Desalegn Atalie, Rotich K. Gideon, (2018) "Extraction and characterization of Ethiopian palm leaf fibers", Research Journal of Textile and Apparel, Vol. 22 Issue: 1, pp.15-25, https://doi.org/10.1108/ RJTA-06-2017-0035.

54. Correia, Carla & Valera, Ticiane. (2019). Cellulose Nanocrystals and Jute Fiber-reinforced Natural Rubber Composites: Cure Characteristics and Mechanical Properties. Materials Research. 22. 10.1590/1980-5373-mr-2019-0192.

55. ("Kaw, A.K., 2006, Mechanics of Composite Materials, CRC Press, Boca Raton FL, and 2nd edition).

56. T. Takeichi, N. Furukawa, in Polymer Science: A Comprehensive Reference, 2012.

57. ASTM international, PA USA, 2010, "ASTM D3039/D3039M Standard Test Method for Tensile Properties of Polymer Matrix Composite Materials".

58. ASTM International, "ASTM D 1822 Standard Test Methods for Determining the Izod Pendulum Impact Resistance of Plastics," 2010.

59. ASTM international, PA USA 2007, "ASTM D7264 Standard Test Methods for Flexural Properties of Unreinforced and Reinforced Plastics and Electrical Insulating Materials".

60. ASTM Standards, , "ASTM D 3410 Standard Test Method for Compressive Properties of Polymer Matrix Composite Materials with Unsupported Gage Section by Shear Loading".

61. ASTM standards D792, "Standard Test Methods for Density and Specific Gravity (Relative Density) of Plastics by Displacement," 2013.

62. 2013, ASTM standards D792 Standard Test Methods for Density and Specific Gravity (Relative Density) of Plastics by Displacement.

63. Agarwal BD and Broutman LJ. Analysis and performance of fiber composites:Thrid Edition. s.l. : John Wiley and Sons,Inc, 2015.

64. 2009, ASTM Standard D2734 − 09 Standard Test Methods for Void Content of Reinforced Plastics.

65. Christopher C. Ihueze, Christian E. Okafor, Chris I. Okoye Journal of King Saud University – Engineering Sciences (January 2013).

66. Belyaev, N.M., 1979. Strength of Materials. MIR publishers, MOSCO.

67. Crawford, R.J., 1998. Plastics Engineering, third ed. Butterwoth-.

68. S. W. Tsai and E. M. Wu, "A general theory of strength for anisotropic materials, "Journal of composite materials, vol. 5, pp. 58-80, 1971.

69. . Staab, George .H, Laminated composite plate analysis, Laminar Composites,Second Edition,Elsevier 2015 : 351-389. s.l., , pp. 351-389.

70. Selvaraj, Dilipkumar, Part, Study on Feasibility and Viability of Applying Eco-Friendly Material for the Car Bonnet for A Sustainable Automotive and Isep, 2018.

71. Fournier, E., "Under Hood Temperature Measurements of Four Vehicles", Biokinetics Report to the Motor Vehicle Fire Research Institute, Report No. R04-13b. September 7, 2004.

72. (Hollaway, L C. "A review of the present and future utilization of FRP composites in the civil infrastructure with reference to their important in-service properties." Construction and Building Materials 24, no. 12 (2010): 2419-2445).

73. Al-Khanbashi A, Al-Kaabi K, and Hammami A 2005 Date palm fibers as polymeric matrix reinforcement: fiber characterization Polym. Compos. 26 486-497.

74. Sunil V Chavan, Rajkumar G R, Ashik K P, Shivalingappa M H, Mechanical Properties of Jute fiber reinforced Polyester based composites under different environmental conditions Advances in Polymer Science and Technology ISSN 2277 – 7164.

75. Uppada Rama Kantha, Putti Srinivasa Raob, Mallarapu Gopi Krishnac,∗ Mechanical behaviour of fly ash/SiC particles jmaterrestechnol . 2 0 1 9 and 2018, 8(1):737–744 5 June.

APPENDIX-A

A. Specimens Geometry and Dimensions

Table A-1Tensile test specimens geometry dimensions

Layer Notation	Test Material	Withd(mm)		Thickness(mm)		Length (mm)
		Mean	SD	Mean	SD	
JJJJJJ	Sample 1	20.1	0.16	4.52	0.13	250
	Sample 2	20.2	0.15	4.50	0.12	250
JGJJGJ	Sample 1	20.2	0.17	4.43	0.14	250
	Sample 2	20	0.19	4.32	0.13	250
JGJGJG	Sample 1	20.3	0.20	4.49	0.05	250
	Sample 2	20.4	0.21	4.50	0.06	250

Table A-2 Compressive test specimens geometry dimensions

Layer Notation	Test Material	Withd(mm)		Thickness(mm)		Length (mm)
		Mean	SD	Mean	SD	
JJJJJJ	Sample 1	20.2	0.15	4.50	0.15	250
	Sample 2	20.2	0.13	4.50	0.16	250
JGJJGJ	Sample 1	20.3	0.14	4.60	0.18	250
	Sample 2	20.4	0.16	4.30	0.13	250
JGJGJG	Sample 1	20.3	0.18	4.52	0.16	250
	Sample 2	20.2	0.17	4.34	0.15	250

Table A-3 Flexural test specimens geometry dimensions

Layer Notation	Test Material	Withd(mm)		Thickness(mm)		Length (mm)
		Mean	SD	Mean	SD	
JJJJJJ	Sample 1	20.5	0.16	4.22	0.15	250
	Sample 2	20.4	0.14	4.35	0.14	250
JGJJGJ	Sample 1	20.3	0.05	4.40	0.09	250
	Sample 2	20.2	0.04	4.42	0.08	250
JGJGJG	Sample 1	20.4	0.19	4.50	0.20	250
	Sample 2	20.5	0.20	4.44	0.19	250

Table A-4 Impact test specimens geometry dimensions

Layer Notation	Test Material	Withd(mm)		Thickness(mm)		Length (mm)
		Mean	SD	Mean	SD	
JJJJJJ	Sample 1	20.4	0.16	4.25	0.15	120
	Sample 2	20.38	0.15	4.46	0.14	120
JGJJGJ	Sample 1	20.3	0.14	4.41	0.15	120
	Sample 2	20.38	0.15	4.37	0.16	120
JGJGJG	Sample 1	20.4	0.19	4.38	0.13	120
	Sample 2	20.48	0.20	4.35	0.13	120

Table A-5 Water Absorption test specimens geometry dimensions

Layer Notation	Test Material	Withd(mm)		Thickness(mm)		Length (mm)
		Mean	SD	Mean	SD	
JJJJJJ	Sample 1	20.15	0.16	4.50	0.14	60
	Sample 2	20.32	0.15	4.43	0.14	60
JGJJGJ	Sample 1	20.31	0.16	4.50	0.15	60
	Sample 2	20.28	0.20	4.48	0.14	60
JGJGJG	Sample 1	20.24	0.21	4.51	0.16	60
	Sample 2	20.3	0.20	4.55	0.15	60

APPENDIX-B

B. Mechanical properties Test Results of composite

Table B-1 Experimental Mechanical Property Test Result of the composite material

Tensile Test Result					Calibrated Tensile Resul	
Specimen	No. of trials	Ultimatetensilestrength(Mpa)	Tensile strength(MPa)	Elongation at break (%)	Ultimate strength (Mpa)	Tensile stre ngth (MPa)
JJJJJJ	T1	357.5	298.2	3.67	308.2	204.7
	T2	355.4	302.6	3.64	304.5	200.4
	Avg	356.0	300.5	3.65	306.0	202.1
JGJJGJ	T1	366.8	336.7	3.62	254.8	206.6
	T2	381.2	328.4	3.6	269.2	204.6
	Avg	374.0	332.0	3.61	309.2	205.6
JGJGJG	T1	390.9	364.3	3.02	278.4	213.6
	T2	374.4	364.3	3.06	262.9	205.3
	Avg	382.6	364.3	3.54	313.8	209.8

Calibrated Result					
Specimen	No. of trials	Compression Load(KN)	Compression Strendth(Mpa)	Impact Strength (KJ/m2)	Flexuralstrength(Gpa)
JJJJJJ	T1	30.98	298.28	338.95	795.02
	T2	28.95	305.32	346.26	795.40
	Avg	29.96	301.80	342.61	795.21
JGJJGJ	T1	31.92	328.40	343.10	795.18
	T2	31.96	352.00	344.78	795.30
	Avg	31.94	340.20	343.94	795.24
JGJGJG	T1	29.00	442.62	350.55	795.28
	T2	31.96	480.28	346.23	795.40
	Avg	30.48	461.45	348.39	795.34

APPENDIX-C

C. Simulation Analysis results from Altair-Hyper Work

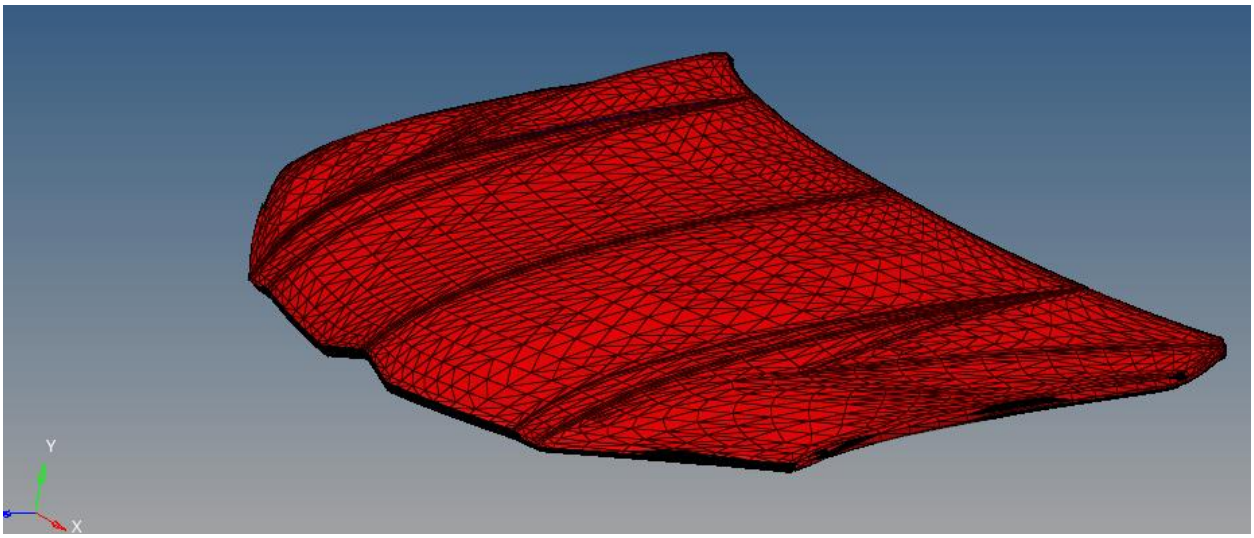

Figure C:1 Meshed part of the laminated composite bonnet

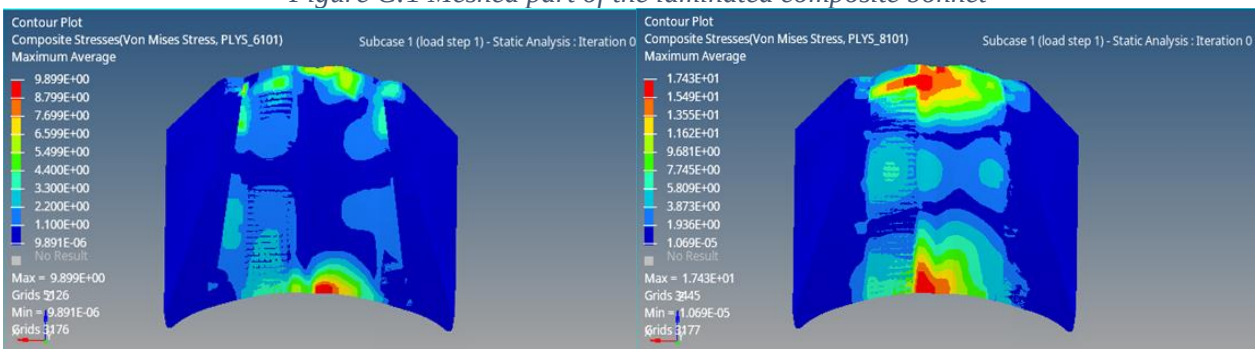

Figure C:2 Composite Stress (Von-mises Stress) of each Plays

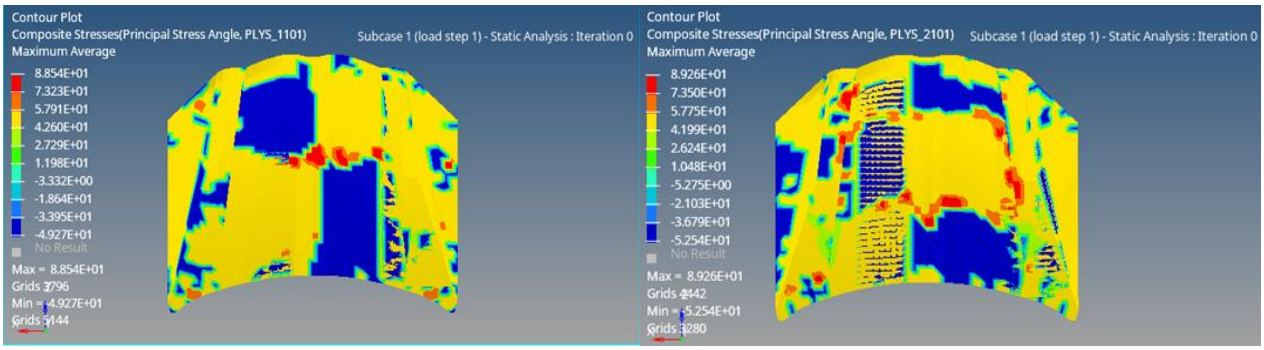

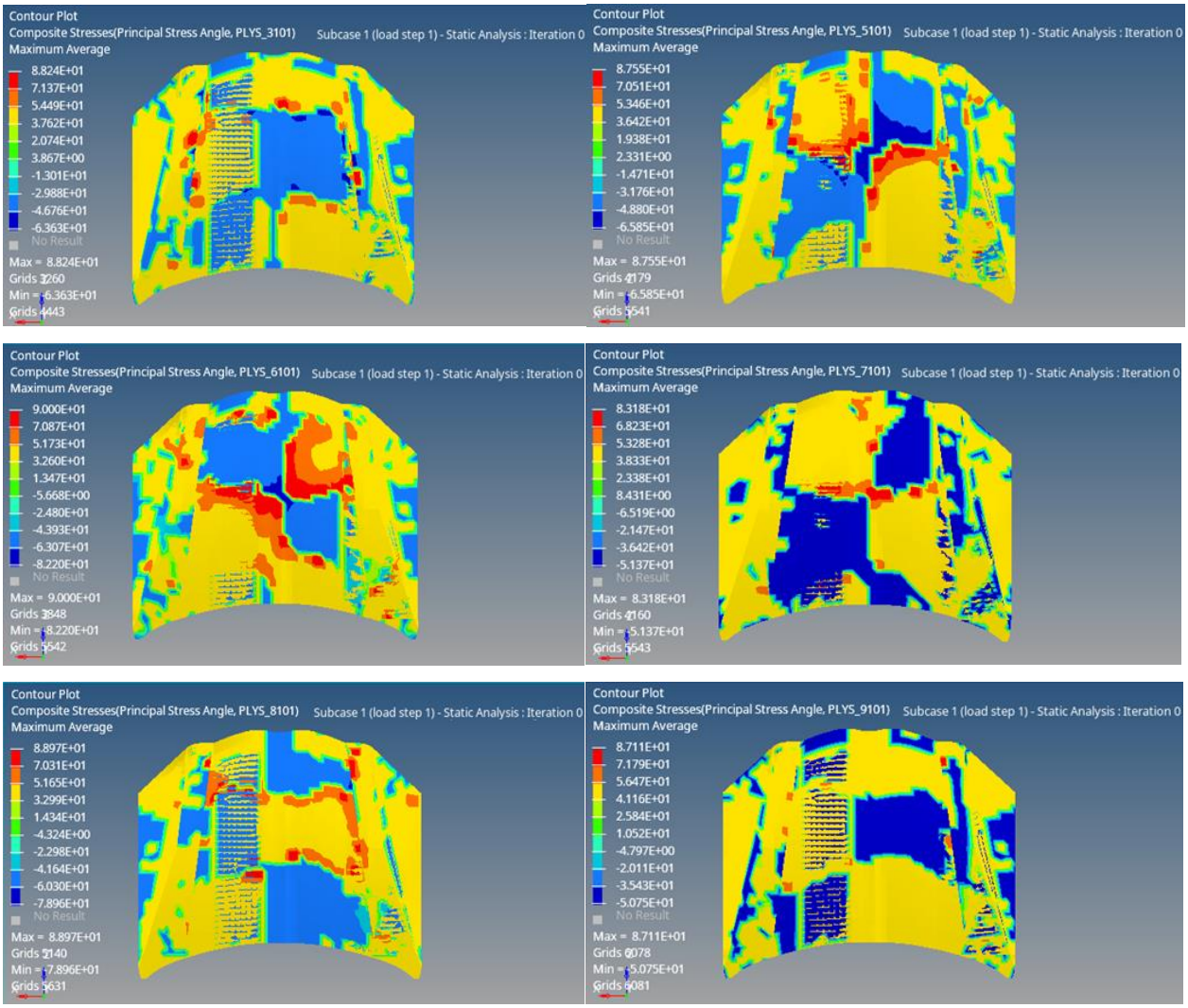

Figure C:3 Composite Stress (Principal Stress) of each Plays

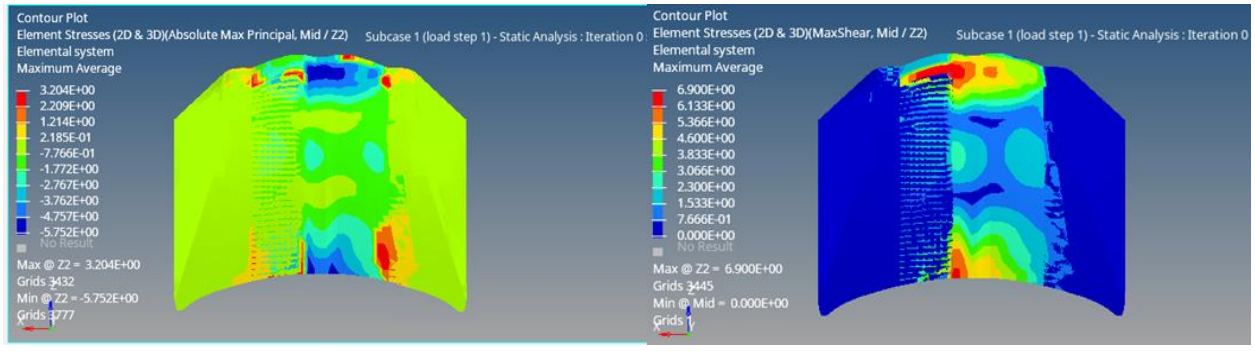

Figure C:4 Element Stress (2D&3D) In-Plane P1 & P2

APPINDIX-D

D. Excell Design of the Bonnet Plate

Plates

i **Check lines: 4.9;**
ii **Project information**

? Input section

1.0 Selection of material and units setting

1.1	Calculation units		SI Units (N, mm, kW...)	
1.2	Material		Structural steel EC 3, EN 10025; Fe 510 / Sy=355 MPa	
1.3	Modulus of elasticity	E	210000	[MPa]
1.4	Modulus of shearing	G	80769	[MPa]
1.5	Poisson's ratio	ν	0.30	
1.6	Temperature coefficient of expansion	γ	11.70	[m/m/C*e-6]
1.7	Specific mass	Ro	7850.00	[kg/m^3]
1.8	Yield strength	σ_y	355.00	[MPa]
1.9	Requested safety coefficient	SF	3.00	

2.0 Circular plates

3.0 Annular circular plates

4.0 Rectangular plates

4.1	Loading and mounting type		02. Uniform pressure q over small concentric circle of radius ro, all edges simply supported	
4.2	Plate thickness	t	1.200	[mm]
4.3	Long edge	a	1980.000	[mm]
4.4	Short edge	b	1450.000	[mm]
4.5	Radial location of loading	ro	25.400	[mm]
4.6	Total applied force	W	48.50	[N]
4.7	Load per unit area	q		[MPa]
4.8	Plate weight	m	27.04	[kg]
4.9	Maximum deflection	ymax	-44.85840	[mm]
4.10	Maximum stress	σ_{max}	87.42	[MPa]
4.11	Safety coefficient	SF	4.06	

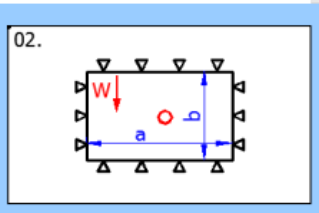

5.0 Circular plates producing large deflection

6.0 Rectangular plates producing large deflection

6.1	Mounting and loading type		07. Held and fixed, at center of long edges (a/b = 1.5 ~ <100), (Uniform pressure q over entire plate)	
6.2	Plate thickness	t	1.200	[mm]
6.3	Long edge	a	1980.000	[mm]
6.4	Short edge	b	1320.000	[mm]
6.5	Load per unit area	q	48.50000	[N]
6.6	Plate weight	m	24.62	[kg]
6.7	Maximum deflection	ymax	-1.70101	[mm]
6.8	Diaphragm stress	σ_d	0.97	[MPa]
6.9	Bending + diaphragm stress (sum)	σ_{sum}	7.30	[MPa]
6.10	Safety coefficient	SF	48.64	

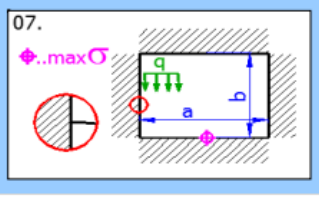

Move values from paragraph [4.0]

Figure D:1 Numerical Design of the Composite bonnet Plate